

**CHARACTERISATION OF TRANSGENIC TOBACCO
PLANTS EXPRESSING SYNTHETIC MOUSE PRION
PROTEIN**

NWORJI OGECHUKWU FRANCES

**A thesis submitted in partial fulfilment of the requirements of the
University of East London for the degree of Dr of Philosophy**

School of Health, Sports and Bioscience

September 2016

Abstract

The cellular prion protein (PrP^{C}) is a glycoprotein with unknown function constitutively expressed in mammalian neurons. PrP^{C} converts to a pathogenic misfolded isomer (PrP^{Sc}) through a poorly understood process, resulting in a group of fatal neurodegenerative diseases collectively known as transmissible spongiform encephalopathy or prion disease. Elucidating the molecular mechanisms behind prion conversion requires production of PrP^{C} in recombinant systems. This study was designed to generate transgenic tobacco plants expressing recombinant mouse prion protein (mPrP). Using a synthetic gene encoding the mouse prion protein, plant expression vectors were constructed for constitutive mPrP expression in the apoplast (pGreen35SmPrP-Apo), cytosol (pGreen35SmPrP-Cyto) and endoplasmic reticulum (pGreen35SmPrP-ER). Putative transgenic plants transformed with either pGreen35SmPrP-Cyto or pGreen35SmPrP-ER were analysed by PCR, ELISA and immunoblot for transgene integration and expression. However, no viable plants were obtained from the pGreen35SmPrP-Apo transformants. ELISA analysis showed that recombinant mPrP accumulated up to 0.0024% of total soluble leaf protein in transgenic tobacco leaves transformed with the pGreen35SmPrP-Cyto construct and 0.0016% of total soluble leaf protein in plants designed to sequester recombinant mPrP to the ER. Furthermore, immunoblot analysis showed that ER-targeted recombinant mPrP was mainly unglycosylated, although a glycosylated mPrP isoform was observed indicating that transgenic tobacco plants process ER-targeted recombinant mPrP in a manner analogous to mammalian systems. The nutrient composition of several transgenic plants were analysed to determine the phenotypic effect of expressing recombinant mPrP in tobacco plants. The

analysis revealed that transgenic lines expressing cytosolic-mPrP had elevated average levels of Mn^{2+} and Fe^{2+} . In addition, kanamycin-treated transgenic plants expressing cytosolic-mPrP developed a non-rooting phenotype. Conversely, the average Cu^{2+} level was increased in analysed transgenic plants designed to sequester recombinant mPrP in the ER. Furthermore, the plants developed no visible phenotype upon kanamycin treatment. This result support studies that suggest that the PrP^C has functional role in metal homeostasis and loss of its thermodynamic structure leads to metal dyshomeostasis which in turn has been linked to prion disease associated neurotoxicity. Finally, the recombinant mPrP was purified via affinity chromatography facilitated by the presence of a C-terminal polyhistidine tag on the synthetic gene constructs.

Table of Content

Table of Content	iii
Table of Figures	vii
Table of Tables.....	xi
Abbreviations.....	xii
Acknowledgement	xvi
Dedication	xvii
1 Literature Review	1
1.1 Prions	2
1.1.1 Prion Protein Structure	2
1.1.2 Function of PrP^C	4
1.1.2.1 PrP^C and Metal Interactions	5
1.1.3 Mechanism of PrP^{Sc} Aggregation	6
1.1.4 Prion Diseases	9
1.1.4.1 PrP^{Sc} Strains	10
1.1.4.2 Prion Disease Diagnosis and Treatment.....	11
1.1.5 Glycosylation profile of PrP	13
1.2 Transgenic Plants.....	14
1.2.1 Choice of Plant	16
1.2.2 Transgene Design	18
1.2.3 DNA delivery systems	20
1.2.4 Glycosylation	21
1.2.5 Downstream Processing	23
1.3 Research Aims.....	24
2 Materials and Method	26
2.1 Introduction	27
2.2 Design of transgene construct	27
2.2.1 Bacterial strains.....	27

2.2.2	Plant growth conditions	27
2.2.3	Transgene design	27
2.2.4	Plasmids	28
2.2.4.1	35S-CaMV	28
2.2.4.2	pGreen	29
2.2.5	Expression cassette construction	30
2.2.5.1	Restriction digestion	30
2.2.5.2	Agarose gel electrophoresis	30
2.2.5.3	DNA recovery	30
2.2.5.4	Subcloning procedure	31
2.2.5.5	E. coli transformation	31
2.2.5.6	Plasmid DNA isolation	32
2.2.6	Transformation of tobacco leaves	32
2.2.6.1	Preparation of electrocompetent cells	32
2.2.6.2	Agrobacterium transformation	32
2.2.6.3	Tobacco leaves transformation	33
2.3	Characterisation of recombinant mPrP in transgenic tobacco leaves ...	34
2.3.1	DNA analysis	34
2.3.1.1	Polymerase chain reaction (PCR)	34
2.3.2	RNA analysis	35
2.3.2.1	Reverse transcription (RT)-PCR	35
2.3.2.2	Real time RT-PCR	35
2.3.3	Protein Analysis	36
2.3.3.1	Western blot	36
2.3.3.2	Enzyme-linked immunosorbent assay (ELISA)	37
2.4	Chemical analysis of transgenic tobacco leaves	37
2.4.1	Analysis of Plant Nutrients	39
2.4.2	Peroxidase Assay	40
	Statistical analysis	40

2.5	Purification of recombinant mPrP	40
2.5.1	Lysis buffers	40
2.5.2	Sample Preparation	42
2.5.3	Purification	43
3	Design of Transgene Constructs	44
3.1	Introduction	45
3.2	Results	46
3.2.1	Synthetic mPrP gene constructs	46
3.2.2	Plant Expression Vectors	52
3.2.2.1	p35S-2-mPrP cassettes	52
3.2.2.2	pGreen-35S-mPrP cassettes	54
3.2.3	Plant Transformation	58
3.3	Discussion	60
4	Characterisation of recombinant mPrP in transgenic tobacco leaves	64
4.1	Introduction	65
4.2	Results	67
4.2.1	Analysis of transgenic plants expressing cytosolic-mPrP	68
4.2.2	Analysis of transgenic plants transformed with the ER-mPrP construct	73
4.3	Discussion	78
5	Phenotypic analysis of transgenic tobacco leaves expressing recombinant mPrP	87
5.1	Introduction	88
5.2	Results	90
5.2.1	Kanamycin induced phenotypic changes in transgenic tobacco plants transformed with the pGreen-35S-mPrP-Cyto construct	90
5.2.2	Chemical analysis of transgenic tobacco plant leaves	91
5.2.2.1	Analysis of macroelements	92
5.2.2.2	Analysis of microelements	96
5.2.3	Effect of recombinant prion expression and kanamycin treatment on peroxidase activity in transgenic tobacco leaves	100

5.3	Discussion	102
6	Purification strategy for recombinant mPrP expressed in tobacco plants..	111
6.1	Introduction	112
6.2	Results	114
6.2.1	Purification Strategy.....	114
6.2.2	Extraction of recombinant mPrP	115
6.2.2.1	Transgenic leaves lysed with buffer A.....	115
6.2.2.2	Transgenic leaves lysed with buffer B.....	117
6.2.2.3	Transgenic leaves lysed with buffer C.....	119
6.2.2.4	Ammonium Sulphate fractionation of extracts.....	120
6.2.2.5	Transgenic leaves lysed with buffers D and E	121
6.2.2.6	Transgenic leaves lysed with buffer F	122
6.3	Discussion	124
7	Discussion	132
8	References	139
9	Appendices	173
9.1	Appendix A: Protease Digestion of recombinant mPrP.....	174
9.2	Appendix B: Deglycosylation of recombinant mPrP	175
9.3	Appendix C: Western Blot analysis of recombinant mPrP	176
9.4	Appendix D: Non-detergent lysis of transgenic tobacco leaves expressing cytosolic-mPrP	178
9.5	Appendix E: Recombinant mPrP concentration.....	179
9.6	Appendix F: qRT-PCR Analysis.....	180

Table of Figures

Figure 1.1: Schematic representation of PrP ^C	3
Figure 1.2: 3 Dimensional Structure of the PrP	4
Figure 1.3: General mechanism of Protein aggregation	7
Figure 1.4: PrP ^{Sc} aggregation models	8
Figure 2.1: 35S-CaMV cassette	28
Figure 2.2: pGreen Binary Vectors	29
Figure 3.1: Creation of a synthetic mPrP gene for expression in tobacco plants	46
Figure 3.2: Comparative codon analysis of native mouse prion protein and synthetic mouse prion protein optimised for expression in <i>Nicotiana Tabacum</i>	47
Figure 3.3: Schematic representation of mPrP transgene constructs	48
Figure 3.4: Annotated mPrP-Cyto nucleotide sequence	49
Figure 3.5: Annotated mPrP-Apo nucleotide sequence	50
Figure 3.6: Annotated mPrP-ER nucleotide sequence	51
Figure 3.7: <i>EcoRV</i> analysis of p35S-2-mPrP constructs	52
Figure 3.8: Schematic representation of p35S-2-mPrP transgene cassettes	53
Figure 3.9: <i>EcoRV</i> Analysis of pGreen-35S-mPrP constructs	54
Figure 3.10: Schematic representation of pGreen-35S-mPrP-Cyto plasmid	55
Figure 3.11: Schematic representation of pGreen-35S-mPrP-Apo plasmid	56
Figure 3.12: Schematic representation of pGreen-35S-mPrP-ER plasmid	57
Figure 3.13: Stages in Plant Transformation	58
Figure 3.14: Schematic representation of recombinant T-DNA region of constructs	59
Figure 4.1: PCR analysis of transgenic tobacco leaves transformed with the pGreen-35S-mPrP-Cyto construct	68
Figure 4.3: qRT-PCR analysis of mPrP mRNA transcript levels in transgenic tobacco leaves transformed with the pGreen-35S-mPrP-Cyto construct	69
Figure 4.2: RT-PCR analysis of transgenic tobacco leaves transformed with the pGreen-35S-mPrP-Cyto construct	69

Figure 4.4: ELISA analysis of recombinant mPrP protein concentration in transgenic tobacco leaves transformed with the pGreen-35S-mPrP-Cyto construct	70
Figure 4.5: Western blot analysis of transgenic tobacco leaves transformed with the pGreen-35S-mPrP-Cyto construct.....	71
Figure 4.6: PCR analysis of transgenic tobacco leaves transformed with the pGreen-35S-mPrP-ER construct.....	73
Figure 4.7: RT-PCR analysis of transgenic tobacco leaves transformed with the pGreen-35S-mPrP-ER construct.....	74
Figure 4.8: qRT-PCR analysis of mPrP expression levels in transgenic tobacco leaves transformed with the pGreen-35S-mPrP-ER construct	74
Figure 4.9: ELISA analysis of recombinant mPrP concentration in transgenic tobacco leaves transformed with the pGreen-35S-mPrP-ER construct.....	75
Figure 4.10: Western blot analysis of transgenic tobacco leaves transformed with the pGreen-35S-mPrP-ER construct.....	76
Figure 4.11: Comparative analysis of recombinant mPrP produced in different subcellular compartments in transgenic tobacco plants.....	77
Figure 4.12: PrP quality control pathway	79
Figure 5.1: 15-day-old transgenic plant transformed with the pGreen-35S-mPrP-Cyto construct grown either in MS media supplemented with kanamycin (A) or MS media only (B).....	90
Figure 5.2: 30-day-old transgenic plants grown either in MS media supplemented with kanamycin: pGreen-35S-mPrP-Cyto construct (A) and pGreen construct (C) or MS media only: pGreen-35S-mPrP-Cyto construct (B) and pGreen construct (D)	91
Figure 5.3: Comparison of nitrogen content of transgenic tobacco leaves from the pGreen, pGreen-35S2-mPrP-Cyto and pGreen-35S2-mPrP-ER constructs grown either in MS media or MS media supplemented with kanamycin (100 µg/ml).	92
Figure 5.4: Comparison of phosphorus content of transgenic tobacco leaves from the pGreen, pGreen-35S2-mPrP-Cyto and pGreen-35S2-mPrP-ER constructs grown either in MS media or MS media supplemented with kanamycin (100 µg/ml).	93
Figure 5.5: Comparison of potassium content of transgenic tobacco leaves from the pGreen, pGreen-35S2-mPrP-Cyto and pGreen-35S2-mPrP-ER constructs grown either in MS media or MS media supplemented with kanamycin (100 µg/ml).	93
Figure 5.6: Comparison of calcium content of transgenic tobacco leaves from the pGreen, pGreen-35S2-mPrP-Cyto and pGreen-35S2-mPrP-ER constructs grown either in MS media or MS media supplemented with kanamycin (100 µg/ml).	94
Figure 5.7: Comparison of magnesium content of transgenic tobacco leaves from the pGreen, pGreen-35S2-mPrP-Cyto and pGreen-35S2-mPrP-ER constructs	

grown either in MS media or MS media supplemented with kanamycin (100 µg/ml).	94
Figure 5.8: Comparison of iron content of transgenic tobacco leaves from the pGreen, pGreen-35S2-mPrP-Cyto and pGreen-35S2-mPrP-ER constructs grown either in MS media or MS media supplemented with kanamycin (100 µg/ml).	96
Figure 5.9: Comparison of manganese content of transgenic tobacco leaves from the pGreen, pGreen-35S2-mPrP-Cyto and pGreen-35S2-mPrP-ER constructs grown either in MS media or MS media supplemented with kanamycin (100 µg/ml).	97
Figure 5.10: Comparison of copper content of transgenic tobacco leaves from the pGreen, pGreen-35S2-mPrP-Cyto and pGreen-35S2-mPrP-ER constructs grown either in MS media or MS media supplemented with kanamycin (100 µg/ml).	97
Figure 5.11: Comparison of boron content of transgenic tobacco leaves from the pGreen, pGreen-35S2-mPrP-Cyto and pGreen-35S2-mPrP-ER constructs grown either in MS media or MS media supplemented with kanamycin (100 µg/ml).	98
Figure 5.12: Comparison of nickel content of transgenic tobacco leaves from the pGreen, pGreen-35S2-mPrP-Cyto and pGreen-35S2-mPrP-ER constructs grown either in MS media or MS media supplemented with kanamycin (100 µg/ml).	98
Figure 5.13: Comparison of zinc content of transgenic tobacco leaves from the pGreen, pGreen-35S2-mPrP-Cyto and pGreen-35S2-mPrP-ER constructs grown either in MS media or MS media supplemented with kanamycin (100 µg/ml).	99
Figure 5.14: Peroxidase assay of transgenic tobacco leaves from the pGreen, pGreen-35S2-mPrP-Cyto and pGreen-35S2-mPrP-ER constructs grown either in MS media or MS media supplemented with kanamycin (100 µg/ml).	101
Figure 6.1: Flowchart of steps involved in recombinant mPrP extraction from transgenic tobacco plants	114
Figure 6.2: Purification of His-tagged cytosolic recombinant mPrP from transgenic tobacco leaves extract	116
Figure 6.3: Purification of His-tagged recombinant mPrP from transgenic tobacco leaves extract.....	118
Figure 6.4: Purification of His-tagged cytosolic recombinant mPrP from transgenic tobacco leaves extract.	119
Figure 6.5: Ammonium sulphate fractionation of transgenic tobacco leaves expressing recombinant mPrP in the ER.....	121
Figure 6.6: Purification of His-tagged recombinant mPrP from transgenic tobacco leaves extract.....	122
Figure 6.7: Purification of His-tagged recombinant mPrP from transgenic tobacco leaves extract.....	123
Appendix 9.1: Proteinase K digestion of transgenic plants expressing mPrP...	174
Appendix 9.2: Deglycosylation of transgenic plants transformed with the ER construct	175

Appendix 9.3: Western blot analysis of recombinant mPrP.	176
Appendix 9.4: Western blot analysis of cytosolic-mPrP in transgenic tobacco lines.	178
Appendix 9.6a: qRT-PCR Efficiency	180

Table of Tables

Table 1.1 Important biopharmaceuticals produced in transgenic plant systems	15
Table 2.1: Primer Sequences	36
Table 2.2: Tobacco leaf protein extraction buffers	41
Table 2.3: Properties of detergents used in lysis buffer	42
Table 4.1: Transformation efficiency of tobacco explants	67
Appendix 9.5: Recombinant mPrP concentration	179
Appendix 9.6b: Relative RNA quantification	181

Abbreviations

ANOVA	Analysis of variance
BAP	6-Benzylaminopurine
β ME	β -Mercaptoethanol
BSA	Bovine serum albumin
BSE	Bovine spongiform encephalopathy
BY-2	Bright yellow-2
CaMV	Cauliflower mosaic virus
cDNA	Complementary deoxyribonucleic acid
CJD	Creutzfeldt-Jakob disease
CMC	Critical micelle concentration
CNS	Central nervous system
CSF	Cerebrospinal fluid
Cu ²⁺	Copper ions
CWD	Chronic wasting disease
DNA	Deoxyribonucleic acid
EEG	Electroencephalogram
ELISA	Enzyme-linked immunosorbent assay
ER	Endoplasmic reticulum
ERAD	Endoplasmic-reticulum-associated protein degradation
fCJD	Familial Creutzfeldt-Jakob disease
FFI	Fatal familial insomnia
FSI	Fatal sporadic insomnia
GPI	Glycosylphosphatidylinositol
GSS	Gerstmann–Sträussler–Scheinker syndrome
HSP	Heat shock protein

IMAC	Immobilised Metal Affinity Chromatography
LB	Luria-Bertani
MCS	Multiple cloning site
mPrP	Mouse prion protein
MRI	Magnetic resonance imaging
mRNA	Messenger RNA
MS	Murashige and Skoog
MWCO	Molecular weight cut-off
NAA	1-Naphthaleneacetic acid
NptI	Neomycin phosphotransferase I
OPRI	Octapeptide repeat insertions
PAGE	Polyacrylamide gel electrophoresis
PBST	Phosphate-buffered saline and Triton X-100
PCR	Polymerase chain reaction
PDC	Protein detergent complex
PEG	Polyethylene glycol
PMCA	Protein Misfolding Cyclic Amplification
PRNP	Prion protein
PrP	Full length prion protein
PrP ^C	Cellular prion protein
PrP ^{Sc}	Misfolded prion protein
qRT-PCR	Quantitative real time polymerase chain reaction
RNA	Ribonucleic acid
RT-PCR	Real time polymerase chain reaction
Rpm	Revolution per minute
sCJD	Spontaneous Creutzfeldt-Jakob disease
SDS	Sodium dodecyl sulphate

TBS	Tris-buffered saline
TME	Transmissible mink encephalopathy
TMV	Tobacco mosaic virus
TSP	Total soluble protein
UPS	Ubiquitin proteasome system
UTR	Untranslated region
vCJD	Variant Creutzfeldt-Jakob disease
YEP	Yeast Extract Peptone

Nucleic Acids

Nucleic Acid	Single Letter Code
Adenine	A
Cytosine	C
Guanine	G
Thymine	T

Amino acids

Amino acid	Three letter code	Single letter code
Alanine	Ala	A
Arginine	Arg	R
Asparagine	Asn	N
Asparagine Or Aspartic Acid	Asx	B
Aspartic Acid	Asp	D
Cysteine	Cys	C
Glutamic Acid	Glu	E
Glutamine	Gln	Q
Glutamine Or Glutamic Acid	Glx	Z
Glycine	Gly	G
Histidine	His	H
Isoleucine	Ile	I
Leucine	Leu	L
Lysine	Lys	K
Methionine	Met	M
Phenylalanine	Phe	F
Proline	Pro	P
Serine	Ser	S
Threonine	Thr	T
Tryptophan	Trp	W
Tyrosine	Tyr	Y
Valine	Val	V

Acknowledgement

To the Holy Spirit, I'm grateful for your guidance and friendship. Especially for helping me understand the wisdom of choosing mercy over justice.

To Dr Andrew Thompsett and Dr David Bringloe, thank you for proofreading this dissertation and your helpful suggestions and comments throughout the duration of this study. To the laboratory technicians, thank you for your assistance.

To my parents and siblings, of all my blessings family comes first. I'm grateful for the support and sacrifices made to help me complete this project. Chichi, thank you for being an emotional anchor.

To Tunde, thank you for your unrequitable kindness, Jennifer, I'm grateful for your unconditional friendship, Ngozi, thank you for ensuring that I always had homemade dinners when I spent weekends in the laboratory, Edith, thank you for your incredible generosity and Damola, thank you for being a much needed confidence prop.

Dedication

To anyone traumatised by bullies

Let nothing disturb you,

Let nothing frighten you,

All things are passing away:

God never changes.

Patience obtains all things

Whoever has God lacks nothing;

God alone suffices.

-- *St. Teresa of Avila*

1 Literature Review

1.1 Prions

The cellular prion protein (PrP^C) is a glycoprotein that is highly conserved and constitutively expressed in mammalian neurons. The function of PrP^C is unknown however the misfolded isoform of the protein causes prion disease (Prusiner, 1998). Prion diseases are a group of progressive and fatal neurodegenerative disorders that affect both human and animals (Prusiner, 1998). The molecular basis for prion infectivity involves the post-translational conversion of cellular prion protein (PrP^C) to an aberrant isoform, designated PrP^{Sc}, which causes prion disease (Prusiner, 1998; Piccardo *et al.*, 2012). The PrP^{Sc} isoform is self-replicating and propagates by converting newly synthesised PrP^C into its aberrant isoform. This hypothesis is supported by the absence of infectivity in PrP *knockout* mice (Prusiner, 1998). In addition, synthetic PrP^{Sc} generated *in vitro* demonstrated low levels of infectivity in wild type animals (Weber *et al.*, 2007). The entire open reading frame of the prion protein (PRNP) is located in a single exon of the prion protein gene (*PRNP*). The PrP^C and PrP^{Sc} isoforms have identical amino acid sequence but vary in their biochemical and biophysical properties due to post-translational modifications (McKintosh *et al.*, 2003; Linden *et al.*, 2008).

1.1.1 Prion Protein Structure

Full length human prion protein has 208 amino acid residues and consists of two domains (Figure 1.1). The N-terminal domain (23-120) is flexible and consists of 4-5 octapeptide repeats with slight variation in consensus sequence (PHGGGWGQ) at amino acid residues 51-90. The C-terminal domain (121-231) folds into a stable conformation of three α -helices (α -helix 1: 144–154, α -helix 2: 173–194, and α -helix 3: 200–228) and an anti-parallel β -sheet (β 1: 128-131 and

β 2:161-164). The second and third α -helices are stabilised by a disulphide bridge between Cys 179 and Cys 214. It also features sites for N-linked glycosylation at Asp 181 and Asp 197. A glycosphosphatidylinositol (GPI) anchor linked at residue 231 attaches the prion protein to the cell membrane (DeArmonda and Bouzamondo, 2002; Mastrianni, 2004).

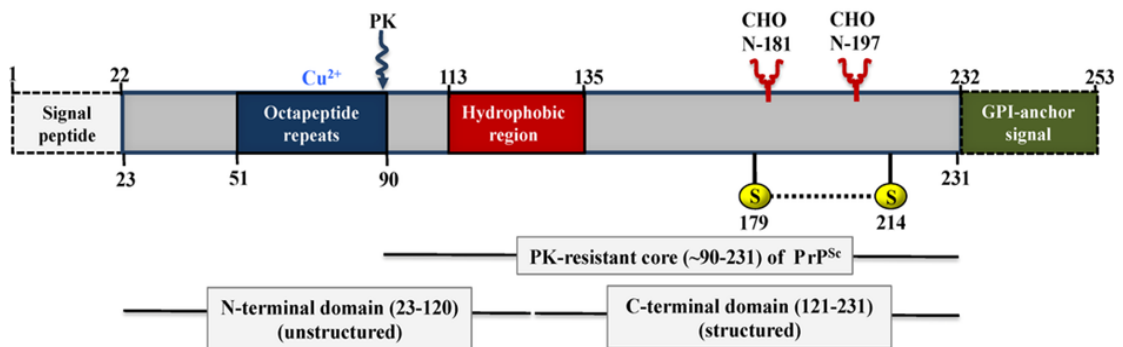


Figure 1.1: Schematic representation of PrP^C

Reproduced with permission from Acevedo-Morantes and Wille (2014)

There are several structural differences between PrP^C and PrP^{Sc} (Figure 1.2). The structure of PrP^{Sc} has not been elucidated due to methodological difficulties associated with the protein's insolubility. Theoretically, PrP^{Sc} synthesis from recombinant PrP^C involves disruption of the α -helices and formation of an amyloidoid β core, comprising of parallelly aligned β -strands at the C-terminal domain (Cobb and Surewicz, 2009). Fully glycosylated PrP^C has a molecular weight of 33-35 kDa, is approximately 42% α -helical with 3% β -sheet, soluble in detergents and sensitive to proteinase K digestion while PrP^{Sc} is theoretically 30% α -helical with 43% β -sheet, insoluble in detergents and proteinase K digestion of PrP^{Sc} results in an N-terminal truncated protease core (amino acid residues 90-231) of molecular weight of 27-30 kDa (DeArmonda and Bouzamondo, 2002;).

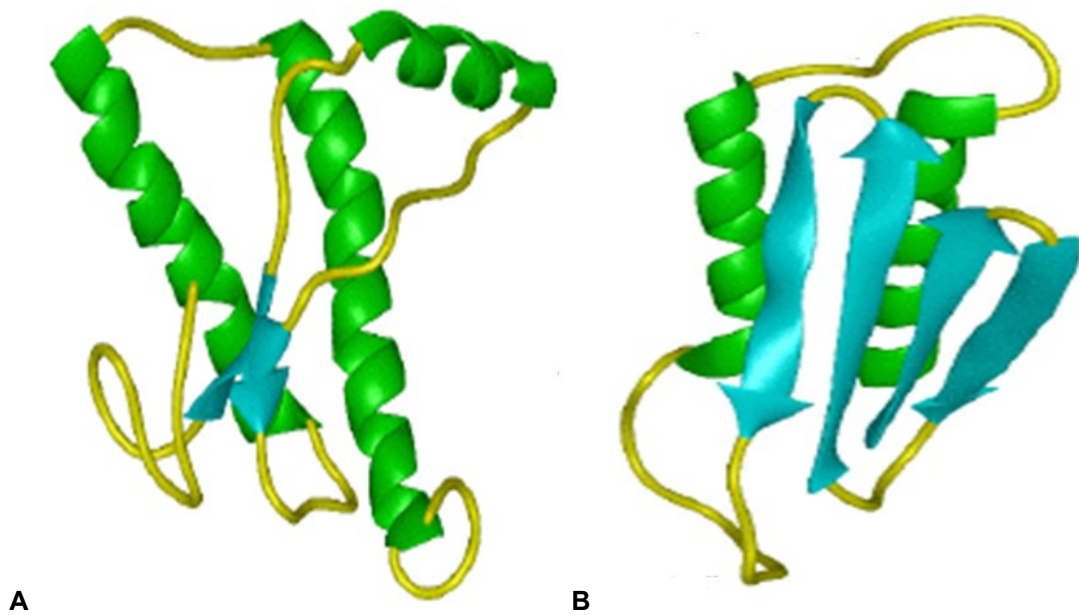


Figure 1.2: 3 Dimensional Structure of the PrP

A, PrP^C; B, Theoretical PrP^{Sc}

Adapted from www.cmpharm.ucsf.edu/cohen

1.1.2 Function of PrP^C

Cellular prion protein is constitutively expressed by neurons and hematopoietic cells but the physiological function of cellular prion protein is yet to be elucidated. Several potential functions have been attributed to the cellular prion protein based on experimental observations including regulation of cell division and apoptosis, antioxidant activity, signal transduction, metal-ion transport and protection of neurons against Bax-mediated cell death (Hu *et al.*, 2008; Jeffrey *et al.*, 2012; Puoti *et al.*, 2012). Researchers have observed that *PRNP* knockout mice are vulnerable to seizures and traumatic brain injury relative to wild-type mice. In addition, *PRNP* ablated mice exhibit normal early development but as they grow older the mice display severe ataxia and death of Purkinje neurons (Prusiner, 1998). It is therefore, plausible that PrP^C has a role in the development and protection of neurons (Hu *et al.*, 2008).

1.1.2.1 PrP^C and Metal Interactions

Prion protein binds several divalent transition metals including copper for which it has a high affinity. This affinity may signify a role for PrP^C in copper metabolism and transport. Furthermore, PrP^C affinity for metals indicates the protein may function as an antioxidant or influence metal-ion transport (Brown *et al.*, 1999; Jeffrey *et al.*, 2012). Brown *et al.* (1997) observed that compared to wild-type mice *PRNP* knockout mice have synaptosomal fractions that are deficient in copper strongly suggesting PrP^C affects the delivery of copper to cells. Also, neurons from *PRNP* knockout mouse were more susceptible to oxidative stress and copper toxicity relative to wild-type neurons in a cell culture system. Consequently, this suggests that PrP^C affinity for Cu²⁺ ion aids in protecting cells against copper toxicity and oxidative stress (Brown *et al.*, 1999; Davies and Brown, 2008). The histidine residues within the octapeptide repeat region coordinate Cu²⁺ ions. The level of copper coordination is determined by the amount of copper that binds to PrP^C. At full copper occupancy, the unstructured N-terminal region of the prion protein becomes more structured with altered biochemical properties. Also, Cu²⁺ ions bind to the hydrophobic region of the prion protein coordinated at histidine residues His 96 and His 111 (Davies and Brown, 2008).

The function of copper in the physiopathology of prion disease is subject to controversy. Evidence exists that copper binding prevents the conversion of PrP^C to PrP^{Sc} and that copper bound PrP^C has an increased α -helical content. Also, copper prevents the development of amyloid fibrils at physiological pH. On the contrary, copper increases proteinase K resistance and induces aggregation in mature prion proteins. Furthermore, recombinant PrP bound to copper has higher

β -sheet content and compared to cellular PrP^C are more prone to aggregation (Davies and Brown, 2008; Moore *et al.*, 2009).

These conflicting observations probably result from the different PrP purification methods that influence the prion protein affinity for copper and other divalent metals. In addition, the original conformation of the prion protein affects its affinity for metals and the metal-bound PrP^C influence on protein aggregation (Moore *et al.*, 2009). Finally, there is a possibility that alternate metal ion occupancy of PrP^C is relevant in prion pathogenesis (Fontaine and Brown, 2009). For instance, brain tissues from sCJD patients showed increased levels of manganese and zinc-bound PrP^C whereas copper levels decreased relative to controls that had no detectable levels of manganese and zinc (Wong *et al.*, 2001).

1.1.3 Mechanism of PrP^{Sc} Aggregation

Misfolded protein aggregation as shown in Figure 1.3, is a feature of common neurodegenerative disorders. The mechanism of prion protein aggregation has been modelled mainly on two kinetic theories (Figure 1.4). These models are template-assisted aggregation and nucleated polymerisation mechanism. In template-assisted aggregation, PrP^{Sc} acts as template to induce the conformational conversion of PrP^C with the aid of a molecular chaperone termed protein X. Then, a heterodimer is formed between PrP^C and PrP^{Sc} that assembles into fibrils. The nucleated polymerisation mechanism involves aggregation of PrP^C monomers to form an oligomer PrP^{Sc}, which acts as a stable nucleus that integrates PrP^C monomers, till amyloid fibrils are formed (Cobb and Surewicz, 2009; Fontaine and Brown, 2009). PrP^{Sc} oligomers, consisting of 25 PrP^C monomers, are the minimal infectious unit of prion disease (Cobb and Surewicz, 2009). This implies that fragmentation of fibrils to oligomeric fractions by

molecular chaperones may contribute to disease pathology (Cobb and Surewicz, 2009; Fontaine and Brown, 2009). Several factors including divalent transition metal ions, polyanions and glycosaminoglycans can influence prion protein aggregation (Fontaine and Brown, 2009).

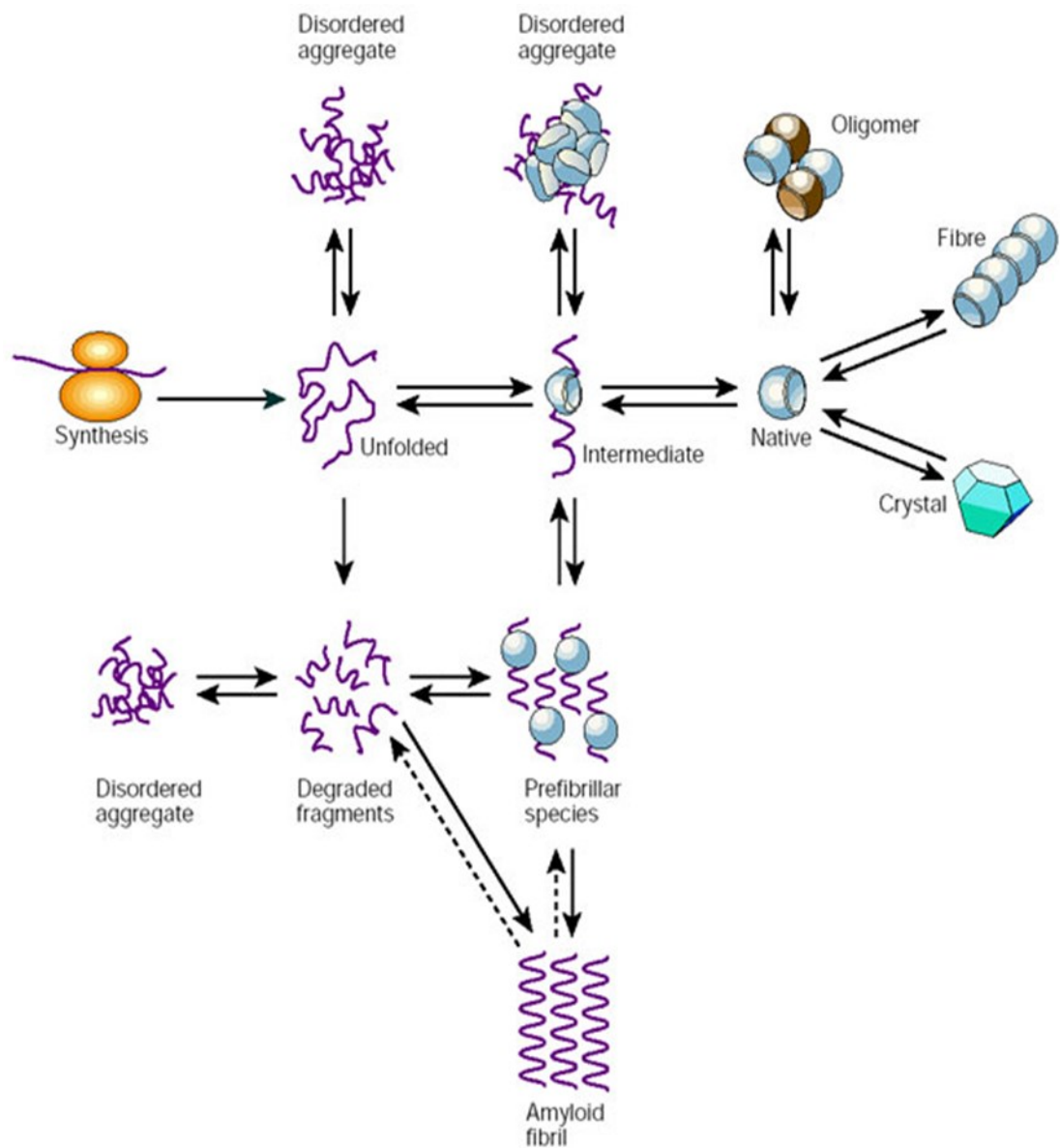
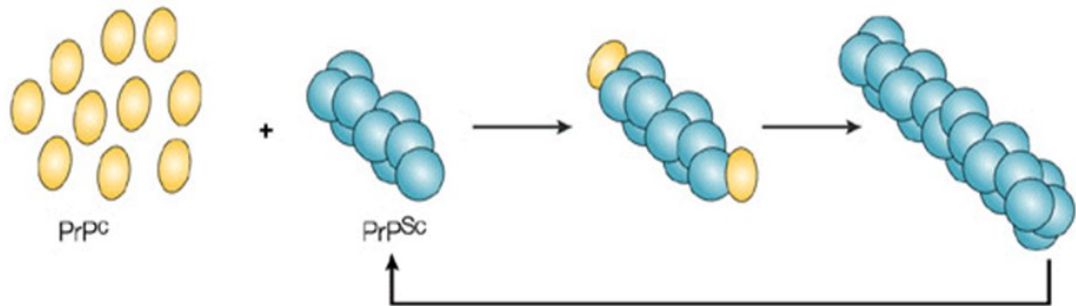


Figure 1.3: General mechanism of Protein aggregation
Reprinted with permission from Dobson (2003).

a Nucleation-polymerization model



b Template-assisted model

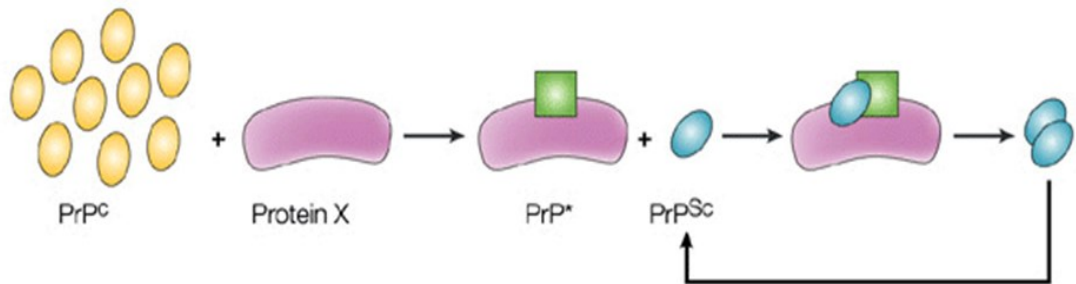


Figure 1.4: PrP^{Sc} aggregation models
Reprinted with permission from Soto (2004).

The ability of misfolded protein monomers to form insoluble aggregates is described as seeding. *In vitro*, proteins associated with other neurodegenerative diseases such as Huntington's, Alzheimer's and Parkinson's diseases display the seeding phenomenon but no evidence for infectivity. Therefore, studies of the prion phenomenon may have implications for other neurodegenerative diseases (Munch and Bertolotti, 2012). In addition, the seeding phenomenon has been demonstrated in yeast. Yeast "prion-like" protein [PSI⁺] regulated by molecular chaperone Hsp104 is cytoplasmically inherited where it modifies and induces aggregation of its newly synthesised monomeric form Sup35 (Cobb and Surewicz, 2009).

Recently, researchers observed that under *ex vivo* conditions human small heat shock protein sHspB5 regulates monomeric disaggregation of α -synuclein

amyloid fibres (pathogenic in Alzheimer's and Parkinson's diseases) by molecular chaperones Hsp40, Hsp70 and Hsp110. This indicates a potential strategy for treatment of neurodegenerative disorders (Duennwald *et al.*, 2012).

1.1.4 Prion Diseases

Prion disease was first identified as scrapie in sheep and goats in the 18th century. Other examples of prion disease in animals include Bovine Spongiform Encephalopathy (BSE) of cattle, Transmissible Mink Encephalopathy (TME) of ranch-raised mink and Chronic Wasting Disease (CWD) of deer and elk (Prusiner, 1998). Human prion diseases are classified according to etiology into sporadic, inherited or acquired. Sporadic prion diseases are generated through spontaneous conversion of PrP^C to PrP^{Sc} or somatic mutation. Also, several researchers have associated the spontaneous occurrence of prion disease with oxidative stress (Jeffrey *et al.*, 2012). Sporadic prion diseases include sporadic Creutzfeldt-Jakob disease (sCJD), which accounts for approximately 80% of human prion diseases and fatal sporadic insomnia (FSI) (Aguzzi and Calella, 2009; Piccardo *et al.*, 2012). The prevalence of sporadic CJD is estimated at 1 in 1,000,000 annually (Hu *et al.*, 2008).

Inherited prion diseases may be due to point mutations in the C-terminal domain or octapeptide repeat insertions (OPRI) in the N-terminal domain of PRNP and are inherited in an autosomal dominant pattern (Prusiner, 1998; McKintosh *et al.*, 2003). The incidence of inherited prion disease is approximately 15% of human prion diseases. Conventionally, inherited prion diseases are classified based on neuropathological features and clinical symptoms into Gerstmann-Straussler-Scheinker disease (GSS), Fatal Familial insomnia (FFI) and Familial CJD (fCJD) (Hill *et al.*, 2006). Commonly investigated mutations include E200K of fCJD,

P102L of GSS and D178N of FFI and OPRI (Hill *et al.*, 2006; Fontaine and Brown, 2009).

PrP^{Sc} cannot be degraded by proteases and conventional sterilisation methods, they are only destroyed by alkaline hydrolysis or incineration, hence its transmissible etiology (Prusiner, 1998). Peripheral pathogenesis of prion disease in humans occurs either orally or iatrogenically. Oral transmission is implicated in variant CJD by consumption of BSE contaminated beef and kuru in people who practiced ritualistic endocannibalism. Iatrogenic prion disease has been induced in patients through transmission of prion infected blood and use of cadaveric human growth hormones and dura matter grafts that contained prion pathogen (Prusiner, 1998; Goni *et al.*, 2005; Hu *et al.*, 2008).

1.1.4.1 PrP^{Sc} Strains

Prion strains are a unique feature of prion diseases that are observed when a host species inoculated with a heterologous PrP^{Sc} agent displays a unique clinical phenotype different from the infectious species. In other words, prion strains are conformational variations of PrP^{Sc} (Caughey *et al.*, 1998; Hu *et al.*, 2008). The ease at which prion strains are generated poses a public health risk in the event that perilous new prion strains similar to vCJD emerge (Morales *et al.*, 2007; Barria *et al.*, 2009). The diversity of prion strains have been attributed to the conformational flexibility of PrP^C, interspecies transmission and PrP polymorphisms (Prusiner, 1998; Morales *et al.*, 2007; Cobb and Surewicz, 2009). For instance, varying clinical phenotypes for sCJD have been observed in patients characterised by homozygosity for methionine or valine and heterozygosity at codon 129 (Prusiner, 1998; McKintosh *et al.*, 2003; Hu *et al.*, 2008; Puoti *et al.*, 2012).

The term interspecies barrier refers to the ability of prion strain to infect only selected species (Castilla *et al.*, 2008). On the other hand, interspecies barrier may be defined as the long incubation period and low transmission rate observed when PrP^{Sc} strains are transmitted to a heterologous species. This suggests that the PrP^C sequence and cellular environment of the host determines prion disease pathology (Cobb and Surewicz, 2009; Fontaine and Brown, 2009). The donor prion strain and differences in the amino acid sequence between the prion host and donor species determines interspecies barriers (Prusiner, 1998; Piccardo *et al.*, 2012). Crossing the interspecies barrier generates a new PrP^{Sc} strain and subsequent passages of the new strain in homologous host species stabilises the new prion strain conformation (Castilla *et al.*, 2008). The mouse-hamster species barrier was crossed *in vitro* (Castilla *et al.*, 2008), using a process known as protein misfolding cyclic amplification (PMCA) (Saborio *et al.*, 2001), this process was previously thought unattainable given lack of symmetry between mouse and hamster generated PrP^{Sc} fragments. The generated synthetic prion strain demonstrated infectivity in wild type animals (Castilla *et al.*, 2008).

1.1.4.2 Prion Disease Diagnosis and Treatment

Prion diseases are associated with relatively long incubation periods usually exceeding three decades and diagnosis is usually by onset of clinical symptoms (Prusiner, 1998). Prion disease strains are confirmed at autopsy by histopathological examination of brain and central nervous system (CNS) tissues. The disease strains are characterised by western blot analysis, neuropathology and immunohistochemistry (McKintosh *et al.*, 2003; Jeffrey *et al.*, 2012). Strains can be classified *in vivo* by variation in vacuolation profile, clinical symptoms and incubation period (Prusiner, 1998; Morales *et al.*, 2007; Hu *et al.*, 2008; Piccardo

et al., 2012). Biochemically, differences in prion strains are diagnosed by their glycosylation profile, exposure to denaturing solvent guanidine hydrochloride and varying electrophoretic mobilities after protease digestion (Morales *et al.*, 2007; Piccardo *et al.*, 2012; Puoti *et al.*, 2012). However, several PrP^{Sc} strains in cattle, humans and sheep are susceptible to protease digestion. Fortunately, the specificity of immunohistochemistry identifies the differences between protease resistant PrP^{Sc} plaques and protease sensitive PrP^{Sc} plaques (McKintosh *et al.*, 2003, Jeffrey *et al.*, 2012). The presence of prion proteins in the lymphoid tissues is also detected by immunohistochemistry (McKintosh *et al.*, 2003).

In brain tissues, immunohistochemical staining depends on the accumulation of PrP^{Sc} plaques in the brain (Jeffrey *et al.*, 2012). However, prion diseases are not always associated with accumulation of PrP^{Sc} plaques indicating that immunolabelling may be insufficient for diagnosis (Jeffrey *et al.*, 2012). Currently, prion disease strain can be identified efficiently in patients who have undergone cerebrospinal fluid (CSF) analysis, electroencephalography (EEG), brain biopsy and magnetic resonance imaging (MRI). Also, gene sequencing can identify inherited forms of prion disease and eliminate several strains (Puoti *et al.*, 2012). There is a need for diagnostic techniques for easy detection of PrP^{Sc} in bodily fluids as this will allow pharmacological intervention before onset of clinical symptoms (Hu *et al.*, 2008). The diverse prion strains hinder the development of a simplified diagnostic procedure because it is almost impossible to exploit PrP^{Sc} biophysical characteristics as an *in vitro* marker of infectivity (Baskakov and Breydo, 2007).

No successful therapies for human prion disease exist. However, immune modulation may prevent prion infectivity and delay clinical onset of disease (Goni *et al.*, 2005; Hu *et al.*, 2008; Puoti *et al.*, 2012).

1.1.5 Glycosylation profile of PrP

Post-translational modifications may alter PrP^C conformation making it amenable for conversion to PrP^{Sc} (Prusiner, 1998). PrP^{Sc} strains have varied affinities for different PrP^C glycoforms (Rudd *et al.*, 2002). Therefore, glycosylation modulates PrP^{Sc} stability and its incubation period prior to disease onset (Prusiner, 1998). The distribution of the diverse glycoforms in a prion strain can be characterised using SDS-PAGE analysis (Cobb and Surewicz, 2009). However, the diagnostic value of this is limited as prion strains may have similar glycoform ratios (Rudd *et al.*, 2002). For instance, in inherited prion disease, point mutations P102L, D178N and E200K have similar glycosylation patterns (Hill *et al.*, 2006). The glycosylation pattern of infectious PrP^{Sc} strain is maintained by the host cells (Rudd *et al.*, 2002). Consequently, the glycosylation pattern of a PrP^{Sc} strain may help explain its neurological phenotype (McKintosh *et al.*, 2003). For instance, similarities between diglycosylation patterns of vCJD and BSE contributed to the theory that vCJD is the human variant of BSE (Yin *et al.*, 2003). Glycosylation patterns may also affect the stability of amino acid residues involved in prion homodimer formation. This implies that understanding glycosylation patterns may aid in elucidating PrP^{Sc}-PrP^C heterodimer structure (Rudd *et al.*, 2002). Hence, analysis of the biochemical and biophysical properties of PrP^{Sc} glycoforms would require substantial quantities of PrP^C glycoforms (Rudd *et al.*, 2002). This indicates that recombinant expression systems capable of glycosylation are essential for the production of PrP^C.

In mammals, transgenic mice and hamsters expressing recombinant PrP^C are the main models for investigating prion phenomenon. However, difficulties associated with purification of recombinant PrP^C from brain tissues resulted in low yields (Yin *et al.*, 2003; Vrentas *et al.*, 2012). Alternatively, sufficient amounts of recombinant PrP^C can be produced in an *Escherichia coli* bacterial expression system (Yin *et al.*, 2003; Pavlicek *et al.*, 2007). But, prion proteins produced in bacteria tend to form inclusion bodies and subsequent purification of inclusion bodies may modify the protein, altering its native conformation (Corsaro *et al.*, 2002; Abskharon *et al.*, 2012). Also, bacterially expressed recombinant PrP^C are unglycosylated. Glycosylation has no effect on PrP^{Sc} infectivity, although it modifies the infection process, hence there is a possibility glycosylation affects PrP^{Sc} conformation (Pavlicek *et al.*, 2007; Tuzi *et al.*, 2008). Therefore, biochemical and structural studies using recombinant PrP from bacteria, may not fully resolve the molecular mechanisms of prion diseases. This dilemma could be possibly circumvented by using transgenic plants as a novel source of recombinant PrP since plant expression systems offers the advantage of producing the different PrP glycoforms.

1.2 Transgenic Plants

Plants are established production system for recombinant protein. Molecular farming is the use of transgenic plants to produce commercially significant biopharmaceuticals such as vaccines, enzymes, therapeutic antibodies and growth hormones (Daniell *et al.*, 2001; Goldstein and Thomas, 2004; Twyman *et al.*, 2005). Examples of important biopharmaceuticals produced in transgenic plants is shown in table 1.1. The use of transgenic plants as an expression system offers advantages in terms of inexpensive production costs, low risk of

contamination with microbial toxins and mammalian pathogens, specialised organs for storing the recombinant protein, scalability, and potential for post-translational modification (Ma *et al.*, 2003; Twyman *et al.*, 2005). Recombinant protein yield in plants is determined by several factors including choice of host plant, design of transgene construct and transformation method.

Table 1.1 Important biopharmaceuticals produced in transgenic plant systems

Recombinant protein	Host plant	Vector/ Transformation technique	Expression level	Notes
Alkaline phosphatase	Tobacco	pBinAR/AMT	3% tsp	Used to treat ovarian and testicular cancer
Aprotinin	Maize	PB	6% tsp	Used as trypsin inhibitor during transplant surgery and for treatment of pancreatitis
Avidin	Maize	PB	3% tsp	Used in biochemical assays. First commercially produced plant biopharmaceutical Commercially produced by ProdiGene
Cholera toxin B subunit	Potato	pPCV701/AMT	0.3% tsp	First chloroplast expressed vaccine
	Tomato	pCAMBIA2301/AMT	0.04% tsp	The recombinant vaccine was immunogenic and protective in mice when delivered orally
	Tobacco	pLDCTV2/PB	4.1% tsp	
Collagen	Tobacco	pBINPLUS/AMT	2% tsp	Used to repair damaged tissue First successful expression of a correctly modified human structural protein polymer Commercially produced as Vergenix by Collplant
Erythropoietin	Tobacco cells	pCAM35/ protoplast electroporation	1 pg/g wet cell	Used to treat anaemia Initial human protein expressed in tobacco suspension cells

Glucocerebrosidase	Carrot cells	pGREENII/AMT		Used to treat Gaucher's disease Commercially produced by Protalix Bio-Therapeutics
	Tobacco	pBI101/AMT		
Herpes simplex virus antibody	Soybean			First expression of a biopharmaceutical in soybean
Hepatitis B surface antigen	Banana	pBI121/AMT	0.7µg/g FW	Immunogenic in human and mice when orally administered Commercially produced by Arizona University
	Potato	pBI121/AMT	97.1 ng/g	
	Tobacco	pBI121/AMT	FW 66 ng/mg tsp	
α-Interferon	Rice	pG121Hm/AMT		First biopharmaceutical produced in rice Used to treat Hepatitis Commercially produced by Biolex
	Carrot cells Tobacco	pCBV16/ Vacuum infiltration PB	3 mg/g FW	
Lactoferrin	Rice	pAPI141/PB	20% tsp	Antimicrobial Commercially produced by Ventria Bioscience
	Tobacco	pCGN1578/AMT	4.3% tsp	
	Sweet Potato	pGA748/PB	3.2 µg/mg tsp	
Rabies Virus Glycoprotein	Tomato	RG-2/AMT	10ng/mg tsp	Rabies vaccine, immunogenic in mice when orally administered. First edible vaccine biopharmaceutical
	Tobacco	Pbi101/AMT	0.38% tsp	
Zmapp (C13C6, C2G4 & C4G7 Ebola antibodies)	Tobacco	BeYDV/ Agroinfiltration	50 µg/g FW	Used to treat Ebola Commercially produced by Mapp Bio
Serum Ablumin	Tobacco	pLD/PB	11% tsp	Used to treat burns and liver cirrhosis First full size biopharmaceutical expressed in plants.
	Potato	pTUB3/AMT	0.2% tsp	
Somatotropin	Tobacco	pPRV112B, pPRV111B/PB	7% tsp - chloroplast	Used to treat pituitary dwarfism First human biopharmaceutical expressed in plants and chloroplast

AMT – Agrobacterium mediated transformation; PB – Particle Bombardment

(Adapted from Daniell *et al.*, 2001; Ma *et al.*, 2003; Twyman *et al.*, 2005; Moustafa *et al.*, 2016)

1.2.1 Choice of Plant

Recombinant proteins have been produced in a variety of plant species.

Transgenic plants are generally classified as leafy crops, fruits & vegetables, oil

& fibre crops and cereal & legume seed. Leafy crops such as *Arabidopsis thaliana*

and *Medicago sativa*, offers high biomass yield but must be processed or frozen at maturity to prevent protein degradation (Twyman *et al.*, 2003; Fischer *et al.*, 2004). Accumulation of recombinant protein in seeds, for instance, soybean and maize, supports long-term storage of recombinant protein, however, potential problems of gene transfer through pollen needs to be addressed (Schillberg *et al.*, 2005; Obembe *et al.*, 2011). Fruits & vegetables, for example tomatoes and potatoes, are desirable for the production of edible vaccines and topically applied antibodies due to minimal downstream processing requirements (Twyman *et al.*, 2005). Recombinant proteins have been targeted to the oil bodies of safflower and rapeseed plants, using the oleosin-fusion technology, to simplify the purification process (Giddings *et al.*, 2000; Ma *et al.*, 2003). Fibre crops such as cotton, offer alternative by-products, which may help offset recombinant protein production costs (Twyman *et al.*, 2003).

In this study designed to produce recombinant mouse prion protein (mPrP) in a plant expression system, tobacco was chosen as the host plant. Tobacco is a model laboratory plant with abundant literature on transgene expression. Extensive research on transgenic tobacco has resulted in established protocols for gene transfer and gene expression. Also, tobacco is environmentally safe because it is a non-food/feed crop and can be produced under greenhouse conditions. Finally, tobacco plants are easily regenerated using micropropagation, have a biomass yield of 100,000kg per hectare and have established prime, large-scale downstream processing facilities. However, tobacco leaves must be processed immediately after harvest to avoid loss of the recombinant protein and also the presence alkaloids in tobacco may interfere with downstream processing (Twyman, 2006).

1.2.2 Transgene Design

Efficient transgene design affects the yield of recombinant proteins. The use of regulatory elements, codon optimisation, and signal sequence for subcellular localisation in the transgene construct mostly improves recombinant protein yield. Transcriptionally gene expression can be controlled by use of suitable promoters. Promoters are important cis-regulatory elements that modulate the rate of transgene expression. They are classified according to their mode of operation into constitutive, tissue-specific, inducible and synthetic promoters (Sharma and Sharma, 2009; Hernandez-Garcia and Finer, 2014). Constitutive promoters drive transgene expression in all plant tissues and at all developmental stages of the plant. Conventional constitutive promoters include CaMV 35S promoter isolated from cauliflower mosaic virus for dicotyledonous plants (Odell *et al.*, 1985) and maize ubiquitin promoter for monocotyledonous plants (Christensen and Quail, 1996). However, the overexpression of certain transgenes may be toxic to the plant, thus the need for regulated promoters.

Tissue-specific promoters restrict transgene expression to certain tissues, organs or developmental stages of the plant (Sharma and Sharma, 2009). Seed-specific promoters are the most common tissue specific promoters and limit transgene expression to seeds. For example, rice globulin 1 promoter was used to express human lysozyme in maize endosperm (Yang *et al.*, 2003). Inducible promoters regulate transgene expression by responding to external stimuli. This stimulus may be chemical, physical or endogenous. Notable inducible promoters include the tetracycline inducible promoter, the most studied chemically inducible plant promoter system, and the wheat wcs120 promoter, a cold inducible promoter that has been tested in wheat, barley and alfalfa (Corrado and Karali, 2009).

The limitations of natural promoters in transcription efficiency, induction conditions and size has led to a demand for synthetic promoters in plant transgenic technology. Synthetic promoters are enhanced natural promoters with tetrameric repeats of regulatory elements to improve strength and/or specificity of the promoter (Hernandez-Garcia and Finer, 2014). Synthetic promoters, such as the MAC promoter derived by combining the MAS element of *Agrobacterium* and the CaMV35S promoter, by comparative analysis are more effective than natural promoters at improving transgene expression (Hernandez-Garcia and Finer, 2014).

Translational efficiency of the transgene can be improved by modifying codon usage and addition of intronic elements. Codon optimisation involves using codon usage tables to alter the coding sequence of the transgene to closely match preferred genes of the host species (Koziel *et al.*, 1996; Kusnadi, 1997). The entire sequence of the transgene may be altered or only codons below a certain threshold in the host species are changed. The results are usually unpredictable, ranging from enhanced expression to no effect. Researchers usually test multiple optimised gene designs to determine the best construct for stable and enhanced expression. Also, codons may be optimised to increase GC content, remove RNA motifs associated with poor expression and alter sequences targeted by endogenous small RNAs involved in silencing (Rouwendal *et al.*, 1997; Lessard *et al.*, 2002). Plant viral mRNAs are effective enhancers of translation. 5' and 3' untranslated regions (UTR) are highly structured intronic regions in viruses that are essential for replication and translation (Gallie and Walbot, 1990; Gallie, 2002). The 5' viral UTR contains signal for effective initiation of translation and contends efficiently with plant cellular mRNA for free ribosomes. In transgenic

tobacco plants, fusing the tobacco mosaic virus (TMV) 5' UTR to the start codon increased transgene expression levels (Gallie, 2002) while the 3'UTR contributes to the stability and translational efficiency of the mRNA (Gallie and Walbot, 1990).

The subcellular compartment, in which a heterologous protein accumulates, affects the associated processes of folding, assembly and post-translational modification, therefore, its yield (Schillberg *et al.*, 2003; Twyman *et al.*, 2003). Recombinant proteins without a signal sequence accumulate in the cytosol where they are usually quickly degraded by proteases. Also, proteins retained in the cytosol lack post-translational modification. Therefore, recombinant proteins can be targeted to the secretory pathway by adding an N-terminal signal sequence to the transgene construct. The protein is then secreted to the apoplast where they are retained (Conrad and Fiedler, 1998). Accumulation levels of recombinant protein can also be increased 2 to 10-fold by retaining them in the lumen of the endoplasmic reticulum (ER) using the H/KDEL C-terminal tetrapeptide tag (Conrad and Fiedler, 1998). The ER is an oxidising environment, lacks proteases and contains molecular chaperones, essential factors for correct protein folding and assembly. Also, recombinant proteins retained in the ER are not altered by the Golgi apparatus, hence they have high mannose glycans but no plant-associated xylose and fucose residues (Conrad and Fiedler, 1998).

1.2.3 DNA delivery systems

Heterologous genes are introduced into plant systems by established methods of co-cultivation with *Agrobacterium tumefaciens* (Holsters *et al.*, 1978) and/or biolistics. *Agrobacterium*-mediated transformation is based on the ability of the bacteria to stably integrate a section of DNA within its tumour inducing (Ti) Plasmid into the nuclear genome of plants (Darbani *et al.*, 2008). It is the most

efficient transformation method because it is associated with transfer of large DNA fragments, stable transgene integration into host genome, low transgene copy number, reduced transgene silencing and stable transgene expression in subsequent generations of transgenic plants (Hansen and Wright, 1999; Desai *et al.*, 2010). However, *Agrobacterium* transformation is suited mainly to dicotyledonous plants although use of super virulent vectors enhances expression in monocotyledonous crops (Birch, 1997; Hansen and Wright, 1999). The transformation efficiency of *Agrobacterium* can be improved by sonication of explants as this allows the *Agrobacterium* to access more plant cells (Trick and Finer, 1997).

Biolistics involves microprojectile bombardment of target plant tissues with transgene-coated gold or tungsten particles. Methodological advantages include introduction of several transgenes at once into plant tissues and elimination of explant necrosis sometimes associated with *Agrobacterium*-mediated transformation (Birch, 1997; Darbani *et al.*, 2008). However, integration of long DNA fragments can be problematic as the DNA is not protected from damage in cells and multiple copies of transgene integrate at the same site leading to gene silencing (Birch, 1997; Hansen and Wright, 1999; Darbani *et al.*, 2008). A later development agrolistics, which involves co-bombardment of the transgene along with the virulence genes of *Agrobacterium*, has improved the efficiency of transgene integration using biolistics (Darbani *et al.*, 2008).

1.2.4 Glycosylation

Protein glycosylation is an important post-translational modification for the correct function of many proteins in eukaryotes. Glycosylation significantly influences the physicochemical properties of proteins such as solubility and protection from

thermal and proteolytic degradation. It also modulates the biological properties of a protein including specific activity, ligand receptor interactions and immunogenicity (Gomord and Faye, 2004). Recombinant glycoproteins are usually associated with N-glycans or O-glycans. Both glycans differ in their sugar composition, biosynthesis and association with amino acid residues (Gomord *et al.*, 2005; Faye *et al.*, 2005). Although, the glycosylation capacity of plants makes them an attractive expression system their glycosylation patterns are structurally different from mammals (Gomord *et al.*, 2005; Sethuraman and Stadheim, 2006). The possible immunogenicity of plant specific glycans may limit the use of plant-made biopharmaceuticals for therapeutic purposes (Ma *et al.*, 2003; Gomord *et al.*, 2005; Faye *et al.*, 2005).

N-glycans are linked to the amide group of asparagine residues. Plants and mammals have similar N- type glycans in the endoplasmic reticulum (Lerouge *et al.*, 2000). However, further processing in the Golgi apparatus leads to dissimilar complex type N-glycans in plants and mammals. Plants have $\alpha(1, 3)$ -fucose and $\beta(1, 2)$ – xylose residues while mammals have $\alpha(1, 6)$ -fucose residues and $\beta(1, 4)$ -galactose residues (Gomord and Faye, 2004). Several strategies to humanise plant N-glycans for the production of non-immunogenic recombinant proteins are being examined. This includes processes to inactivate plant glycostransferases, *de novo* expression of heterologous glycosyltransferases similar to those in mammals, RNA interference to reduce fucosyl and xylosyl glycans levels and retention of the recombinant protein in the endoplasmic reticulum (Ma *et al.*, 2003; Lerouge *et al.*, 2000; Sethuraman and Stadheim, 2006). For example, Zmapp an antibody cocktail for treatment of Ebola, is produced in *Nicotiana benthamiana* plants engineered to produce humanised glycans (Olinger *et al.*, 2012)

O-glycosylation occurs in both intracellular and extracellular proteins. O-glycans are linked to the hydroxyl groups of serine or threonine residues in mammals and hydroxylproline residues in plants. Mammals have a preference for mucin type O-glycans while plants have a preference for hydroxylproline rich O-glycans of extensins and arabinogalactan proteins (AGP) (Gomord *et al.*, 2010). Despite the problem of immunogenicity, the presence of plant-specific O-glycans can improve protein stability and resistance to proteolysis. For example, AGP O-linked glycomodule in chimeric human interferon $\alpha 2b$ (IFN $\alpha 2$) improved protein stability and increased recombinant protein yield up to 1400-fold (Xu *et al.*, 2007).

1.2.5 Downstream Processing

The downstream processing requirements for any heterologous protein depends on the proposed use of the recombinant protein. For instance, edible vaccines require no downstream processing while a recombinant protein required for pharmaceutical or diagnostic purposes requires a high purification threshold (Menkhaus *et al.*, 2004). Downstream processing is the most expensive aspect of recombinant protein production in transgenic plants (Nikolov and Woodard, 2004). Insufficient data on recombinant protein purification is probably because of suboptimal expression levels and substandard purification processes (Nikolov and Woodard, 2004). Therefore research to identify easily scalable, efficient and economical purification is important to reduce the significant downstream processing costs associated with plant based systems (Nikolov and Woodard, 2004; Menkhaus *et al.*, 2004). There are several ways to design transgenic plants to reduce processing costs. For example, targeting the recombinant protein to tissues such as maize seed, which are easily separated from other plant tissues, reduces purification burden (Kusnadi *et al.*, 1997).

The efficiency of recombinant protein purification from plants is influenced by the host system, purification requirements and the concentration of the recombinant protein (Wilken *et al.*, 2012). The recombinant protein is released from seed-based and leaf-based production systems by homogenisation of the biomass followed by buffer extraction and centrifugation to clarify the extracts. Detergents are a necessary buffer additive for extraction of membrane-associated proteins (Kusnadi *et al.*, 1997; Wilken *et al.*, 2012). Protease inhibitors and antioxidants are usually added to extraction buffers to prevent structural modification of the recombinant protein due to proteolytic activity and interaction with phenolic compounds (Kusnadi *et al.*, 1997). Prior to purification, plant extracts are pre-treated to remove most of the host plant proteins and contaminants. Pre-treatment strategies include pH adjustment, aqueous two-phase extraction and precipitation followed by another clarification step (Wilken *et al.*, 2012). Most purification strategies usually involves chromatography. Affinity chromatography based on a Protein A or G ligand is used for purifying antibodies while histidine-tagged proteins are purified using immobilised-metal affinity chromatography (IMAC) (Wilken *et al.*, 2012). For example, fusing a 6X His-tag to lactate dehydrogenase improved protein purification and increased the yield and purity of the recombinant protein (Mejare *et al.*, 1998). However chromatographic purification is not commercially scalable because of resin fouling (Menkhaus *et al.*, 2004).

1.3 Research Aims

This research aims to investigate the possibility that recombinant mPrP produced in transgenic tobacco plants, may better reflect the properties of the prion protein in experimental studies. By directing heterologously expressed mPrP to the ER,

post-translational glycosylation will produce a recombinant protein more representative of mammalian protein than that expressed in *E.Coli*.

The research objectives include

- Design of transgene constructs
- Characterisation of transgenic tobacco plants expressing recombinant mPrP
- Phenotypic analysis of transgenic tobacco leaves expressing recombinant mPrP
- Purification of recombinant mPrP from transgenic tobacco leaves

2 Materials and Method

2.1 Introduction

This chapter details the experimental procedures used in this study. Except where stated, all protocols were carried out according to manufacturer's guidelines. Antibiotics were obtained from Melford Laboratories Ltd and the various growth media reagents from Sigma-Aldrich. GraphPad prism 7 software was used for data analysis.

2.2 Design of transgene construct

2.2.1 Bacterial strains

Escherichia coli strain DH5 α [*fhuA2* Δ (*argF-lacZ*) *U169 phoA glnV44 Φ 80 Δ (*lacZ*) M15 gyrA96 recA1 relA1 endA1 thi-1 hsdR17*] (Hanahan, 1985) was procured from New England Biolabs and used for all molecular cloning procedures.

Agrobacterium tumefaciens strain AGL1 [*AGL0recA::blapTiBo542deltaT Mop+ CbR*] (Lazo *et al.*, 1991) used for all plant transformation procedures was provided by David Bringloe's Laboratory at University of East London.

2.2.2 Plant growth conditions

Nicotiana tabacum L. cultivar Samsun was provided by David Bringloe's Laboratory at the University of East London. The plants were grown under aseptic conditions in Phytatray(s) II (Sigma-Aldrich) placed in an incubator (LMS 600 Series 4 Cooled Incubator) at 25°C under a 16:8 light: dark photoperiod.

2.2.3 Transgene design

The mouse *PRNP* gene was codon-optimised for expression in the nuclear genome of tobacco plants using GENEius software (Eurofin Genomics). Three

synthetic constructs were designed to direct gene expression to various subcellular locations. Subsequently, the synthetic constructs were synthesised by Eurofins MWG Operon and delivered inserted into the *NotI* site of the pEX-A vector.

2.2.4 Plasmids

2.2.4.1 35S-CaMV

The 35S CaMV cassette (Figure 2.1) contains a promoter and terminator region, *cis*-acting factors, essential for constitutive expression of a foreign gene in transgenic plants (Hellens *et al.*, 2000). It also features a multiple cloning site (MCS) for insertion of the transgene between the promoter and terminator region. The vector backbone pJIT60 has an ampicillin resistance gene for selection of transformants in *E. coli*.

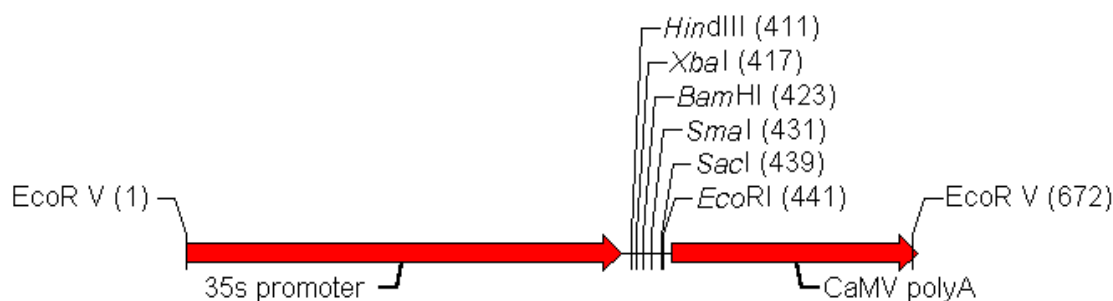


Figure 2.1: 35S-CaMV cassette
Reproduced from www.pgreen.ac.uk

2.2.4.2 pGreen

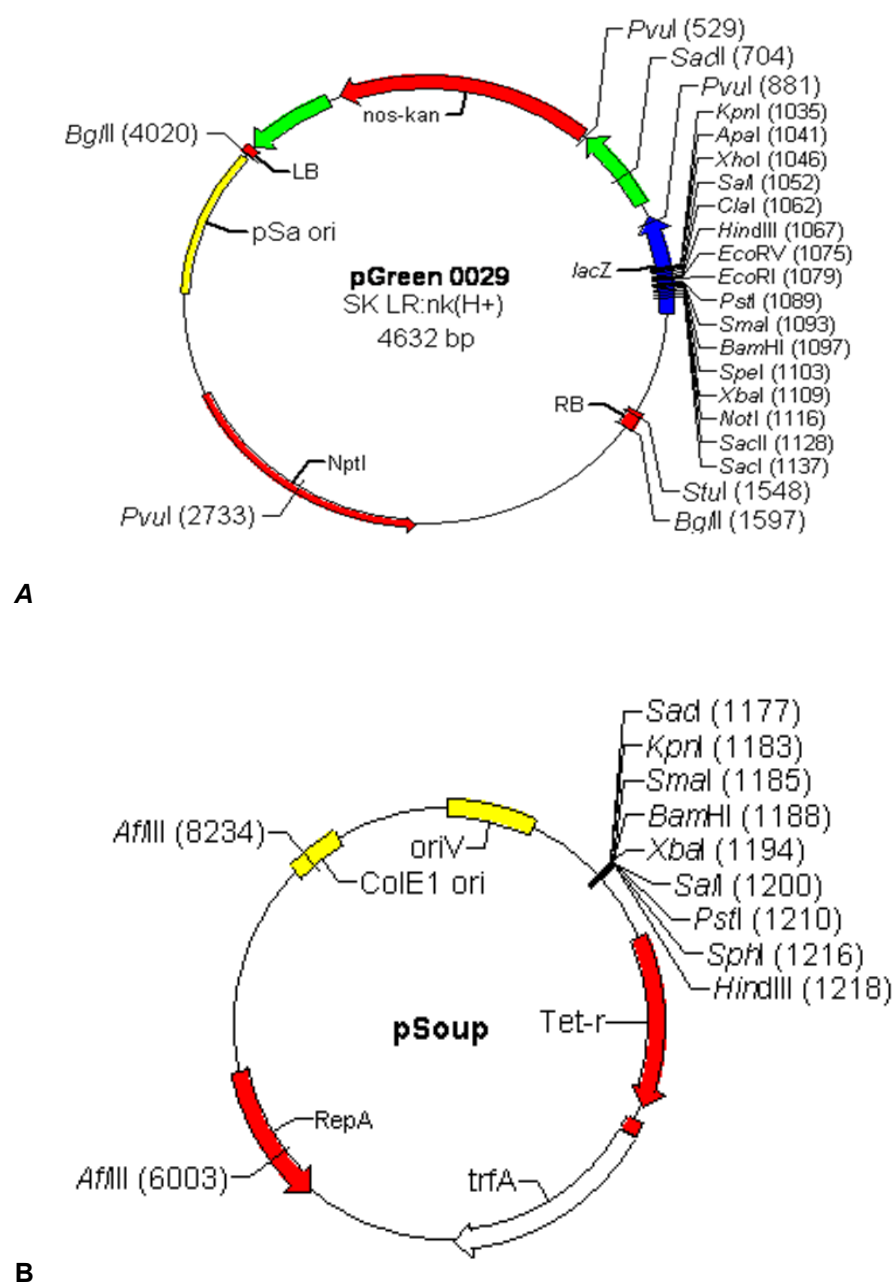


Figure 2.2: pGreen Binary Vectors

A: pGreen plasmid map. B: pSoup plasmid map.

Reproduced from www.pgreen.ac.uk

The plasmids pGreen0029 and pSoup (Figure 2.2) are binary vectors created for *Agrobacterium*-mediated plant transformation. The pGreen vector features a pSa-ori (origin of replication) gene, kanamycin resistance *NptI* gene and a pBluscript based MCS. The pSoup construct contains a pSa-RepA gene for *in trans* replication of pGreen0029 in *Agrobacterium* (Hellens *et al.*, 2000).

2.2.5 Expression cassette construction

2.2.5.1 Restriction digestion

Recombinant plasmids were digested with the appropriate FastDigest restriction enzymes (Thermo Fisher Scientific) in 20 µl reaction volume. For subcloning reactions, restriction digests were carried out 100 µl reaction volume for 1 hour. Afterwards, digested samples were analysed using agarose gel electrophoresis.

2.2.5.2 Agarose gel electrophoresis

Agarose gels (1-2%) were prepared for analysis of DNA samples in 1X TAE buffer (1 Litre: 40 mM Tris (pH 7.6), 20 mM Acetic acid and 1 mM EDTA). To visualise DNA fragments, SYBR Safe stain (Invitrogen) was added to molten agarose while DNA gel loading dye (Thermo Fisher Scientific) was added to DNA samples in a 1:5 ratio before electrophoretic analysis. The gels were submerged in HU6 mini electrophoresis tanks containing 1X TAE buffer and 20 µl or 50 µl samples were electrophoresed at 75 volts for ~ 45 minutes. Results were then visualised on an ultraviolet transilluminator (ChemiDoc MP Imager, Bio-Rad).

2.2.5.3 DNA recovery

DNA fragments required for subcloning reactions were excised from electrophoresed gels. The DNA fragments were visualised with UV light on a

ChemiDoc MP imager (Bio-Rad) and excised with a scalpel. Subsequently, the DNA fragments were extracted from the gel slices using QIAquick Gel Extraction Kit (Qiagen).

2.2.5.4 Subcloning procedure

Subcloning procedure was as described by Sambrook *et al.* (1989). Purified DNA fragments excised from the recombinant vectors pEX-A-mPrP or pJIT-mPrP were ligated into restriction enzyme sites of linearised pJIT or pGreen plasmid respectively using Lyo-Ligase (Bioline). Linearised plasmids were dephosphorylated with Antarctic Phosphatase (New England Biolabs) to prevent religation of the plasmid since a single restriction enzyme was used for all pGreen subcloning procedures. The dephosphorylated pGreen vector was purified with the MinElute Reaction Cleanup Kit (Qiagen) before the ligation process. Ligation reactions were incubated overnight at 16°C, then purified with the MinElute Reaction Cleanup Kit (Qiagen) before *E. coli* transformation.

2.2.5.5 E. coli transformation

Purified recombinant plasmids (5ng) were added to 50 µl ice-cold electrocompetent DH5α cells (New England Biolabs) and mixed. The mixture was transferred to a 1 mm electroporation cuvette (Bio-Rad) and electroporated using the MicroPulser Electroporator (Bio-Rad). Luria-Bertani (LB) broth (1 Litre: 10 g tryptone, 10 g NaCl and 5 g yeast extract) was added in 0.95 ml aliquots to the electroporated cells and gently mixed. The mixture was incubated at 37°C for 1 hour in an Eppendorf thermomixer at 100 rpm to induce expression of the plasmid's antibiotic-resistance gene. Subsequently, the transformed cells were pelleted by centrifugation at 13,000 rpm for 1 minute and resuspended in 200 µl

LB broth. 50 µl of the suspension was spread on LB plates (1 Litre: LB broth and 15 g agar) supplemented with either kanamycin (100 µg/ml) or ampicillin (100 µg/ml) depending on the selective marker expressed by the plasmid. The LB plates were then incubated at 37°C overnight.

2.2.5.6 Plasmid DNA isolation

Recombinant pJIT-mPrP and pGreen-35S-mPrP plasmids were isolated from transformed *E. coli*. DH5α colonies using a QIAprep Spin Miniprep Kit (Qiagen). Afterwards, the integrity of the recombinant plasmids was confirmed by restriction enzyme analysis as described (Sections 2.2.5.1 and 2.2.5.2)

2.2.6 Transformation of tobacco leaves

2.2.6.1 Preparation of electrocompetent cells

Electrocompetent *Agrobacterium* AGL1 cells were prepared as described by Lin (1995) and Den Dulk-Ras & Hooykaas (1995). A 200 µl aliquot of log phase AGL1 stock was added to 100 ml of YEP broth (1 Litre: 10 g peptone, 10 g yeast extract and 5 g NaCl) containing rifampicin (100 µg/ml) and incubated at 28°C overnight in an orbital shaker at 300 rpm. Subsequently, cells were pelleted by centrifugation at 5,000 rpm for 10 minutes and washed 3 times in 20 ml of sterile ice cold glycerol and finally resuspended in 2 ml of sterile, ice-cold 1 M sorbitol. Electrocompetent AGL1 cells were stored in 100 µl aliquots in Eppendorf tubes at -80°C.

2.2.6.2 *Agrobacterium* transformation

Aliquots containing 2.5 µg of recombinant pGreen-35S-mPrP plasmid and 2 µg of the pSoup plasmid was added to 50 µl of electrocompetent AGL1 cells and

mixed. The mixture was transferred to a 2 mm electroporation cuvette and electroporated with the MicroPulser Electroporator (Bio-Rad). Aliquots of 0.95 ml YEP broth was added to the electroporated cells and the mixture incubated at 28°C for 4 hours in an Eppendorf thermomixer at 100 rpm to induce expression of the plasmid's antibiotic-resistance gene. Subsequently, the transformed cells were pelleted by centrifugation at 13,000 rpm for 1 minute and resuspended in 200 µl YEP broth. Aliquots of 50 µl of the suspension was spread on kanamycin (100 µg/ml) YEP plates (1 Litre: YEP broth and 15 g Agar). The YEP plates were incubated at 28°C for three days. Transformed AGL1 colonies were identified by antibiotic resistance and plasmids isolated and characterised by restriction enzyme analysis (Sections 2.2.5.1, 2.2.5.2 and 2.2.5.6).

2.2.6.3 Tobacco leaves transformation

Leaf disks were excised from axenic tobacco plants using a sterilised Eppendorf Snap Cap (Fisher Scientific). The leaf disks (explants) were transformed as described by Horsch *et al.* (1989). Transformed AGL1 cells were grown in 10 ml of YEP broth containing kanamycin (100 µg/ml) in an orbital shaker at 250 rpm till log phase. The cells were centrifuged at 5,000 rpm for 10 minutes and the pellets washed twice with 10 ml ice cold MS broth (1 Litre: 4.4 g Murashige and Skoog basal medium and 30 g sucrose) (Murashige and Skoog, 1962). Subsequently, the cells were resuspended in MS broth at an optical density (OD₆₀₀) of 0.4.

Sterile leaf disks were immersed in 25 ml *Agrobacterium* suspension in a petri dish. After 30 minutes, the explants were blotted on sterile filter paper and transferred to MS plates (1 Litre: MS broth and 8.8 g Plant agar). The plates were sealed and kept in the dark for three day for callus induction. The explants were

transferred to MS plates containing plant growth hormones (1 Litre: 2 mg BAP and 0.2 mg NAA) and antibiotics, kanamycin (100 µg/ml), cefotaxime (500 µg/ml), carbenicillin (500 µg/ml), and incubated at 25°C on a 16 hour photoperiod. A 10-fold difference in cytokinin to auxin ratio is required for maximum callus formation (Ali *et al.*, 2007; Barendse *et al.*, 1987). Shoot regeneration occurred after about 6 weeks. The shoots were excised and transferred to Phytatray(s) II containing MS media and kanamycin (100 µg/ml) for root induction and selection of transgenic plants.

2.3 Characterisation of recombinant mPrP in transgenic tobacco leaves

2.3.1 DNA analysis

2.3.1.1 Polymerase chain reaction (PCR)

Healthy and fully extended transgenic plant leaves (100 mg) frozen in liquid nitrogen was homogenised in an Eppendorf tube with a micropestle. Genomic DNA was isolated from the leaves of transgenic tobacco plants using a DNeasy Plant mini kit (Qiagen). PCR amplification of 100 ng of genomic DNA was performed with the iProof high-fidelity Master Mix kit (Bio-Rad) using 0.2 µM of each mPrP primer (Table 2.1) specific for the synthetic transgene. The reaction was carried out on the T100 Thermal Cycler (Qiagen) under the following conditions: Initial denaturation for three minutes at 98°C, 30 cycles with the temperature sequence (98°C for 10 seconds, 58°C for 20 seconds and 72°C for 15 seconds) and final elongation at 72°C for 5 minutes. Afterwards, PCR products were analysed by electrophoresis on 2% agarose gels.

2.3.2 RNA analysis

2.3.2.1 Reverse transcription (RT)-PCR

Total RNA was extracted from homogenised transgenic tobacco leaves with the RNeasy Plant mini kit (Qiagen). To remove DNA contamination, the RNA was treated with RNase-free DNase (Qiagen) during the isolation procedure then the purity of the RNA was determined using the Nanodrop ND-1000 spectrophotometer (Thermo Fisher Scientific). RT-PCR reactions were performed in two steps. Firstly, cDNA was synthesised from 0.5 µg of isolated RNA, using the iScript reverse transcription Supermix (Bio-Rad). Secondly, cDNA was subjected to PCR using the conditions described in section 2.3.1.1.

2.3.2.2 Real time RT-PCR

RNA expression levels were quantified using real time PCR as described by Pfaffl (2001). After cDNA synthesis, real-time amplification of the samples was performed using the SsoAdvanced Universal SYBR Green Supermix kit (Bio-Rad). The Elongation factor 1 α gene (*EF1 α*) was used as an internal reference gene (Schmidt and Delaney, 2010). cDNA (50 ng) and either the PrP or EF1 primers (0.25 µM each) (Table 2.1) were added the reaction mix. The reaction was carried out in replicates on the Stratagene Mx3000P QPCR System (Agilent Technologies) under the following conditions: Initial denaturation for two minutes at 98°C, 40 cycles with the temperature sequence (Denaturation: 95°C for 10 seconds; Annealing/Extension: 60°C for 30 seconds). At the end of the reaction a melt curve analysis was carried out to ensure the efficiency of the primers.

To create a standard curve to determine efficiency of the reaction, serial dilutions of PCR amplified cDNA products of both the PrP and the EF1 primers were

analysed by real time PCR. Quantitative RT-PCR calculations are shown in Appendix F.

Table 2.1: Primer Sequences

Primer	Sequence	Amplicon Size (bp)
CaMV (Sequencing)	Forward: ACGCACAATCCCACTATCC Reverse: GCGAAACCCTATAAGAACCC	Varied
EF1	Forward: AATGGGTGCTTCAGCTTTAC Reverse: AGCATATCCATTGCCAATCT	72
PrP	Forward: AACCAATGGAACAAACCATC Reverse: AAGTCCTCCAACAACAGCTC	87
mPrP	Forward: ATGTTGGGATCTGCAATGTC Reverse: CTGTTCAACAACCTCTCTCCATC	252

2.3.3 Protein Analysis

2.3.3.1 Western blot

Homogenised transgenic tobacco leaves (100 mg) were resuspended in 200 µl of 2X Laemmli sample buffer (Bio-Rad). The solution was incubated at 90°C for 10 minutes and centrifuged. The clarified lysate (20 µl) was electrophoresed on a 12% Mini-PROTEAN TGX precast gel (Bio-Rad) at 200 volts for 40 minutes. Subsequently, the separated proteins were transferred to a nitrocellulose membrane using the Trans-Blot turbo system (Bio-Rad). The membrane was

blocked with 5% powdered milk in TBS buffer (20mM Tris, 500mM NaCl, pH 7.5), incubated overnight in a 1:2,500 dilution of either the horse radish peroxide (HRP) conjugated anti-6X His-tag antibody (Abcam) or 1:1000 dilution of the PrP polyclonal antibody C-20 (Santa Cruz Biotechnology) in blocking solution. The C-20-probed membrane was washed three times in TBST buffer (TBS, 0.05% Tween-20) for 5 minutes each then incubated in a 1:2000 dilution of HRP-conjugated goat anti-mouse IgG (Santa Cruz Biotechnology) in blocking solution and washed three times in TBST buffer and once with TBS. The anti-6X His-tag antibody-probed membrane was washed five times in TBST buffer and once with TBS. Subsequently, blots were developed with the ECL chemiluminescent reagent (Bio-Rad) prior to chemiluminescent imaging on the ChemiDoc MP Imaging System (Bio-Rad).

2.3.3.2 Enzyme-linked immunosorbent assay (ELISA)

PRNP standards (10 ng/ml, 5 ng/ml, 2.5 ng/ml, 1.25 ng/ml, 0.625 ng/ml, 0.312 ng/ml, 0.156 ng/ml and a blank solution 0 ng/ml made up with standard diluent only) were prepared by serial dilution from the standard stock solution (20 ng/ml). Healthy and fully expanded tobacco leaves (100 mg) were homogenised and solubilised in 250 µl of PBST buffer (1 litre: 8 g NaCl, 0.2 g KCl, 1.44 g Na₂HPO₄, 0.24 g KH₂PO₄ and 1% Triton X-100). The solution was clarified by centrifugation and the clarified lysate used for the protein assay. 100 µl of the standards, transformed and untransformed plant lysate samples were added to predetermined wells on a 96 well plate, the plates were sealed and incubated at 37°C for 2 hours. Afterwards, the solution was removed from each well using an aspirator and 100 µl of detection reagent A was added to the wells and the plates were sealed and incubated for 1 hour at 37°C. Then the solution was aspirated

and wash solution was added to the wells and allowed to sit for 2 mins then aspirated. This process was repeated thrice before 100 µl of detection reagent B was added to the wells and the plates sealed and incubated for 30 minutes at 37°C. The wells were washed 5 times as described above and 90 µl of Tetramethylbenzidine (TMB) substrate was added to the wells and the plate covered and incubated for 15 minutes at 37°C. 50 µl of the stop solution was then added to the wells and absorbance measured immediately at 450 nm on a Thermomultiskan microplate reader (Thermo Fisher Scientific). To calculate the recombinant mPrP concentration in the plant samples analysed an average of the duplicate reading for each standard was determined and the average optical density (O.D.) of the blank standard was subtracted and a standard curve created by plotting the O.D. of the standards against the concentration of the standards. To account for background, the O.D. of the untransformed plant sample was subtracted from the O.D. of the transgenic plant samples analysed and the recombinant mPrP concentration was determined from the standard curve.

2.3.3.3 Bradford Assay

Bovine serum albumin (BSA) protein standards (1.5 mg/ml, 1.0 mg/ml, 0.75 mg/ml, 0.5 mg/ml, 0.375 mg/ml, 0.25 mg/ml and 0 mg/ml, the blank which contained only distilled water) were added to 96 well plate. The tobacco leave lysate samples were diluted 10-fold with distilled water. For the assay, 5 µl of the protein standards and the plant samples were added to predetermined wells of a 96 well plate then 250 µl of the Bradford reagent was added to the wells used and the plate mixed on a shaker for 30 secs. The samples were incubated at room temperature for 10 mins and absorbance measured at 595nm. The soluble protein concentration of the plant samples was determined from the BSA

standard curve. The mPrP concentration in the plant samples was expressed as a percentage of the total soluble protein concentration as shown in Appendix E.

Chemical analysis of transgenic tobacco leaves

2.3.4 Analysis of Plant Nutrients

Healthy fully expanded leaves from 30 day old transgenic tobacco plants, grown on MS media only or with kanamycin (100 µg/ml) included in the media, were excised and mailed in an antistatic package to the Alice Holt forest research institute where the samples were analysed for macro elements (Nitrogen, Phosphorus, Potassium, Calcium and Magnesium) and micro elements (Iron, Manganese, Copper, Boron, Nickel and Zinc).

The leaves were dried and homogenised using a mill (Cyclotec). The homogenate was re-dried at ~70°C for 8 hours or overnight to remove any residual moisture content. 100 mg of the homogenised leaves were digested with 1 ml of concentrated sulphuric acid in a 15 ml borosilicate or quartz tube. Then two doses of 30% hydrogen peroxide (0.4 ml) was added to the mixture. The tubes were then heated at 335°C for 30 minutes. Afterwards an additional dose of hydrogen peroxide was added to the solution and placed on the heating block for another 10 minutes. The process was repeated until the digests were clear. The samples were made up to 15 ml with distilled water and analysed for metal content on a dual view inductively coupled plasma optical emission spectrometry (ICP-OES) (THERMODROP 6500). The total nitrogen content of the re-dried homogenate was analysed using reference method ISO 13878. All results are expressed based on the dry weight of the plant samples.

2.3.5 Peroxidase Assay

Leaves from 30 day old transgenic plants (10 mg), grown either on MS media only or with kanamycin (100 µg/ml) included in the media, were homogenised in 200 µl of Assay Buffer. The clarified lysate (50 µl) was analysed for peroxidase activity using the peroxidase activity assay kit (Sigma-Aldrich). Absorbance was measured at 570 nm on a Thermo Multiskan microplate reader (Thermo Fisher Scientific) at 3 minutes intervals. Peroxidase activity was calculated from the initial and penultimate spectrophotometer readings using the manufacturer's protocol.

Statistical analysis

The effect of the expression of heterologous mPrP on plants nutrients was analysed by two-way analysis of variance (ANOVA) and Bonferroni *post hoc* analysis.

2.4 Purification of recombinant mPrP

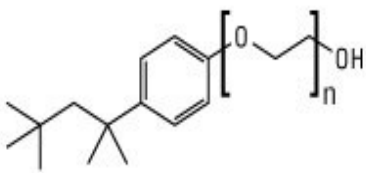
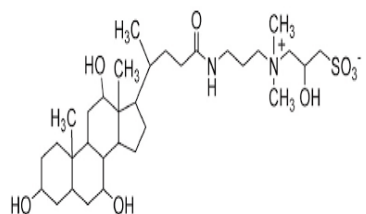
2.4.1 Lysis buffers

The buffer component of the various lysis buffers are shown in Table 2.2 and properties of detergents used in Table 2.3.

Table 2.2: Tobacco leaf protein extraction buffers

Buffer	Components
A	50 mM Tris-HCl, 500 mM NaCl, 2 mM PMSF and 8 M urea
B	20 mM Sodium phosphate, 500 mM NaCl, 2 mM PMSF and 1% Triton X-100
C	50 mM HEPES, 500 mM NaCl, 2 mM PMSF, 1% Triton X-100 and 8M urea
D	50 mM HEPES, 150 mM NaCl, 2 mM PMSF, 1% Triton X-100, 30 mM 2-Mercaptoethanol and 8M urea
E	50 mM HEPES, 10 mM NaCl, 2 mM PMSF, 1% Triton X-100, 30 mM 2-Mercaptoethanol and 8M urea
F	50 mM HEPES, 500 mM NaCl, 2 mM PMSF, 2% CHAPS , 30 mM 2-Mercaptoethanol and 8M urea

Table 2.3: Properties of detergents used in lysis buffer

Detergent	Triton X-100	CHAPS
Structure		
Type	Non-ionic	Zwitterionic
MW monomer	647	615
MW micelle	90000	6000
CMC mM	0.24	8-10
(%w/v)	(0.0155)	(0.5-0.6)
Aggregation No	140	10
Cloud Point °C	64	>100
Dialyzable	No	Yes

2.4.2 Sample Preparation

Transgenic tobacco leaves from healthy plants (10 g) was homogenised in various lysis buffer listed in Table 2.2 in the presence of EDTA-free protease inhibitor tablets (Thermo Fisher Scientific). Plant to lysis buffer ratio were varied to determine optimal concentration for the purification process. The various lysates were clarified by centrifugation at 20, 000 rpm for 30 minutes.

2.4.3 Purification

Recombinant mPrP was isolated from the clarified lysate by immobilised metal affinity-chromatography (IMAC) using either the 1 ml HiTrap Chelating HP columns loaded with either Nickel or Cobalt ions (GE Healthcare Life Sciences) or the His GraviTrap TALON columns precharged with Co^{2+} ions (GE Healthcare Life Sciences). The HiTrap column is advantageous for optimising the purification process and choice of metal ion while the GraviTrap column offers advantages in terms of convenience, binding capacity (15 mg/column), binding affinity and ability to run large sample volumes. After the lysate was passed through the columns, the flow-through was collected then the column was washed with 10X lysate volume of wash buffer (lysis buffer (without detergent and protease inhibitor) + 5 mM imidazole) and the wash fraction collected. The recombinant protein was eluted in 500 μl fractions with elution buffer (Lysis buffer without detergent + 300 mM imidazole). Afterwards the various fractions were mixed with 2X Laemmli sample buffer in a 1:3 ratio and analysed by western blot as described in section 2.3.3.1.

3 Design of Transgene Constructs

3.1 Introduction

Prion diseases are a group of neurodegenerative diseases that affect mammals, transmitted by an infectious protein called prion (Prusiner, 1998). Post-translational changes in the structure of PrP^C converts it to PrP^{Sc}. The various PrP^{Sc} isoforms differ in their sensitivity to proteases, solubility and cellular distribution (Prusiner, 1998; Harris, 1999). The molecular mechanism underlying the conversion to the aberrant isoform is poorly understood. Problems with adequate yields from the purification of PrP^C from brain homogenates and insolubility of the infectious isoform has prevented the advancement of research in this area. Although, recombinant mPrP has been produced in bacteria (Hornemann *et al.*, 1997), bacteria expression systems do not have the capacity for post-translational modification. Hence, production of recombinant mPrP in plant expression systems, which offer post-translational modification, may help researchers elucidate the process of PrP^C to PrP^{Sc} conversion and understand PrP^{Sc} neurotoxicity.

To address the possibility of plant expression systems producing recombinant mPrP, a synthetic mouse *PRNP* gene for heterologous expression in tobacco plants was designed. The choice of tobacco plant was based on convenience due to the availability of established transformation protocols for recombinant protein production. Research to improve recombinant protein production and stability in plants has established that the rate of transcription and translation may be improved by adding regulatory elements and modifying codon usage of the transgene. Furthermore, protein stability may be enhanced by adding sequences conserved for subcellular localisation to the transgene construct (Birch, 1997; Sharma and Sharma, 2009).

3.2 Results

3.2.1 Synthetic mPrP gene constructs

The DNA sequence of the mature peptide of the mouse *PRNP* gene (GenBank ID: NM_011170.2) was optimised for expression in tobacco. Using GENEius software (Eurofins MWG Operon), the codon usage of mouse *PRNP* gene was changed to reflect the preferred codons of tobacco nuclear genes (Figure 3.1). Alignment of the synthetic and native gene gave a sequence similarity of 74%. As shown in Figure 3.2, altering the codon improved the codon adaptation index from 0.68 to 0.92 and reduced the GC content from 60.21% to 44.80%.

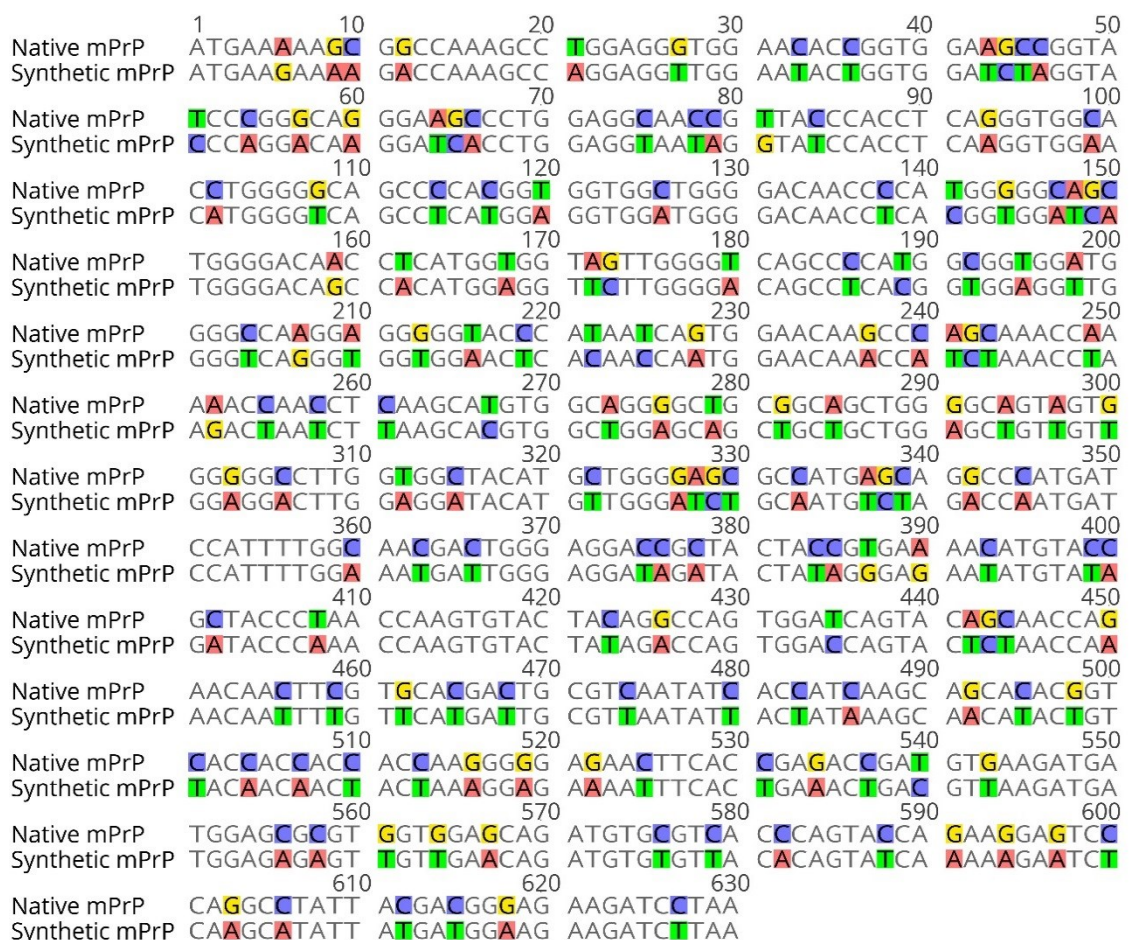
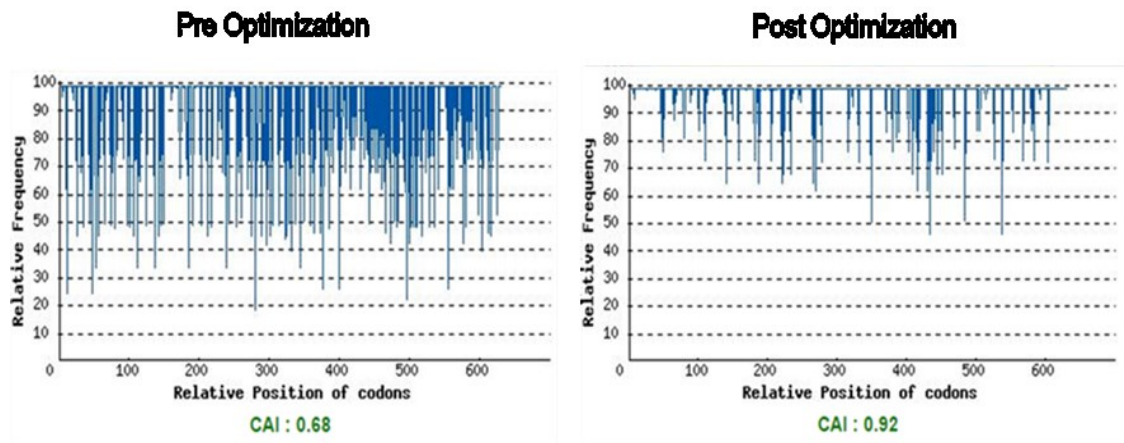


Figure 3.1: Creation of a synthetic mPrP gene for expression in tobacco plants
Sequence alignment of the native mPrP gene and the synthetic gene. Altered nucleotides are coloured. Image design: Geneious Software Version 9.1.5 (<http://www.geneious.com>, Kearse *et al.*, 2012)

Codon Adaptation Index (CAI)



GC Content Adjustment

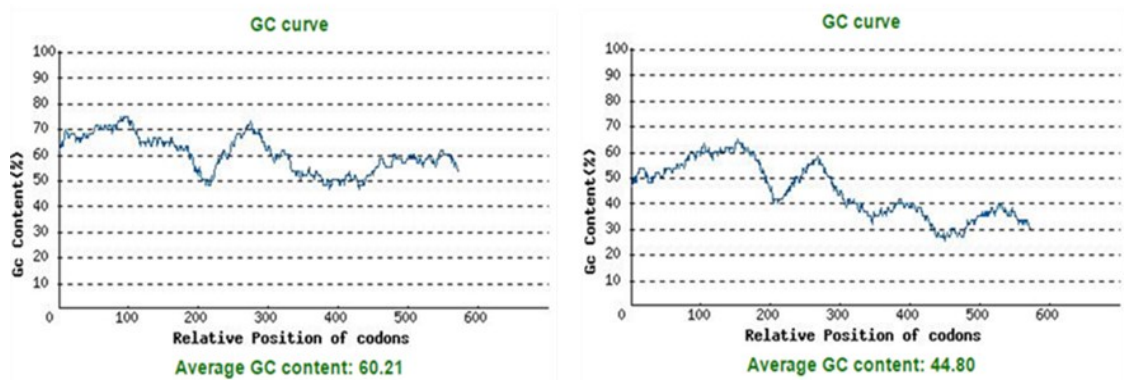


Figure 3.2: Comparative codon analysis of native mouse prion protein and synthetic mouse prion protein optimised for expression in *Nicotiana Tabacum*. Nucleotide alterations increased the CAI from 0.68 to 0.92 and decreased the % GC content from 60.21 to 44.80. Analysis: GenScript Rare Codon Analysis Tool

Several regulatory elements were added to the synthetic mouse *PRNP* gene sequence of all three constructs, mPrP-Cyto (Figure 3.4), mPrP-Apo (Figure 3.5) and mPrP-ER (Figure 3.6). Restriction sites for *Bam*HI and *Eco*RI were added for subcloning purposes, a C-terminal hexahistidine-tag for affinity purification and the translation enhancers, TMV omega sequence (GenBank ID: M24955.1) and 3' UTR TMV (GenBank ID: V01406.1:801-1004). Also, the signal peptide of

PR1a of tobacco (GenBank ID: X06361.1) was added to the apoplast and ER constructs for subcellular localisation. Finally, the “SEKDEL” ER retrieval sequence was added to the ER constructs for ER retention of the recominant protein. All constructs were synthesised and cloned into pEX-A plasmid (Eurofins MWG Operon).

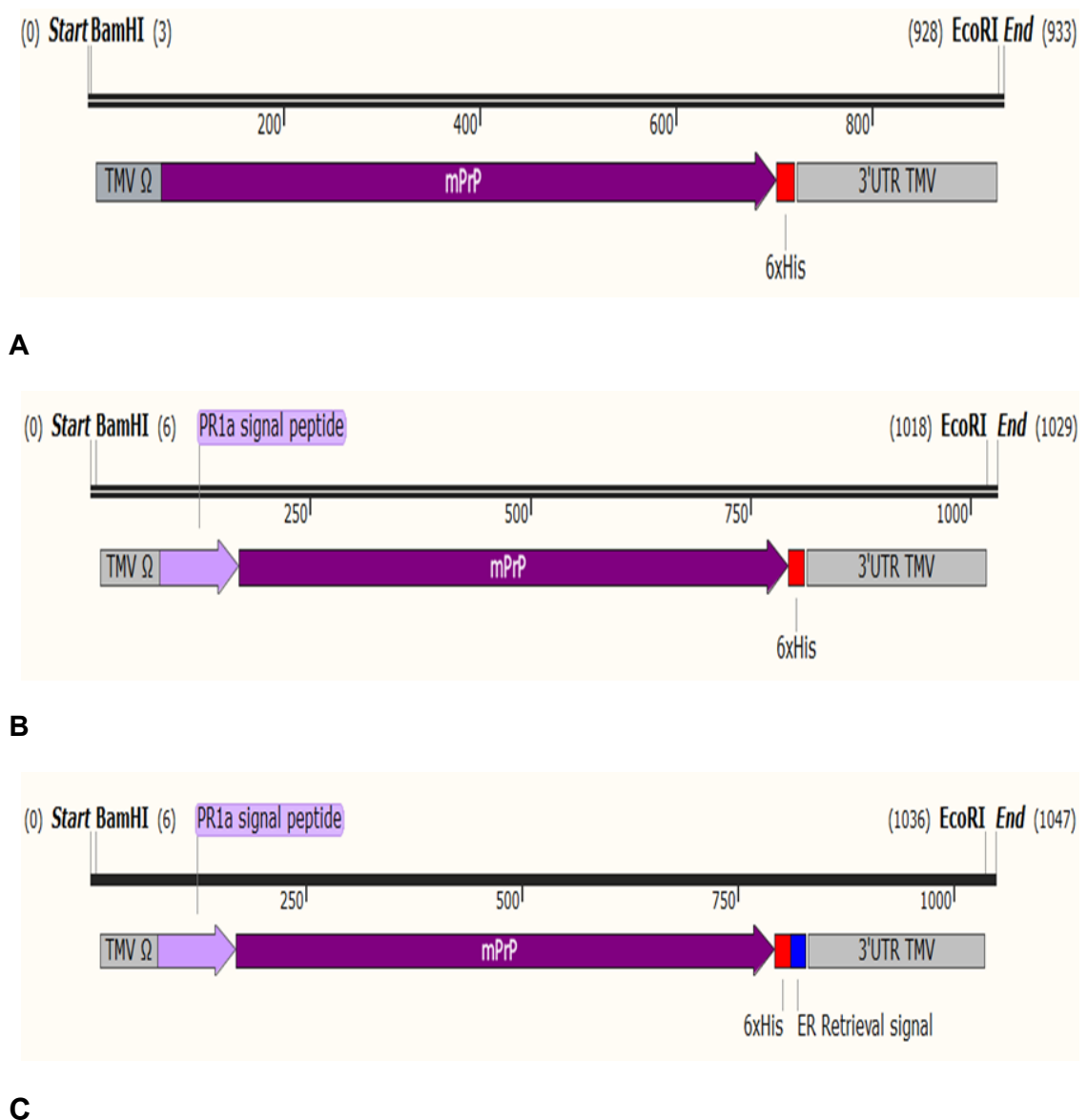


Figure 3.3: Schematic representation of mPrP transgene constructs. A: mPrP-Cyto (933 bp). B: mPrP-Apo (1029 bp). C: mPrP-ER (1047 bp). Image design: SnapGene Software Version 1.5.3 (GSL Biotech).

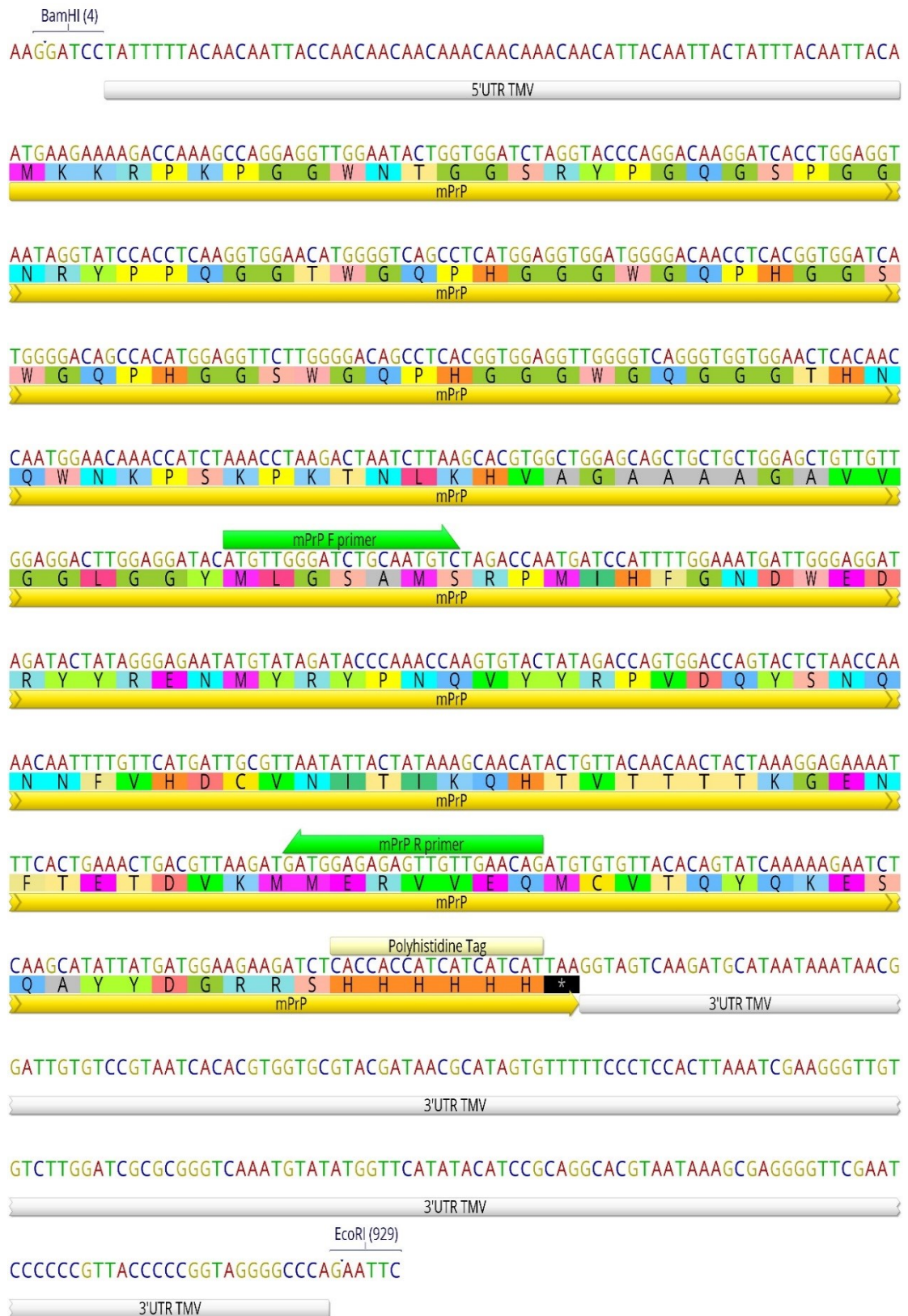


Figure 3.4: Annotated mPrP-Cyto nucleotide sequence. Features: restriction sites *Bam*HI and *Eco*RI, (5'UTR and 3'UTR) TMV, location of mPrP primer site for PCR analysis and polyhistidine-tag. Image Design: Geneious Software Version 9.1.5 (<http://www.geneious.com>, Kearse *et al.*, 2012).

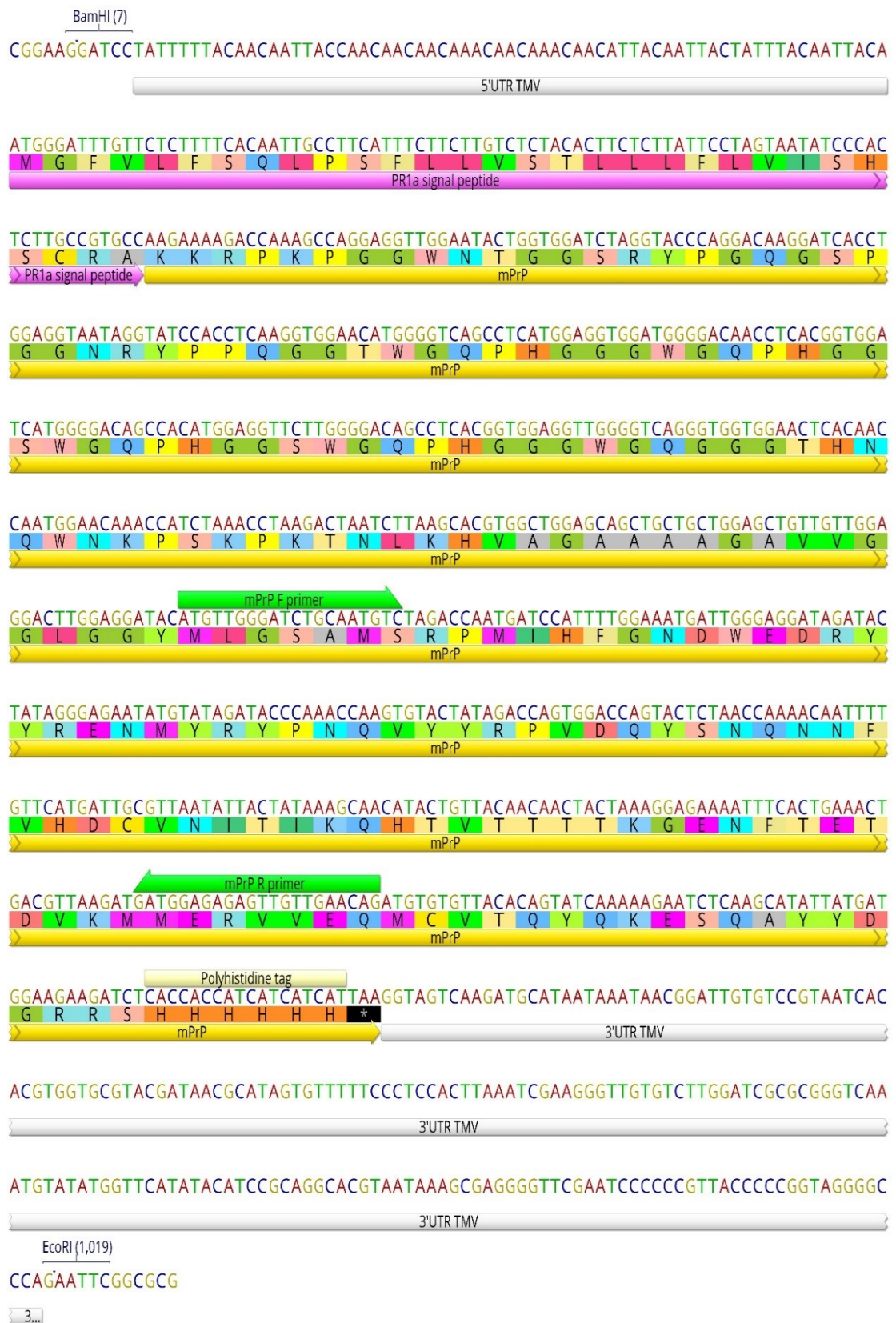


Figure 3.5: Annotated mPrP-Apo nucleotide sequence. Features: restriction sites *Bam*HI and *Eco*RI, (5'UTR and 3'UTR) TMV, location of mPrP primer site for PCR analysis, polyhistidine-tag and *PR1a* signal peptide. Image Design: Geneious Software Version 9.1.5 (<http://www.geneious.com>, Kearse *et al.*, 2012).

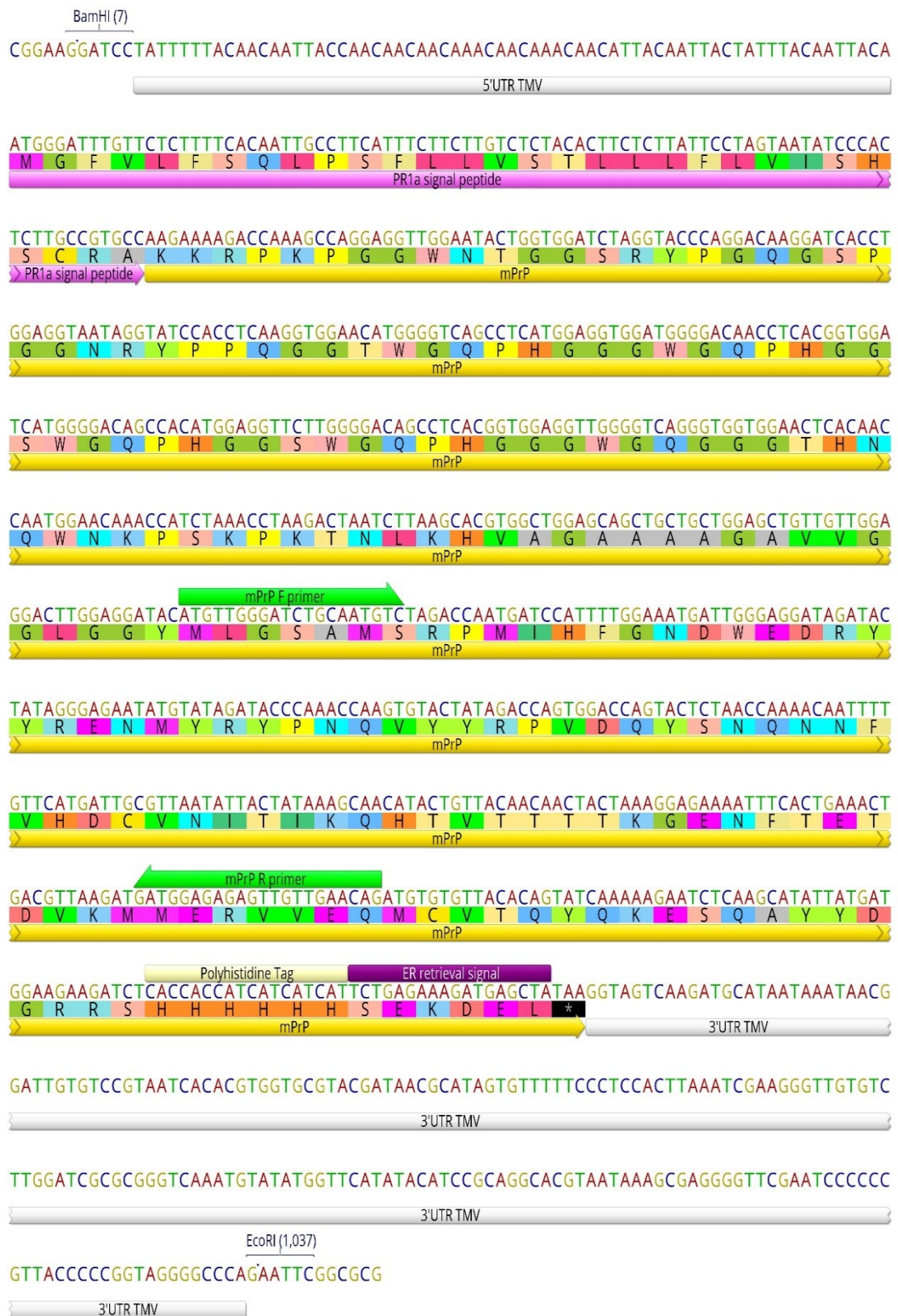


Figure 3.6: Annotated mPrP-ER nucleotide sequence. Features: restriction sites *Bam*HI and *Eco*RI, (5'UTR and 3'UTR) TMV, *PR1a* signal peptide, location of mPrP primer site for PCR analysis, polyhistidine-tag and ER retrieval sequence. Image Design: Geneious Software Version 9.1.5 (<http://www.geneious.com>, Kearse *et al.*, 2012).

3.2.2 Plant Expression Vectors

3.2.2.1 p35S-2-mPrP cassettes

The mPrP constructs, mPrP-Cyto (0.9 kb), mPrP-Apo (1.0 kb) and mPrP-ER (1.0 kb), were excised from pEX-A with *Bam*HI and *Eco*RI restriction enzymes and inserted into the p35S-2 cassette (Hellens *et al.*, 2000) also digested with *Bam*HI and *Eco*RI. All digested fragments were ligated using Lyo-Ligase (Bioline) to generate p35S-2-mPrP-Cyto, p35S-2-mPrP-Apo and p35S-2-mPrP-ER. Subsequently, the modified p35S-2 constructs were transformed into *E. coli* DH5α cells and positive clones were identified by their growth on ampicillin LB plates. The p35S-2-mPrP recombinant plasmids were purified from positive colonies using a plasmid miniprep protocol (Qiagen). Restriction analysis of the isolated plasmids (Figure 3.7) using *Eco*RV produced two fragments, a 2.2 kb vector backbone and either 35S-mPrP-Cyto (1.58 kb), 35S-mPrP-Apo (1.66 kb) or 35S-mPrP-ER (1.68 kb). The results confirmed the integrity of the recombinant p35S-2-mPrP constructs.

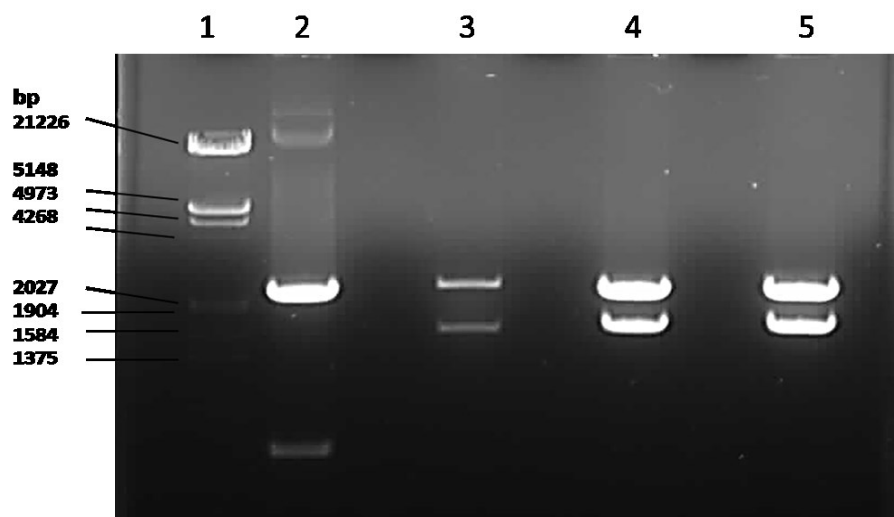
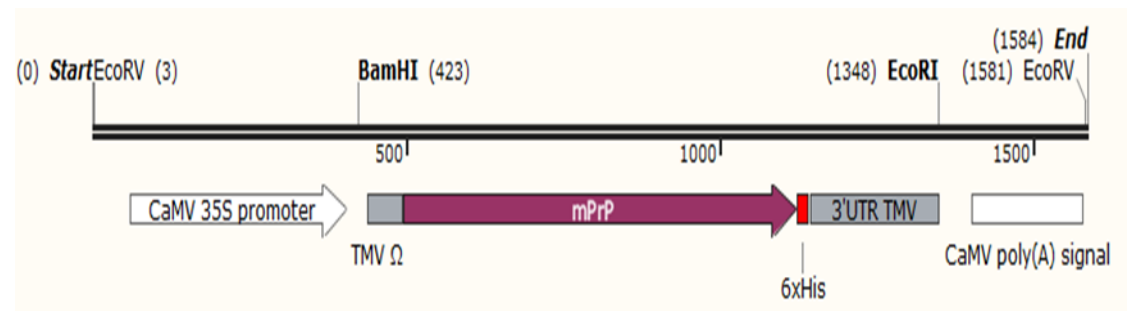
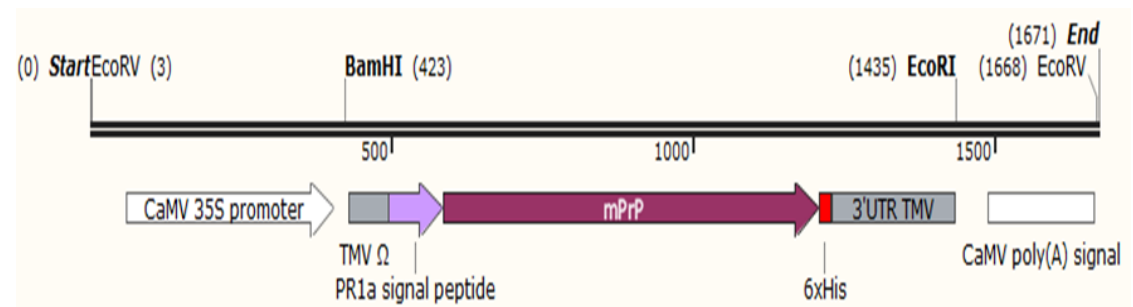


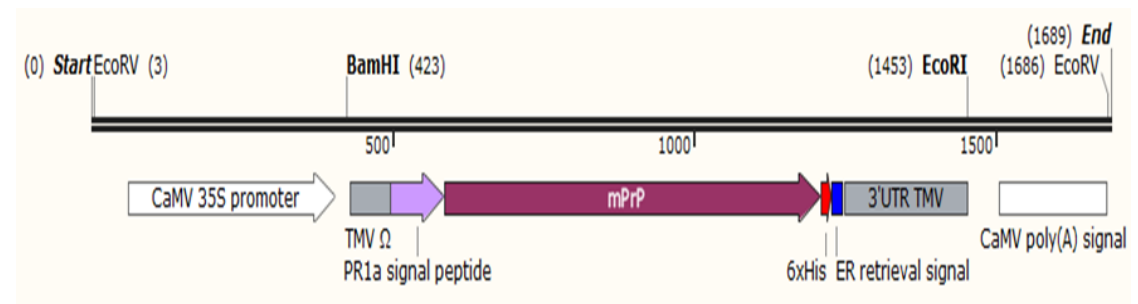
Figure 3.7: *Eco*RV analysis of p35S-2-mPrP constructs. Lane 1: Molecular Weight Marker. Lane 2: p35S-2. Lane 3: p35S-2-mPrP-Cyto. Lane 4: p35S-2-mPrP-Apo. Lane 5: p35S-2-mPrP-ER.



A



B



C

Figure 3.8: Schematic representation of p35S-2-mPrP transgene cassettes. A: 35S-mPrP-Cyto, 1.58 kb. B: 35S-mPrP-Apo, 1.66 kb. C: 35S-mprp-ER, 1.68 kb. Image design: SnapGene Software Version 1.5.3 (GSL Biotech).

3.2.2.2 pGreen-35S-mPrP cassettes

The p35S-2-mPrP cassettes were excised with restriction enzyme *EcoRV* and each insert ligated into a pGreen0029 vector (Hellens *et al.*, 2000) also digested with *EcoRV*, using Lyo-ligase (Bioline). The resultant pGreen-35S-mPrP recombinant plasmids were transformed into *E. coli* DH5 α cells and positive clones were identified by their growth on kanamycin LB plates. Subsequently, plasmids were isolated by miniprep (Qiagen) and digested with *EcoRV* for analysis. As shown in Figure 3.9, restriction analysis of the constructs produced two fragments, a 4.6 kb vector backbone and either pGreen-35S-mPrP-Cyto (1.58 kb), pGreen-35S-mPrP-Apo (1.66 kb) or pGreen-35S-mPrP-ER (1.68 kb). The lower molecular weight bands present in lane 2, figure 3.9 are thought to be due to star activity of *EcoRV*. The results indicate the integrity of the recombinant pGreen-35S-mPrP plasmids (Figures 3.10 - 3.12). Results were confirmed by sequence analysis. The recombinant pGreen-35S-mPrP plasmids obtained were suitable for *Agrobacterium tumefaciens*-mediated plant transformation.

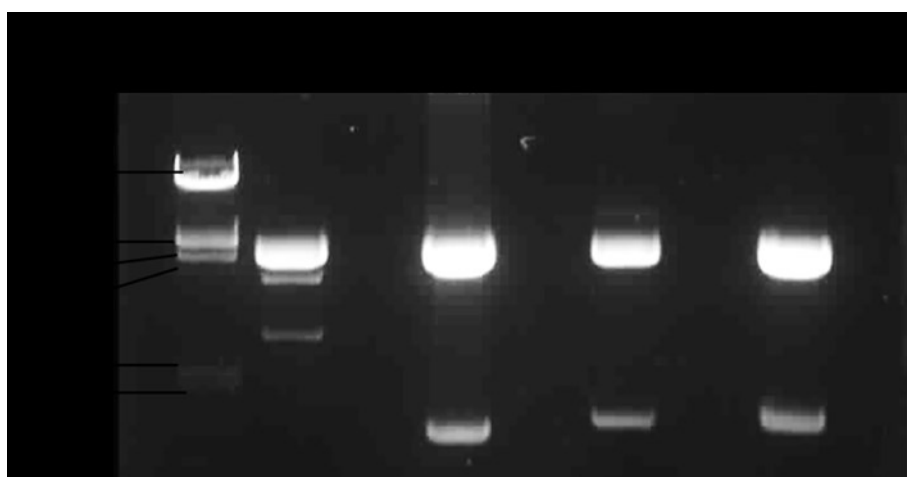


Figure 3.9: *EcoRV* Analysis of pGreen-35S-mPrP constructs. Lane 1: Molecular Weight Marker. Lane 2: pGreen. Lane 3: p35S-2mPrPCyto. Lane 4: p35S-2mPrPApo. Lane 5: p35S-2mPrPER.

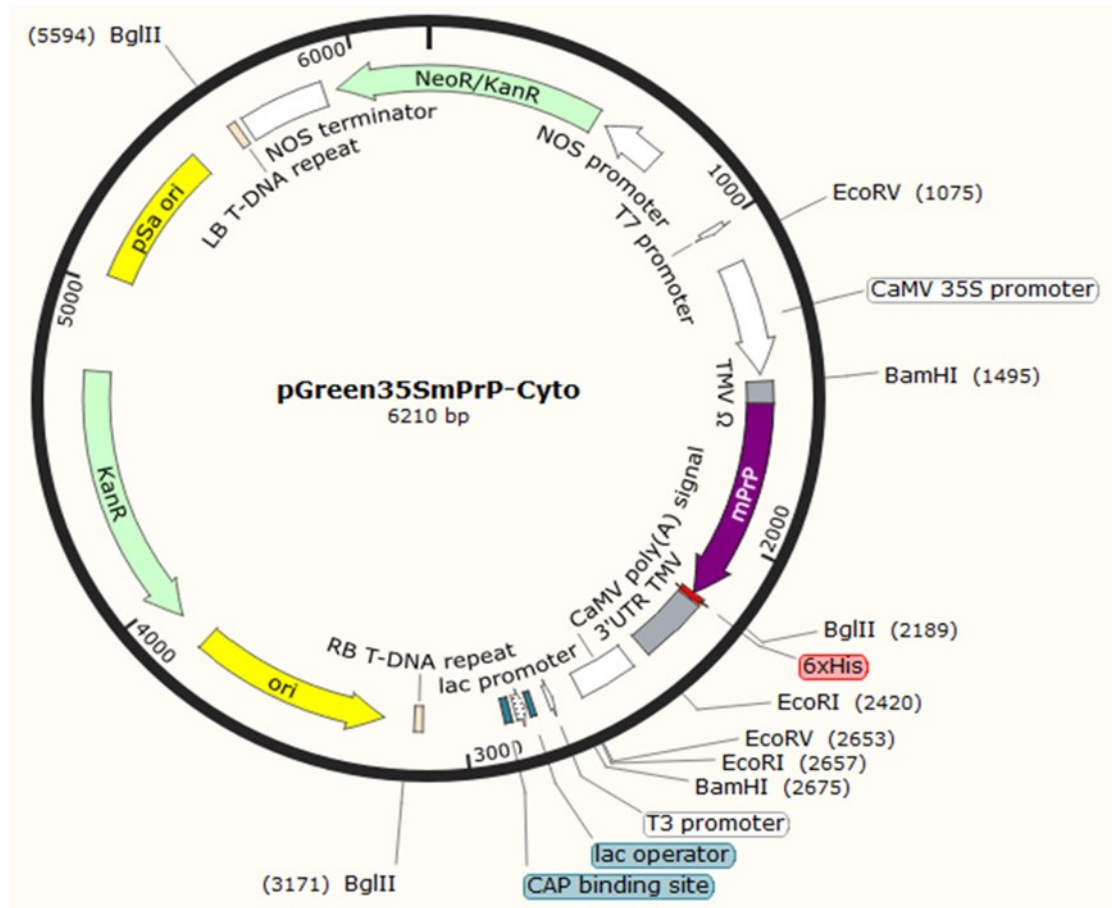


Figure 3.10: Schematic representation of pGreen-35S-mPrP-Cyto plasmid.

The 35S-mPrP-Cyto cassette forms a 1.58 kb insert between the *EcoRV* sites at 1075 bp and 2653 bp. Image design: SnapGene Software Version 1.5.3 (GSL Biotech)

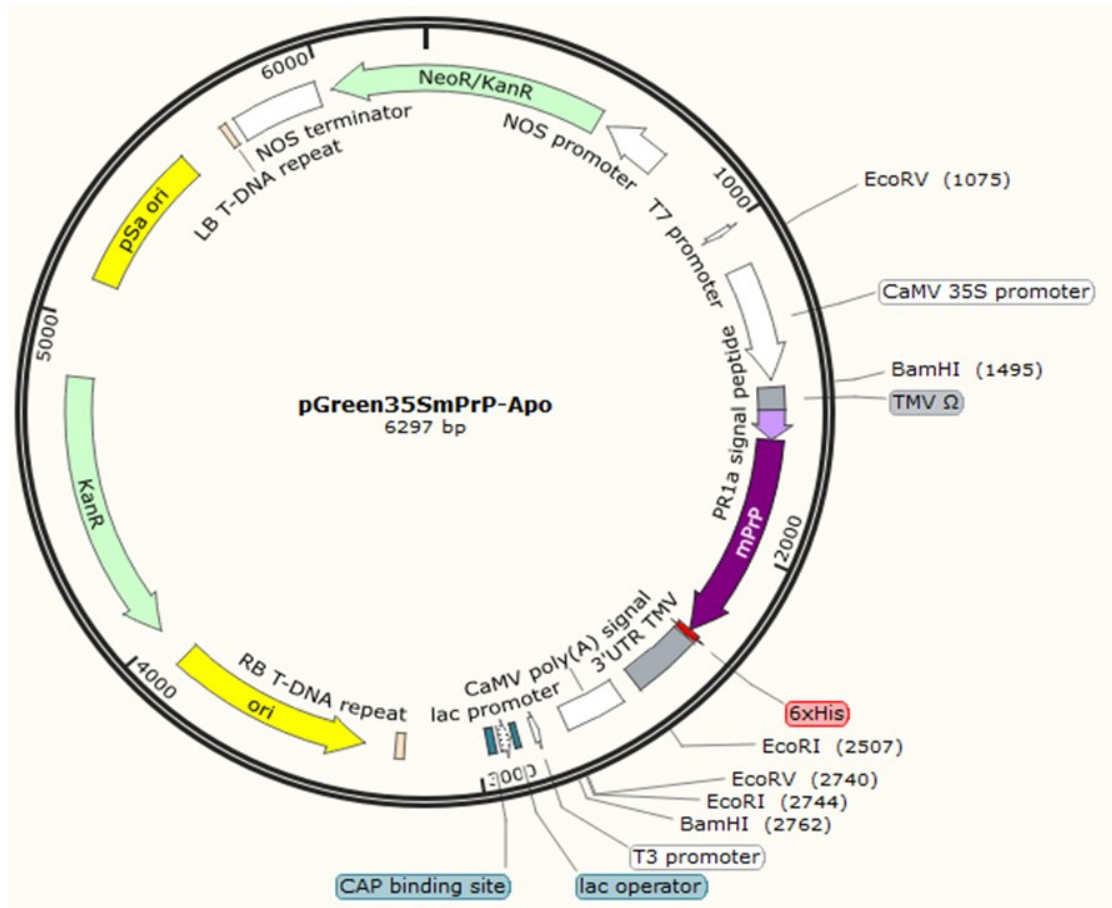


Figure 3.11: Schematic representation of pGreen-35S-mPrP-Apo plasmid. The 35S-mPrP-Apo cassette forms a 1.66 kb insert between the *EcoRV* sites at 1075 bp and 2740 bp. Image design: SnapGene Software Version 1.5.3 (GSL Biotech)

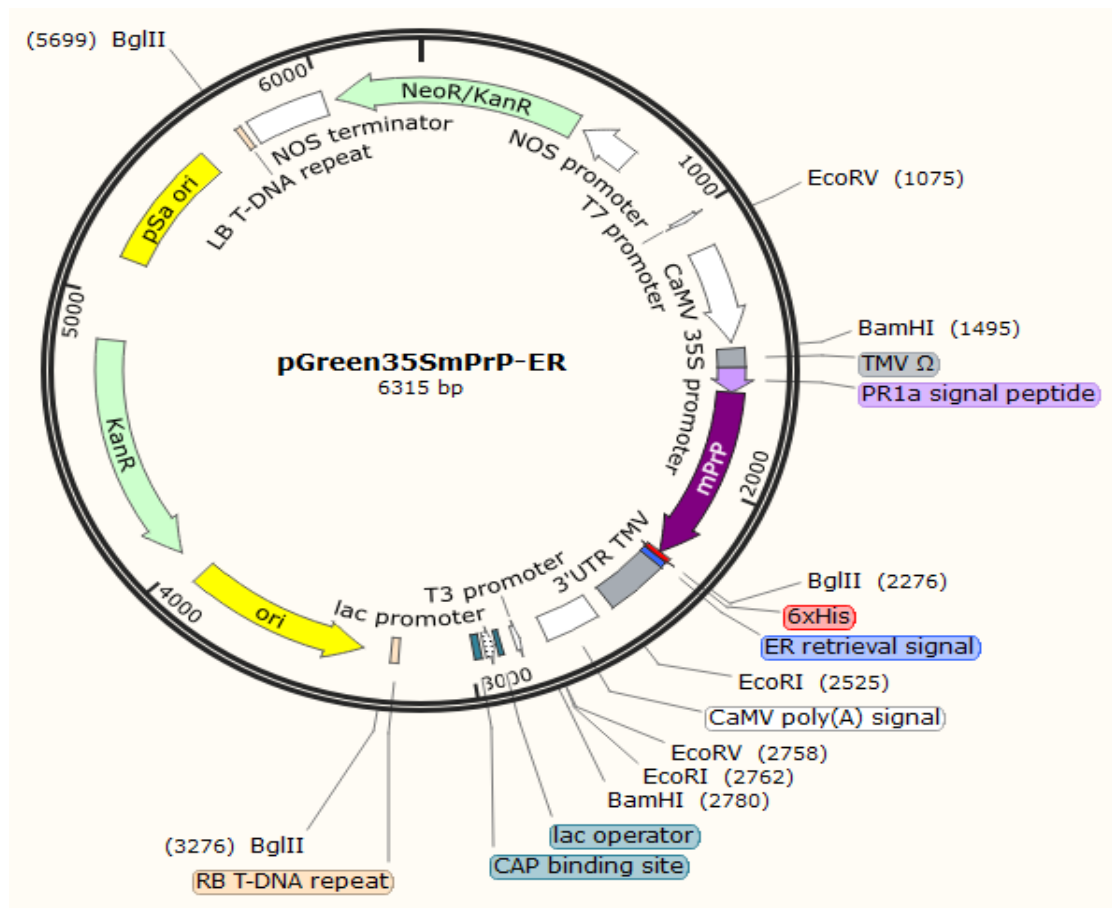


Figure 3.12: Schematic representation of pGreen-35S-mPrP-ER plasmid. The 35S-mPrP-ER cassette forms a 1.68 kb insert between the *EcoRV* sites at 1075 bp and 2758 bp. Image design: SnapGene Software Version 1.5.3 (GSL Biotech)

3.2.3 Plant Transformation

Tobacco plants were transformed by *Agrobacterium* (Horsch, 1985), based on its ability to integrate the recombinant T-DNA (Figure 3.14) into the plant's nuclear genome. The plant expression constructs were each transformed into *Agrobacterium tumefaciens* cells alongside the helper plasmid pSoup by electroporation. Positive clones were identified by growth on kanamycin YEP plates. Subsequently, leaf discs from axenic tobacco plants were infected with *Agrobacterium* suspension that contained the pGreen-35S-mPrP-Cyto, pGreen-35S-mPrP-Apo or pGreen-35S-mPrP-ER recombinant plasmid. The explants were cocultured with *Agrobacterium* in the dark for three days on MS media for callus induction and transferred to kanamycin MS media for selection of putative transgenic shoots (Section 2.2.6.3).

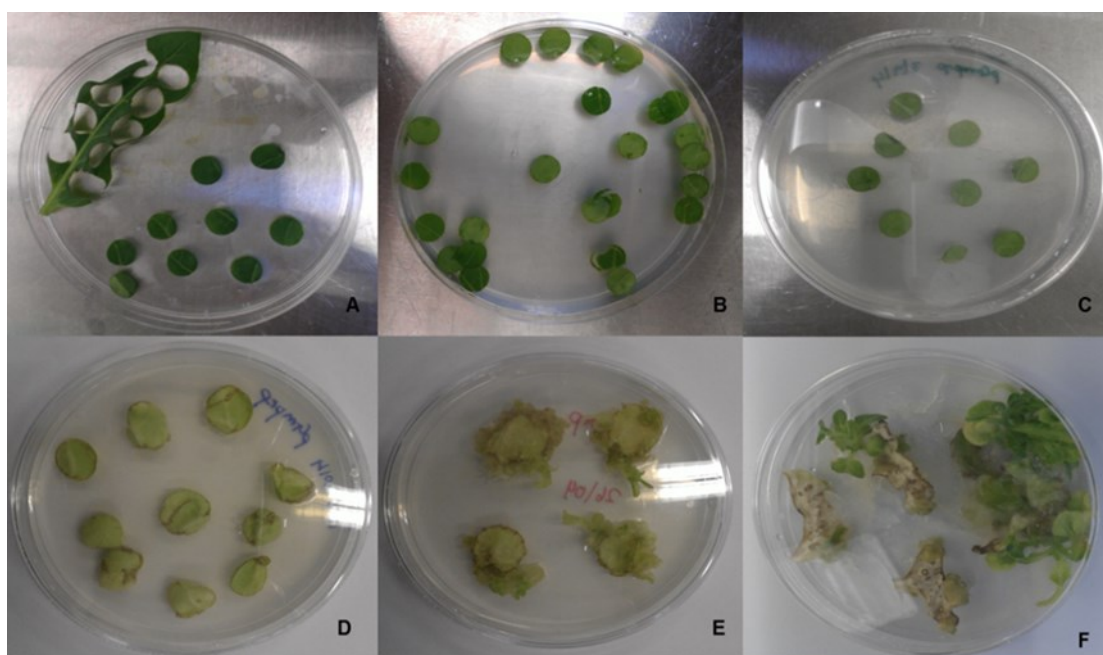
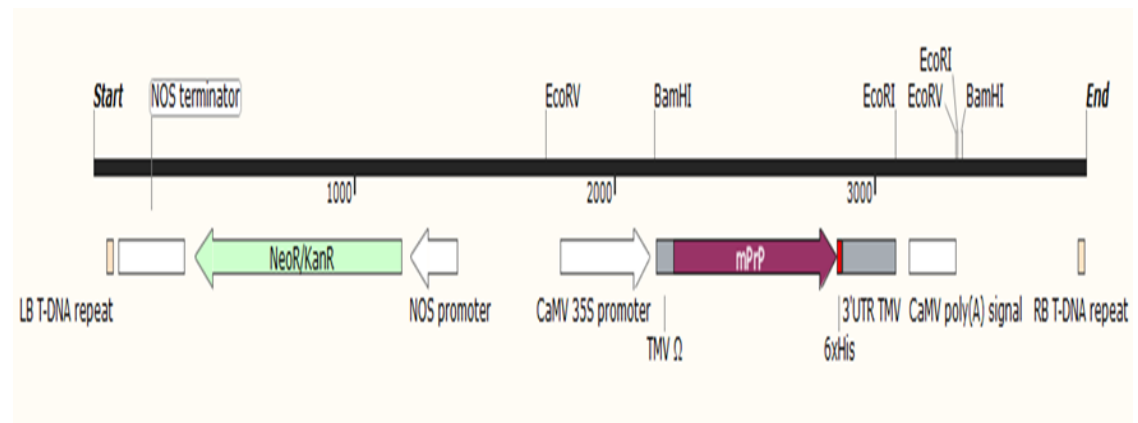
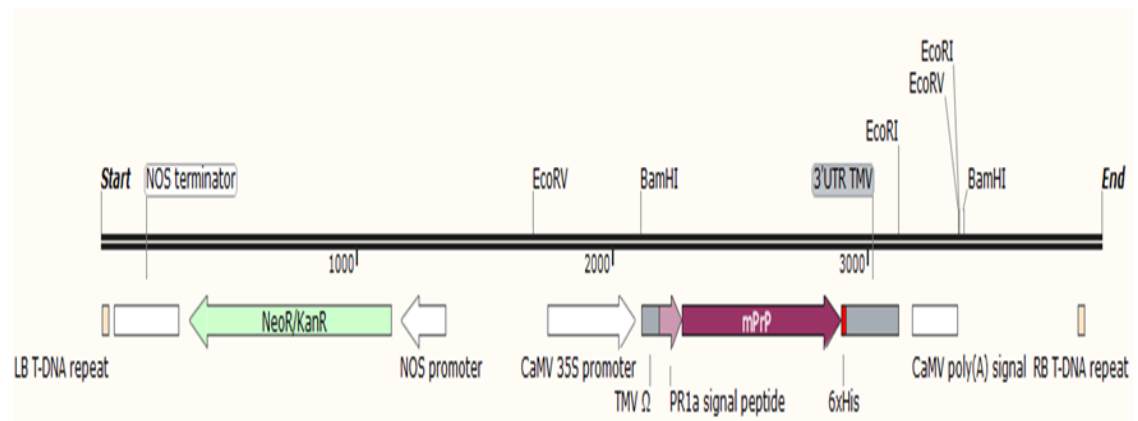


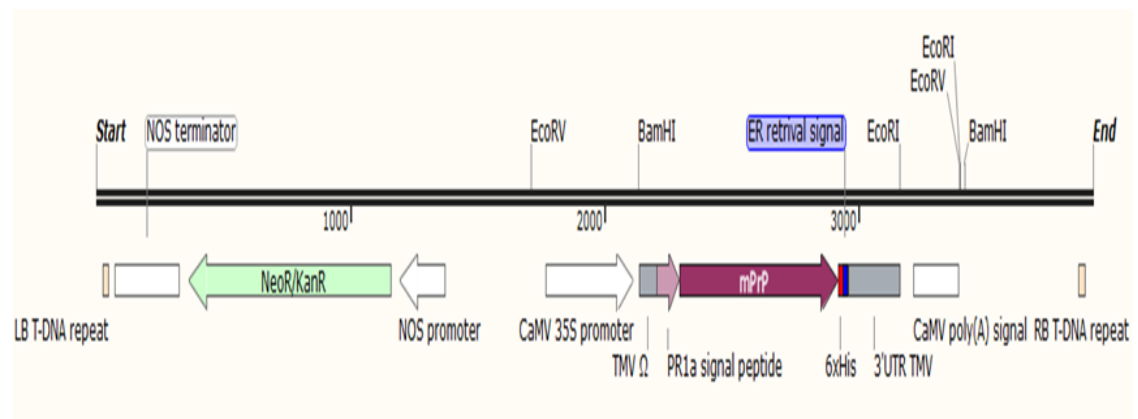
Figure 3.13: Stages in Plant Transformation. A: Excision of Tobacco Leaf discs (Explants). B: Inoculation of explants with *Agrobacterium*. C: Coculturing of explants with *Agrobacterium*. D: Callus on kanamycin MS media. E: Shoot regeneration. F: Mature transgenic shoots.



A



B



C

Figure 3.14: Schematic representation of recombinant T-DNA region of constructs A: pGreen-35S-mPrP-Cyto. B: pGreen-35S-mPrP-Apo. C: pGreen-35S-mPrP-ER. Image design: SnapGene

3.3 Discussion

Plants are a conventional heterologous expression system for the production of recombinant proteins. The quality and yield of plant-expressed recombinant protein depends considerably on the design of an effective transgene expression cassette (Ma *et al.*, 2003; Ullrich *et al.*, 2015). In plant expression systems recombinant protein yields may be low because of codon bias. Codon usage bias is the event that a given species prefers using a particular codon to other synonymous codons during gene translation (Hershberg and Petrov, 2008). Protein expression levels are influenced by codon bias, as they reflect the tRNA levels in the expression system (Gustafsson *et al.*, 2004; Ullrich *et al.*, 2015). For instance, if the recombinant protein being expressed contains a high frequency of a codon less frequently used in the host plant, the tRNA pool will be exhausted leading to low expression of the recombinant protein. Therefore, the nucleotide sequences of transgenes are usually altered, using codon bias tables and gene optimisation software, to reflect the codon usage of the host organism. In this study, to create the recombinant mouse prion gene suitable for expression in tobacco we modified 50% of the codons of mPrP to reflect the codon bias of *Nicotiana tabacum* using the GENEius software. The effect of this modification was measured by CAI and %GC content. The probability of high protein expression level correlates with the value of the codon adaptation index (Sharp *et al.*, 1987). Optimising the mouse prion gene increased CAI to 0.92 which is above the 0.8 threshold for good gene expression in a heterologous system. Also, the synthetic gene had a reduced GC content of 44.8% which is analogous to the 43.38% GC content of tobacco nuclear genes.

The addition of regulatory elements to a transgene construct usually enhances the rates of transcription and translation. Promoters are important regulatory elements that direct the transcription rate of transgenes. The CaMV 35S promoter is a strong constitutive promoter mostly effective for stable nuclear transformation (Odell *et al.*, 1985). Studies have shown that the CaMV 35S confers the highest expression level of transgenes in dicotyledonous plants, hence, its extensive use in plant expression systems (Fang *et al.*, 1989; Comai *et al.*, 1990). Almost 80% of transgenes expressed in plants are driven by the CaMV 35S promoter (Hull *et al.*, 2000). In addition to codon optimisation, translational efficiency of heterologous genes is significantly improved by including the 5' and 3' untranslated regions of plant viral mRNAs in the transgene construct. The 5' UTR and 3' UTR of TMV enhances translation of transgenes independently. The 5'UTR of TMV acts as a binding site for the translational enhancer, heat shock protein HSP101 (Gallie, 2002). The 3' UTR of TMV increases mRNA stability and translation. Studies have shown adding the 3'UTR of TMV to foreign gene constructs may increase transgene expression by 100-fold (Gallie and Walboth, 1990). Ideally, improved transcription and translation should increase recombinant protein levels. However, this rarely correlates with protein levels due to degradation of protein by proteases in the host system (Conrad and Fiedler, 1998).

Plant recombinant protein levels are affected by their subcellular location (Egelkrout, 2012). In the absence of targeting signals most recombinant proteins are directed to the cytosol. Cytosolic proteins typically have no post-translational modification and are quickly degraded by abundant proteases present in the cytosol. Addition of an N-terminal signal peptide to the recombinant protein

normally directs the recombinant protein to the apoplast. Proteins in the apoplast are post-translationally modified in the endoplasmic reticulum and the Golgi apparatus (Stoger *et al.*, 2005). The N-terminal signal sequence of the pathogenesis related protein (PR1a) of tobacco has been successfully used to direct recombinant proteins to the apoplast of tobacco plants (Pen *et al.*, 1992). Also, recombinant protein levels are significantly improved due to depleted protease activity in the apoplast. Alternatively, the protein may be retained in the endoplasmic reticulum by addition of the SEKDEL ER retrieval sequence (Munro and Pelham, 1987) to the transgene construct. The ER has lower protease activity than both the cytosol and the apoplast (Egelkrout, 2012). Also, recombinant proteins in the ER lack complex plant glycans that cause immunogenicity, hence, it is the favoured location for recombinant proteins. However, it is important to note that since proteins are distinct, accumulation levels of a particular protein in different subcellular compartments can only be determined directly by experimentation.

Purification of recombinant protein is essential for biochemical and biophysical characterisation of the protein. A standard purification strategy involves fusing the recombinant protein to a peptide affinity tag followed by affinity chromatography purification, usually in a single step process (Bornhorst and Falke, 2000). The polyhistidine affinity tag, utilising its affinity to immobilised metal ion in immobilised metal affinity chromatography (IMAC), is the most studied affinity tag for protein purification. Therefore, it is a good choice for a novel purification attempt of a heterologously expressed protein. Additionally, polyhistidine-tagged recombinant mPrP has been successfully purified from *E.coli* and the peptide tag had no effect on the quality of the protein (Hornemann *et al.*, 1997). Examples of

histidine-tagged recombinant protein purified from tobacco includes recombinant interferon gamma (Leelavathi and Reddy, 2003) and recombinant HIV-Nef antigen (Marusic *et al.*, 2007)

Agrobacterium has the ability to integrate its T-DNA into the plant nuclear genome. This involves a complex mechanism where wounded plants secrete low molecular weight compounds such as acetosyringone that are recognised by *Agrobacterium* as a signal to instigate expression of virulence genes and initiate transfer of T-DNA into the plant nuclear genome (Gelvin, 2003). Transgenes which require post-translational modifications are best transformed via *Agrobacterium* because they are integrated into the plant nuclear genome (Ma *et al.*, 2003). Stable integration of T-DNA into the plant genome is influenced by factors such as ~~time~~, density of *Agrobacterium* suspension, light and length of cocultivation. For instance, *Agrobacterium* suspensions with an optical density above 0.5 usually causes necrosis of explants (Binns, 2002) while light impedes motility of *Agrobacterium* (Oberpichler *et al.*, 2008). Plant transformation via *Agrobacterium* offers significant advantages over other documented methods including ease, affordability, established protocols, high transformation efficiency, low transgene copy number and stable integration of the transgene (Binns, 2002).

Years of plant biotechnology research has elucidated various approaches to enhance recombinant protein yield in transgenic plants. Several of the strategies described in previous paragraphs, were used to create three transgene constructs pGreen-35S-mPrP-Cyto, pGreen-35S-mPrP-Apo and pGreen-35S-mPrP-ER for enhanced production of recombinant mPrP in tobacco plants.

4 Characterisation of recombinant mPrP in transgenic tobacco leaves

4.1 Introduction

Proteins are complex biological molecules that self-assemble into adaptable three dimensional structures. The most thermodynamically stable conformation of a protein under physiological conditions is known as its native structure. The native structure of a protein determines its function while its intermediate structure determines cellular transport and trafficking, regulation of its biological activity and interaction with other molecules and its environment (Dobson *et al.*, 2003; Gaggelli *et al.*, 2006). The tertiary structure of a protein is encoded by its amino acid sequence. Therefore, mutations affecting the amino acid sequence may cause genetic disorders which are frequently characterised by pathogenic misfolded protein aggregates (Dobson *et al.*, 2003). However, evidence shows that changes in physiological conditions can also alter the conformation of most proteins (Soto, 2003).

Protein conformational disorders occur when a protein deviates from its native structure and maintains a stable alternate conformation by aggregation and accumulation into amyloid fibrils (Soto, 2003; Chiti and Dobson, 2006; Brundin *et al.*, 2010). Neurodegenerative diseases such as Alzheimer's, prion and Parkinson's diseases are protein conformational disorders that affect the brain. Evidence has shown that the aforementioned neurodegenerative diseases may share a common pathogenic mechanism due to similar features. Firstly, neurodegenerative diseases are late onset possibly due to increased oxidative stress and change in metal homeostasis (Sayre *et al.*, 2000; Gaggelli *et al.*, 2006). Secondly, they are mostly sporadic with genetic mutation accounting for only 20% of cases (Prusiner, 2001). Thirdly, they share similar pathological symptoms including misfolded protein deposits that bind amyloid specific dyes,

neuronal loss and abnormal synaptic function (Soto, 2003; Chiti and Dobson, 2006). Finally, structural studies have shown that the misfolded protein aggregates are created via a nucleation mechanism and characterised by soluble oligomeric intermediates and β -sheet rich fibrils (Dobson *et al.*, 2003; Ross and Poirier, 2004). However, the distinct clinical symptoms exhibited by each neurodegenerative disease is determined by the specific protein, brain region and class of neurons affected (Dobson *et al.*, 2003; Soto, 2003).

4.2 Results

Regenerated shoots were obtained from tobacco calli transformed with either the pGreen-35S-mPrP-Cyto or pGreen-35S-mPrP-ER construct, as shown in table 4.1. Unfortunately, all explants transformed with the pGreen-35S-mPrP-Apo construct were lost to contamination even though the experiment was repeated thrice. Putative transformants from the surviving constructs were selected by subculturing on kanamycin-treated MS media. Five randomly chosen transgenic plants from each construct were characterised for transgene integration and mRNA transcription levels. The accumulation of recombinant mPrP from both constructs were determined by ELISA assay.

Table 4.1: Transformation efficiency of tobacco explants

Transgene Construct	Inoculated Explants	Kanamycin Resistant Shoots	Transformation Efficiency (%)
pGreen-35S-mPrP-Cyto	150	23	15.33
pGreen-35S-mPrP-ER	150	10	6.6
pGreen-35S-mPrP-Apo	150	0	0.00

4.2.1 Analysis of transgenic plants expressing cytosolic-mPrP

Integration of mPrP transgene into the nuclear genome of plants transformed with the pGreen-35S-mPrP-Cyto construct was determined by PCR-screening of DNA from putative transformants (Figure 4.1). The mPrP primers designed from the synthetic mouse prion gene generated a 250 bp product in transformants while the control plant transformed with the pGreen vector showed no PCR product. The result confirms stable integration of the synthetic *PRNP* gene in the five transgenic lines tested.

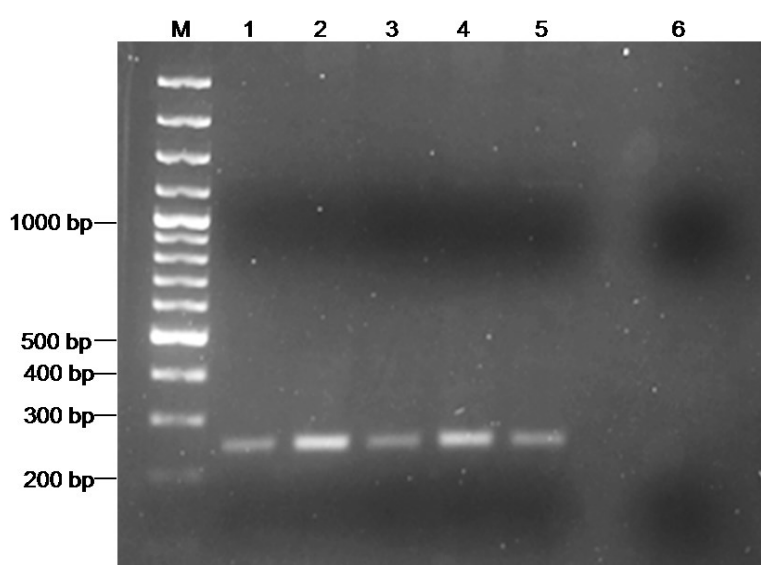


Figure 4.1: PCR analysis of transgenic tobacco leaves transformed with the pGreen-35S-mPrP-Cyto construct. M: DNA size marker, Lanes 1-5: DNA amplification product from transgenic lines C4, C7, C9, C12 and C15 respectively. Lane 6: Control – DNA amplification product from transgenic tobacco leaves transformed with the pGreen vector.

Expression of recombinant mPrP was determined by RT-PCR analysis (Figure 4.2) and measured by qRT-PCR analysis with transgenic line C4 used as calibrator (Figure 4.3). *PRNP* transcripts of size 250 bp were detected from PCR analysis of cDNA from the transgenic lines tested while no transcript was detected in cDNA from a pGreen transgenic plant used as a control (Figure 4.2).

The result indicates that all transgenic lines tested expressed *PRNP* mRNA at varying levels. Transgenic line C15 had the highest expression level while C7 had the lowest expression level.

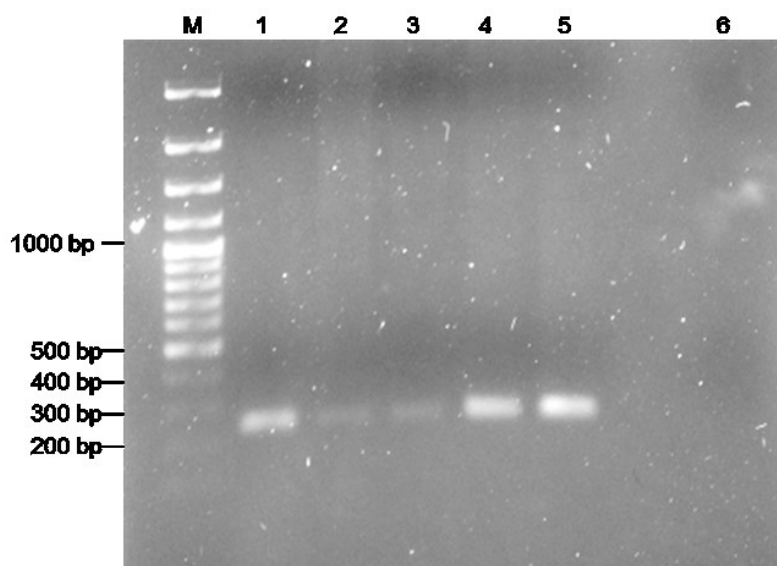


Figure 4.2: RT-PCR analysis of transgenic tobacco leaves transformed with the pGreen-35S-mPrP-Cyto construct. M: DNA size marker. Lanes 1-5: cDNA amplification product from transgenic lines C4, C7, C9, C12 and C15 respectively. Lane 6: Control – cDNA amplification product from transgenic tobacco leaves transformed with the pGreen vector.

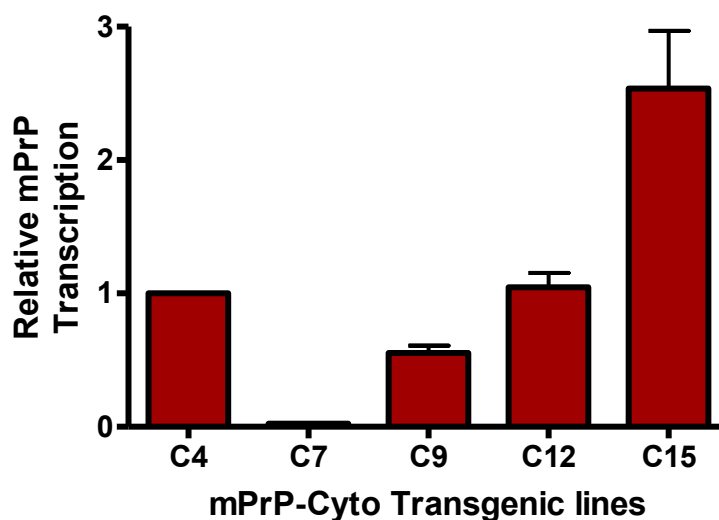


Figure 4.3: qRT-PCR analysis of mPrP mRNA transcript levels in transgenic tobacco leaves transformed with the pGreen-35S-mPrP-Cyto construct. Data represents mean and standard error of the mean for triplicate measurements from 5 independent transgenic lines.

Recombinant mPrP protein concentration in transgenic tobacco leaves was determined by ELISA analysis (Figure 4.4). The result indicates protein accumulation varied from 0.0004% TSP in in transgenic line C4 to 0.0024% TSP in transgenic line C7. Furthermore, the results show no apparent correlation between mPrP transcription levels and protein accumulation levels. This scenario is not unusual in transgenic plants since each transformation event results in a unique transgene location within the plant genome. The differences in mRNA transcription and protein translation rates, mRNA degradation rate and protein half-life accounts for the observed variation (Vogel and Marcotte, 2012).

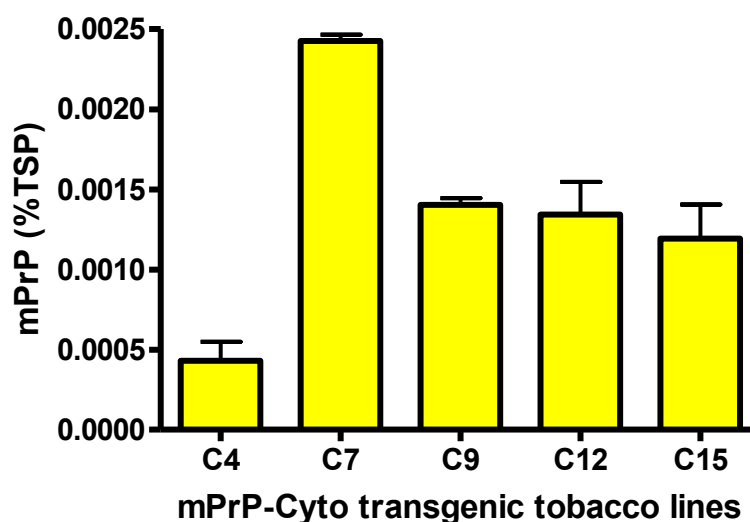


Figure 4.4: ELISA analysis of recombinant mPrP protein concentration in transgenic tobacco leaves transformed with the pGreen-35S-mPrP-Cyto construct. Data represents mean and standard error of the mean for duplicate measurements from 5 independent transgenic lines.

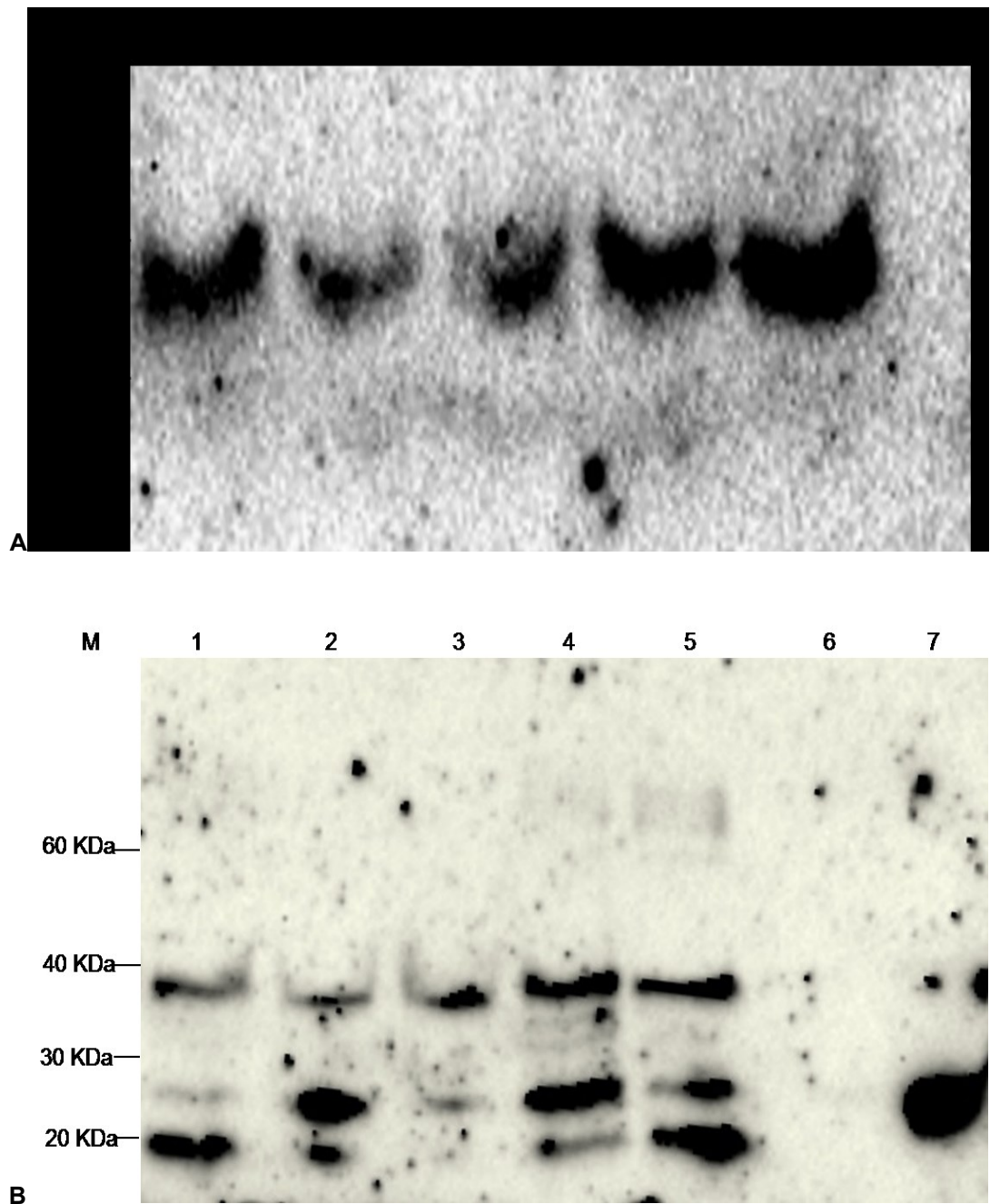


Figure 4.5: Western blot analysis of transgenic tobacco leaves transformed with the pGreen-35S-mPrP-Cyto construct. A: Membrane probed with PrP antibody C-20 (1:1,000 dilution). B: Membrane probed with HRP conjugated anti 6X-HisTag antibody (1:2,500 dilution). M: protein ladder. Lanes A6 & B6: Control – transgenic tobacco leaves transformed with the pGreen vector. Lane B7: Recombinant mPrP isolated from *E.coli*. Lanes A1-A5 and B1-B5: Transgenic lines C4, C7, C9, C12 and C15 respectively.

The molecular weight of the recombinant protein was determined by Western blot analysis using either a PrP antibody C-20 or an anti 6X His-tag antibody (Figure 4.5). His-tag antibody had a higher affinity for the recombinant mPrP protein than the PrP antibody due to the presence of additional histidine residues at the C-terminal end of the synthetic *PRNP* gene. His-tag antibody analysis indicated three bands. The ~24 kDa band indicates aglycosylated full-length mPrP while the ~19 kDa band represents aminoterminally truncated aglycosylated mPrP. The presence of the 19 kDa band when analysed with the His-tag antibody confirms N-terminal truncation. Finally the ~38 kDa band indicates the dimeric form of the truncated mPrP protein (19 kDa). Analysis with the C-20 PrP antibody indicated only the ~38 kDa dimer. The difference in antibody affinities accounts for the observed variation in the western blot assay. The results indicate effective production of recombinant mPrP in the cytosol of transgenic tobacco plants.

4.2.2 Analysis of transgenic plants transformed with the ER-mPrP construct

PCR analysis of transgenic tobacco plants transformed with the pGreen-35S-mPrP-ER construct yielded a 250 bp PCR product which confirms successful integration of the transgene into nuclear genome of the transgenic tobacco lines analysed (Figure 4.6).

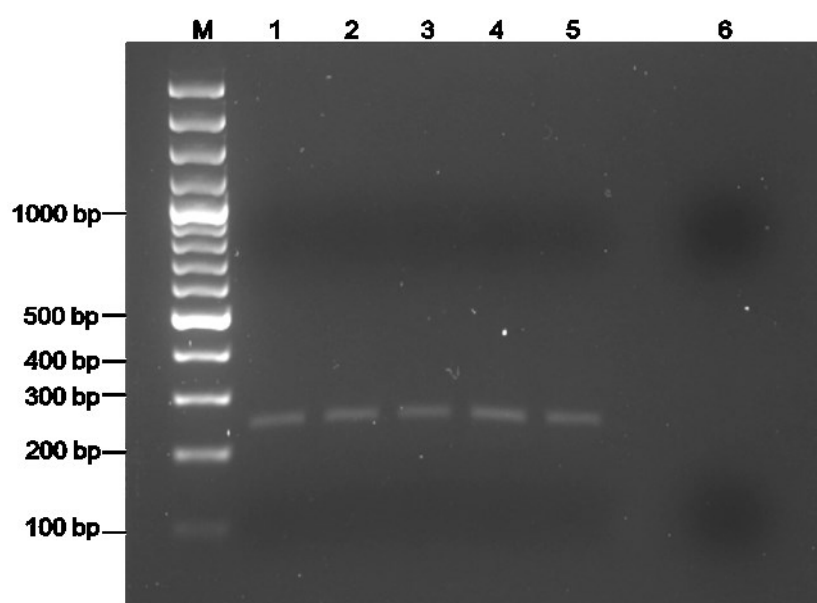


Figure 4.6: PCR analysis of transgenic tobacco leaves transformed with the pGreen-35S-mPrP-ER construct. M: DNA size marker. Lanes 1-5: DNA amplification product from transgenic lines E1, E2, E4, E7 and E10 respectively. Lane 6: Control – DNA amplification product from transgenic tobacco leaves transformed with the pGreen vector.

Expression levels of *PRNP* mRNA was established by qRT-PCR analysis (Figure 4.8). Transgenic line E1 was used as the calibrator, the result shows variation in the expression levels of *PRNP* mRNA. Transgenic line E10 had the highest expression level while E2 had lowest expression level. The variation in mPrP mRNA transcription level can be explained by epigenetic influences of flanking plant DNA and the chromosomal location of the transgene (Stam *et al.*, 1997; Matzke and Matzke, 1998). Also, *PRNP* mRNA transcripts were detected in RNA

isolated from the transgenic lines by the presence of a 250 bp amplicon after PCR analysis while no transcript was detected in RNA isolated from the control plant transformed with pGreen vector (Figure 4.7).

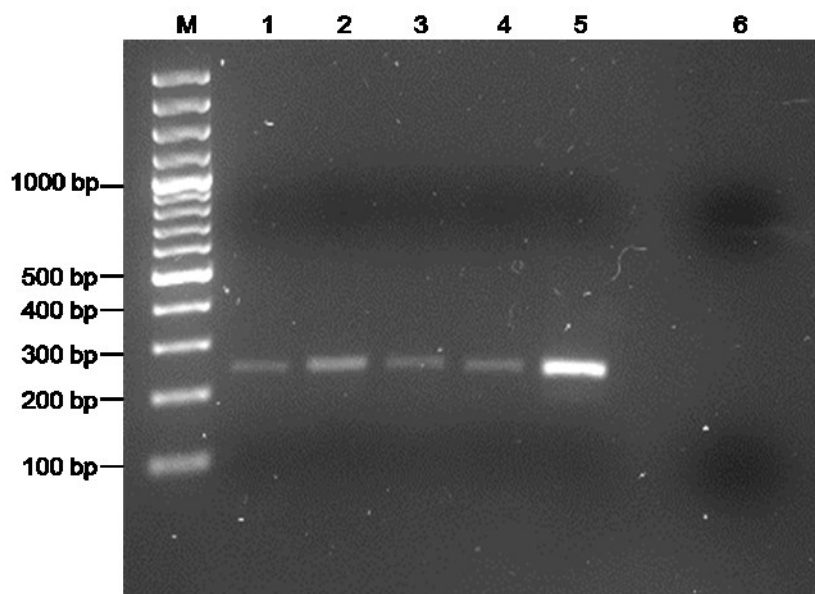


Figure 4.7: RT-PCR analysis of transgenic tobacco leaves transformed with the pGreen-35S-mPrP-ER construct. M: DNA size marker. Lanes 1-5: cDNA amplification product from transgenic lines E1, E2, E4, E7 and E10 respectively. Lane 6: Control – cDNA amplification product from transgenic tobacco leaves transformed with the pGreen vector.

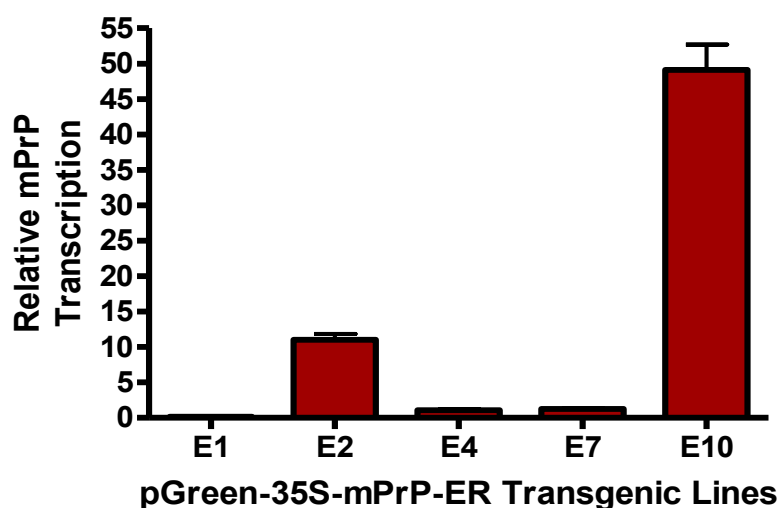


Figure 4.8: qRT-PCR analysis of mPrP expression levels in transgenic tobacco leaves transformed with the pGreen-35S-mPrP-ER construct. Data represents mean and standard error of the mean for triplicate measurements from 5 independent transgenic lines.

Recombinant mPrP accumulation and molecular weight was determined by ELISA analysis (Figure 4.9) and western blot analysis (Figure 4.10) respectively. ELISA analysis showed variation in recombinant mPrP protein levels across the selected transgenic lines. Transgenic line E4 had the highest expression level at 0.0016% TSP while E7 had the lowest expression level at 0.0003% TSP. Again, there was no apparent correlation between transgene expression and protein accumulation. Western blot detection with the His-tag antibody revealed 3 bands. The ~24 kDa band represents full-length unglycosylated mPrP protein, the ~31 kDa band represents the mPrP high mannose glycoform (Figure 4.10b; lanes 4 & 5) while the ~38 kDa band represents the dimeric form of the truncated unglycosylated mPrP. Comparatively, the ELISA assay result correlates with the result from the immunoblot analysis using the His-tag antibody. Analysis with PrP antibody C-20 indicated two bands after resolution, the ~38 kDa truncated dimer and ~31 kDa protein. The results show that various forms of the recombinant mPrP accumulated in transgenic plants transformed with the pGreen-35S-mPrP-ER construct.

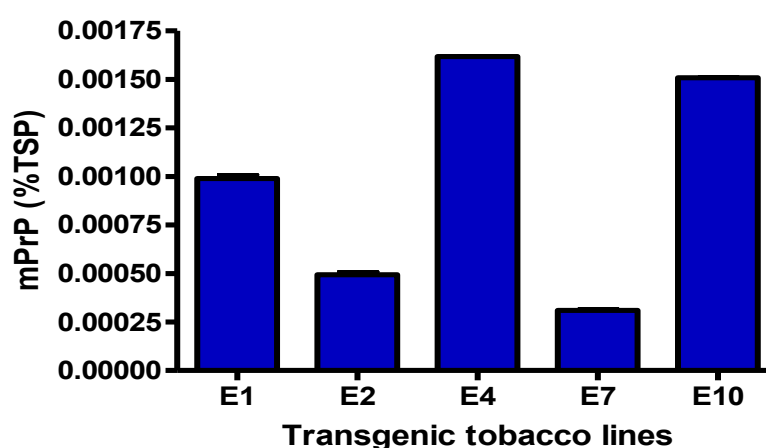


Figure 4.9: ELISA analysis of recombinant mPrP concentration in transgenic tobacco leaves transformed with the pGreen-35S-mPrP-ER construct. Data represents mean and standard error of the mean for duplicate measurements from 5 independent transgenic lines.

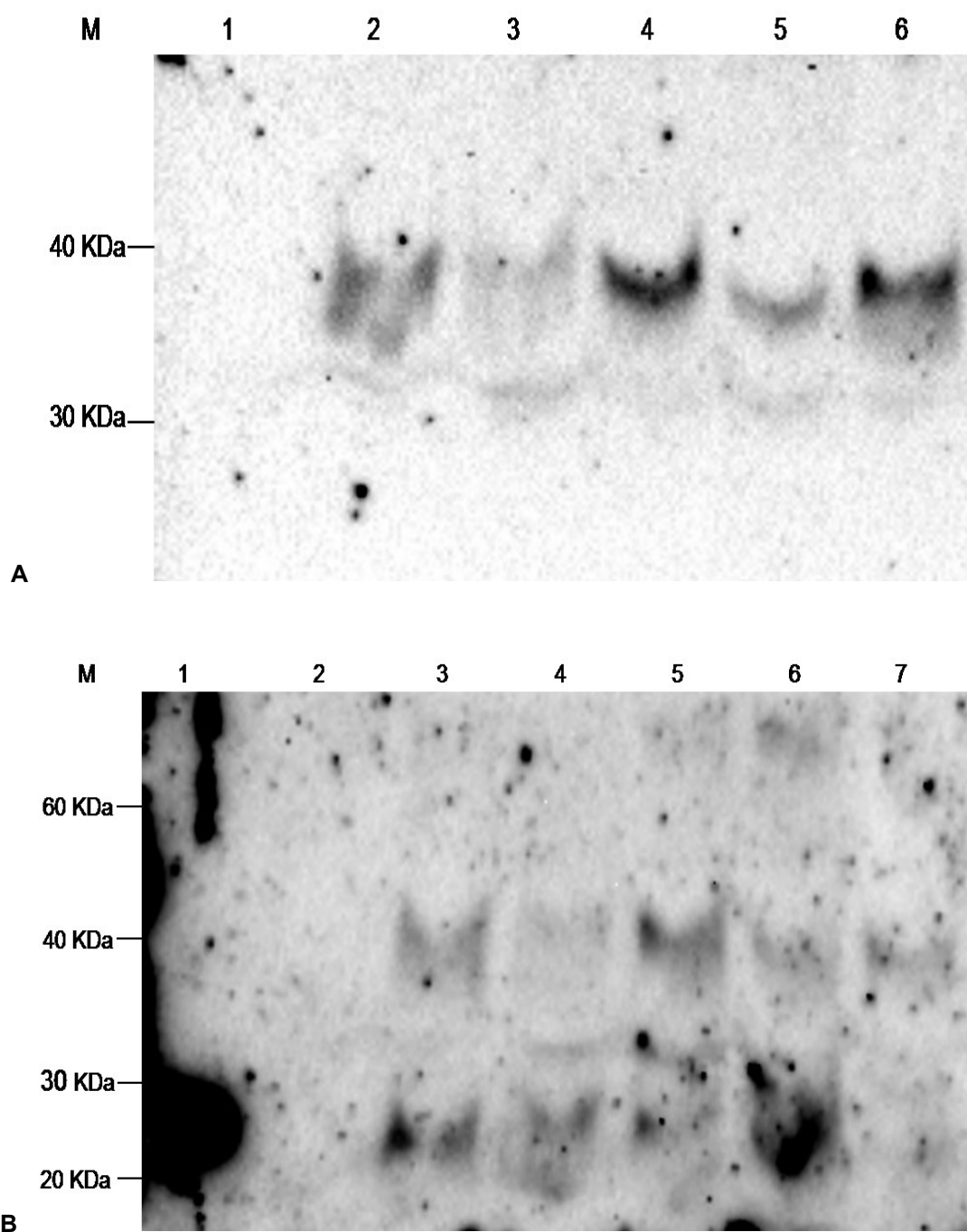


Figure 4.10: Western blot analysis of transgenic tobacco leaves transformed with the pGreen-35S-mPrP-ER construct. A: Membrane probed with PrP antibody C-20 (1:1,000 dilution). B: Membrane probed with HRP conjugated anti 6X-HisTag antibody (1:2,500 dilution). M: protein ladder. Lanes A1 & B2: Control – transgenic tobacco leaves transformed with the pGreen vector. Lane B1: Recombinant mouse prion protein isolated from *E.coli*. Lanes A2-A6 and B3-B7: Transgenic lines E1, E2, E4, E7 and E10 respectively.

Comparative analysis of recombinant protein from both constructs is shown in Figure 4.11. Analysis of recombinant mPrP sequestered in the endoplasmic reticulum with the PrP C-20 antibody indicated two bands of ~38kDa and ~31kDa in lane 2 representing the aminoterminally truncated dimer and the high mannose glycoform respectively while lane 1 showed only the ~38kDa aminoterminally truncated dimer.

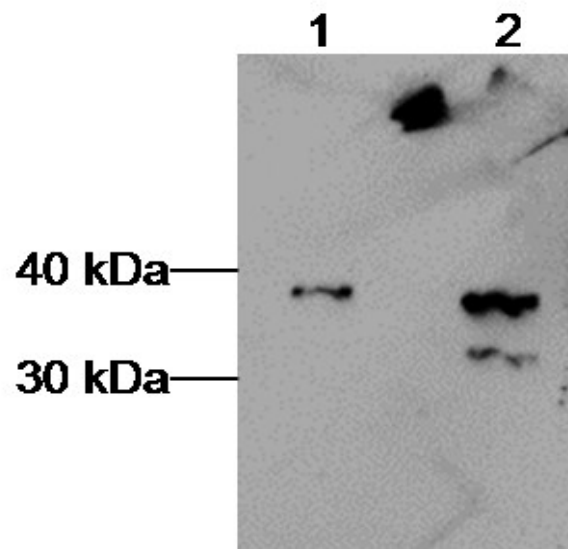


Figure 4.11: Comparative western analysis of recombinant mPrP transformed with the cytosolic construct (Lane 1) and the ER construct (Lane2) using PrP antibody C-20 (1:1000 dilution) Lane 1: Transgenic line C23. Lane 2: Transgenic line E1.

4.3 Discussion

The rate of cellular prion protein replication determines prion disease pathology. Therefore, the steps involved in PrP^C biogenesis and/or degradation pathway are important in demystifying the mechanisms of PrP^{Sc} pathogenesis (Taraboulos *et al.*, 1995; Holscher *et al.*, 2001; Neuendorf *et al.*, 2004; Kiachopoulos *et al.*, 2005). PrP^C is heterogeneously synthesized in several isoforms and differentially expressed at varying glycoform ratios in tissues and neurons (Pan *et al.*, 2002; Russelakis-Carneiro *et al.*, 2002). As shown in figure 4.12, PrP^C biosynthesis involves cotranslational import of the protein into the lumen of the endoplasmic reticulum via its N-terminal signal sequence. In the endoplasmic reticulum, the N-terminal and C-terminal GPI signal sequences are cleaved, disulphide bond is formed then the GPI anchor and N-linked core glycans are added. Correctly folded protein matures through the secretory pathway to the Golgi where the glycans are processed into complex structures that are trafficked via endosomes to the cell surface (Heske *et al.*, 2004; Wang *et al.*, 2006; Rambold *et al.*, 2006; Ashok and Hegde, 2008) while mutant and misfolded protein are sorted for degradation either by the ubiquitin proteasome system (UPS) of the cytosol, endoplasmic reticulum-associated degradation (ERAD) or post ER degradation via the lysosomal pathway (Ashok and Hegde, 2009). The PrP^C quality control pathway is complex, therefore, its dysregulation may significantly affect the physiology of an organism (Hegde *et al.*, 1998). Several studies have postulated that age-related defects in the quality control pathway of PrP^C may induce neurodegeneration (Russelakis-Carneiro *et al.*, 2002; Hetz and Soto, 2006; Ashok and Hegde, 2009).

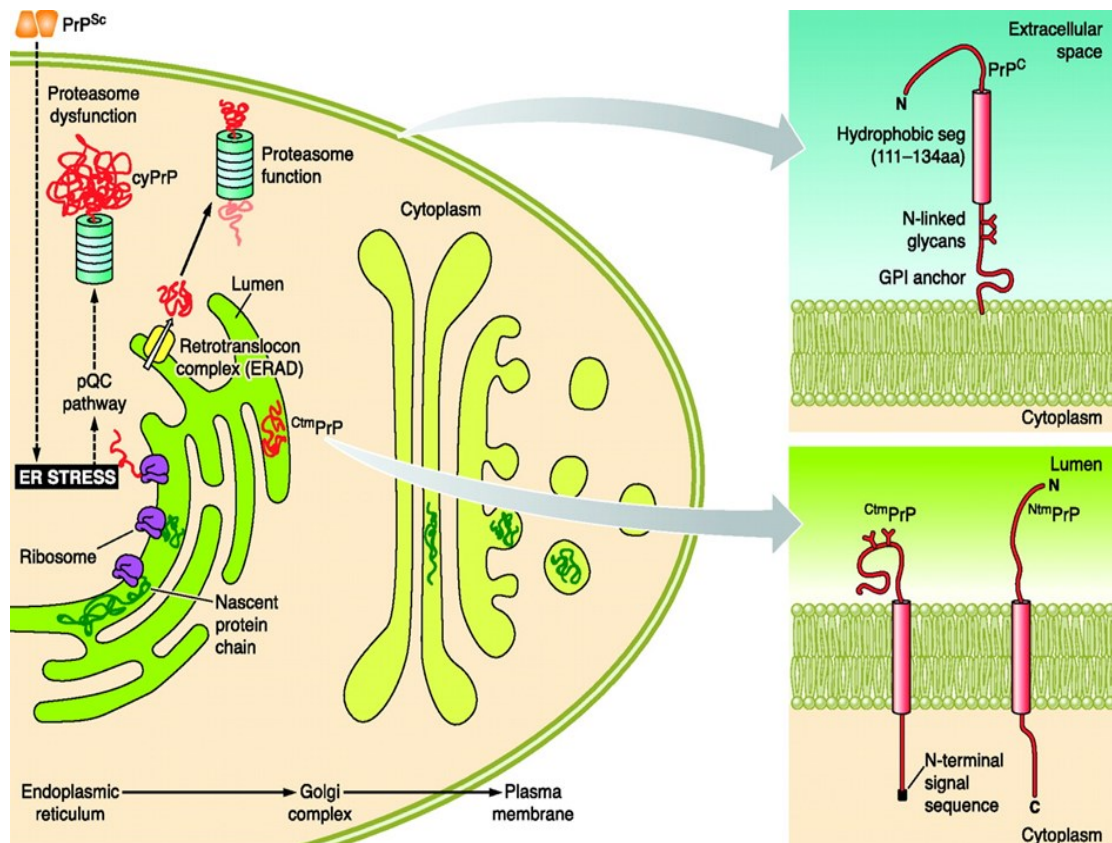


Figure 4.12: PrP quality control pathway
Reproduced from Aguzzi and Calella (2009)

The native N-terminal signal peptide of PrP^C is reported to be inefficient at translocating mutated PrP molecules with premature stop codon, linked to inherited prion diseases, to the ER compared to heterologous signal peptides (Holscher *et al.*, 2001; Heske *et al.*, 2004; Rane *et al.*, 2010). For instance, increased production of CtmPrP molecules associated with GSS syndrome, was limited by replacing PrP signal peptide with the extremely proficient signal peptide of prolactin (Prl) (Rane *et al.*, 2010). Also, Holscher *et al.* (2001) showed that mature PrP molecules with ablated N-terminal signal peptide were translocated to the endoplasmic reticulum via a signal sequence located in the C-terminal hydrophobic region of the prion protein, however, this process was inefficient and resulted in mainly CtmPrP molecules. In validation, Heske *et al.* (2004) showed

that the deletion of the C-terminal hydrophobic domain interfered with import of PrP molecules into the ER. This implies that a regulatory element in the C-terminal hydrophobic domain is important for efficient translocation to the endoplasmic reticulum, (Heske *et al.*, 2004; Rambold *et al.*, 2006. Norstrom *et al.*, 2007; Miesbauer *et al.*, 2010).

The prion protein N-terminal signal sequence and the C-terminal hydrophobic domain work in tandem for efficient translocation of PrP molecules to the ER. Therefore, pathogenic mutations in either the N-terminal signal sequence or the C-terminal hydrophobic domain results in accumulation of PrP in the cytosol or increased formation of the ^{Ctm}PrP transmembrane topology. The accumulation of PrP in the cytosol is a consolidatory feature of the neurodegenerative process in most prion disorders (Ma *et al.*, 2002; Kristiansen *et al.*, 2005; Rambold *et al.*, 2006; Norstrom *et al.*, 2007) and increased synthesis of ^{Ctm}PrP topological forms is an important marker of neurodegeneration in inherited prion diseases not associated with fibrillar PrP^{Sc} deposits (Hegde *et al.*, 1999). In neurons, the mutations W145Stop and Q160Stop linked to GSS syndrome, are associated with increased presence of cytosolic PrP due to impaired ER translocation in spite of the N-terminal signal sequence. Also, retrograde transport of misfolded prion protein via the ERAD pathway results in cytosolic accumulation of PrP (Yedidia *et al.*, 2001; Wang *et al.*, 2006).

Physiologically, cytosolic PrP is present at low levels in a subset of neurons found in the thalamus, hippocampus and neocortex and it protects primary neurons from Bax-mediated cell death (Mironov *et al.*, 2003; Wang *et al.*, 2006; Rambold *et al.*, 2006; Westergard *et al.*, 2007). Experimentally, overexpression of PrP^C and proteasome inhibition causes accumulation of cytosolic PrP with similar

biochemical properties to PrP^{Sc} in transfected cells (Ma and Lindquist, 2001; Hetz and Soto, 2006; Rambold *et al.*, 2006; Westergard *et al.*, 2007). Furthermore, cytosolic PrP produced by deleting the N-terminal signal sequence and C-terminal GPI signal sequence induced neurodegeneration in the cerebellar granular neurons of transgenic mice, with symptoms of prion disease including ataxia and gliosis (Ma *et al.*, 2002) and induced apoptosis in human neuroblastoma cell lines (Rambold *et al.*, 2006). Lastly, cytosolic PrP produced by inhibiting protease activity is specifically toxic to neuroblastoma cells (Ma and Lindquist, 2001) and cytosolic expression of recombinant PrP is toxic to yeast cells (Heller *et al.*, 2003).

Cytosolic PrP from various neuroblastoma cell lines and yeast had PrP^{Sc}-like properties including insolubility in non-ionic detergents, aggregation and protease resistance (Ma and Lindquist, 2001; Heller *et al.*, 2003; Rambold *et al.*, 2006; Norstrom *et al.*, 2007). However, cytosolic accumulation of PrP, due to overexpression of PrP^C is not neurotoxic (Kristiansen *et al.*, 2005). Also, Norstrom *et al.*, (2007) demonstrated that cytosolic PrP-associated neurotoxicity is independent of PrP^{Sc} infectivity and PrP^C expression. Hypothetically, the neurotoxicity of cytosolic PrP has been linked to its association with the lipid core of membranes (Heske *et al.*, 2004; Wang *et al.*, 2006, Westergard *et al.*, 2007; Miesbauer *et al.*, 2010) and its interaction with the anti-apoptotic protein B-cell lymphoma 2 (Bcl-2) (Rambold *et al.*, 2006).

In this study, cytosolic-mPrP was produced in plants by adding the mature peptide segment (PrP23-230) of the sequence to the transgene construct. The expression of cytosolic-mPrP in plants either generated membrane-associated PrP or the cytosolic mPrP binds to membrane associated protein(s) as leaves

lysed without detergent yielded low intensity immunoreactive bands (Appendix D) compared to leaves lysed with detergent added to the buffer (Figure 4.5 & Appendix C). In addition, western blot analysis of the recombinant mPrP showed three bands of ~19 kDa, ~24 kDa and ~38 kDa. Furthermore, transgenic tobacco plants transformed with the cytosolic construct had no visible or toxic phenotypical alternations except kanamycin treatment of the transgenic plants resulted in a non-rooting phenotype. Discussion on this aberrant phenotype is detailed in the next chapter.

The truncated 19 kDa protein indicates limited proteolysis resulting in truncation of the N-terminal segment of the recombinant protein (Pan *et al.*, 2002). The 19 kDa protease-resistant core is usually indicative of the aberrant PrP isomer (Ma and Lindquist, 2001). However, recombinant mPrP produced in bacteria was shown to be susceptible to limited proteolysis resulting in a truncated 19 kDa protein (Hornemann *et al.*, 1997). Additionally, studies examining the various PrP^C isoforms revealed that the truncated 19 kDa protein is also present in the brain tissues of healthy mice (Yedidia *et al.*, 2001; Pan *et al.*, 2002). Therefore, the presence of this fragment is not indicative of PrP^{Sc} molecules. In this study, as shown in Appendix A, recombinant mPrP from plants transformed with both the cytosolic and ER constructs was completely digested by proteinase K treatment indicating that the truncated 19 kDa protein doesn't represent a true PrP species.

The pathophysiological mechanisms of PrP^{Sc}-associated neurodegeneration may include changes in the expression, folding, topology, trafficking and subcellular localisation of PrP^C (Hegde *et al.*, 1998; Walmsley *et al.*, 2001; Russelakis-Carnerio *et al.*, 2002; Gasperini *et al.*, 2015). Post-translational

modifications of PrP^C especially glycosylation regulates the aforementioned processes (Heske *et al.*, 2004; Gasperini *et al.*, 2015). Modifications in the glycosylation pattern of PrP^C during aging has been linked to disease development (Gasperini *et al.*, 2015). Also, prion transmission alters the PrP^C glycoform patterns of infected tissues. For example, prion pathogenesis caused by infection with PrP^{Sc} strains ME7 and 139A, is associated with increased production of aglycosylated PrP^C (Russelakis-Carneiro *et al.*, 2002). Although, glycosylation is not essential for PrP^{Sc} infectivity, it influences the stability of PrP^C and therefore the incubation time for prion disease (Walmsley and Hooper, 2003; Neuendorf *et al.*, 2004).

Researchers have shown that the glycosylation pattern of PrP^C is determined by the presence of the GPI anchor and the membrane topology of PrP (Kiachopoulos *et al.*, 2005). Therefore, mutations that either disrupt the globular domain of PrP^C or change the acceptor amino acid in the GPI anchor signal sequence interferes with the processing of core glycans and addition of the GPI anchor, possibly inducing the generation of PrP^{Sc} isomers (Rogers *et al.*, 1993; Chesebro *et al.*, 2005; Kiachopoulos *et al.*, 2005; Puig *et al.*, 2016). Prion proteins that lack the GPI anchor are slowly trafficked through the endoplasmic reticulum and secreted as mainly the ~24 kDa aglycosylated or ~31 kDa high mannose glycoform (Kiachopoulos *et al.*, 2005; McNally *et al.*, 2009). For example, pathogenic PrP mutations PrPT183A and PrPF198S when synthesised lack the GPI anchor, have mainly high mannose glycoforms and are partially protease resistant (Kiachopoulos *et al.*, 2005).

Corroboratively, retention of wildtype PrP^C in the endoplasmic reticulum using ER-targeted anti-prion single chain variable fragments hindered the maturation

of the prion protein resulting in increased production of unglycosylated and high mannose PrP^C isoforms (Cardinale *et al.*, 2005). Furthermore, deletion of the GPI anchor signal sequence resulted in production of mainly unglycosylated PrP isoforms in scrapie infected mouse neuroblastoma cells (Rogers *et al.*, 1993) and transgenic mice (Chesebro *et al.*, 2005). In addition to the endoglycosidase H sensitive glycoforms, prion protein retained in the endoplasmic reticulum was insoluble in non-ionic detergents and had limited sensitivity to protease digestion indicating the protein was misfolded (Rambold *et al.*, 2006; Ashok and Hegde, 2008). Finally, prevention of complex glycosylation in geldamycin-treated neuroblastoma cells increased the formation of high mannose PrP glycoforms that were the ideal substrate for conversion of PrP^C to PrP^{Sc} in scrapie infected neuroblastoma cells (Winklhofer *et al.*, 2003). Conversely, Rambold *et al.* (2006) reported that PrP^{Sc} molecules in the ER were a poor substrate for prion propagation and non-toxic to cells. In addition, Walmsley *et al.* (2001) reported that prolonged retention of PrP^C in the endoplasmic reticulum by collapsing the Golgi did not induce glycosylation of the protein.

Recombinant mPrP was targeted to the endoplasmic reticulum of transgenic tobacco plants using a C-terminal SEKDEL retention sequence and the N-terminal signal peptide from PR1a. Western blot analysis revealed three bands with molecular weights of ~24 kDa indicating the full length prion protein, a ~31 kDa isomer possibly indicating the high mannose glycoform and a ~38 kDa truncated dimer. The results also indicate that the PR1a signal peptide translocated recombinant mPrP to the ER of transgenic tobacco plants although there was limited production of the ~31 kDa glycosylated isoform. The results in this study is consistent with reports from other studies that expressed GPI-ablated

PrP or ER-retained-PrP. Furthermore, a deglycosylation assay to determine if the 31 kDa band present in plants transformed with the ER construct represents glycosylated mPrP was inhibited by aggregation of the isolated recombinant protein as shown in Appendix B.

According to Ashok and Hegde (2008), A4 mutant cells unable to process the GPI anchor signal peptide produced PrP^C with high mannose glycoforms that were rapidly degraded with a half-life of 1-2 hours. This probably explains the low level of high mannose PrP glycoform seen in transgenic tobacco plants and mammalian cell lines. Walmsley and Hooper (2003) produced anchorless mature glycosylated PrP^C by modifying the GPI signal peptide of the protein. Therefore, mature glycosylated mPrP may be produced in plants using this modified peptide. However, given the conformational instability of PrP^C, addition of plant specific glycans may affect the structure of the prion protein. This can be rectified by using transgenic plants engineered to produce human glycans (Strasser *et al.*, 2009).

Misfolded PrP species are usually aggregates and are insoluble in non-ionic detergents (Yedidia *et al.*, 2001; Ma and Lindquist, 2001; Kiachopoulos *et al.*, 2005). Lysis with non-ionic detergent yielded oligomeric mPrP species of various molecular weight in plants transformed with both constructs indicating that the protein was probably synthesised in a misfolded isoform and aggregated (Section 6.2.2.2 – 6.2.2.5). Therefore, this study has shown that transgenic tobacco plants can successfully synthesise two mutant mPrP species in a similar manner to mammalian transgenic lines. However, expression levels of the protein were low with the highest expression level for plants transformed with the cytosolic construct at 0.0024% TSP and for plants transformed with the ER construct at

0.0016% TSP. A possible reason for the low expression levels of recombinant mPrP is its very short half-life. Wild-type PrP^C has a half-life of ~2.6 hours while N-terminally truncated PrP^C has a half-life of ~4.8 hours (Nunziante *et al.*, 2003).

This study has characterised recombinant mPrP targeted to different cellular compartments in transgenic tobacco leaves. As described earlier, comparable features of neurodegenerative diseases implies that understanding the pathological mechanism of any neurodegenerative disease may significantly impact diagnostics and therapy for other neurodegenerative diseases. Therefore, the infectious nature of the prion protein makes it uniquely primed for designing studies to explain the pathogenic mechanisms underlying neurodegenerative diseases (Ross and Poirier, 2004; Chiti and Dobson, 2006; Prusiner, 2012).

5 Phenotypic analysis of transgenic tobacco leaves expressing recombinant mPrP

5.1 Introduction

The prion protein binds several divalent metal ions mainly within its octapeptide repeat region. Therefore, several speculative functions were assigned to PrP^C in relation to metal homeostasis particularly copper transport and protection of cells against oxidative damage (Jackson *et al.*, 2001; Rana *et al.*, 2009; Singh *et al.*, 2010). Experimental evidence suggests that prion metal interactions have structural and functional consequences. For instance, PrP^C expressed in neuronal cells are endocytosed rapidly in the presence of physiological relevant concentrations of copper and zinc (Perera and Hooper, 2001). Furthermore, spectroscopic studies have shown that the unstructured N-terminal region of the prion protein undergoes a conformational change when bound to copper ions. Finally, PrP^C expression levels are affected by metal ions. For example, reducing dietary copper levels or increasing dietary manganese levels has a corresponding effect on PrP^C expression levels (Kralovicova *et al.*, 2009).

Metals are associated with the physiopathology of prion disease and prion pathogenesis is dependent on its association with Cu²⁺, Zn²⁺ and Mn²⁺ ions (Wong *et al.*, 2001; Lehmann, 2002). Researchers hypothesised that PrP^{Sc} results from metal altered conformation of PrP^C, hence PrP^{Sc} associated neurotoxicity is a deleterious consequence of metal dyshomeostasis (Lehmann, 2002; Rana *et al.*, 2009). Corroboratively, toxic levels of cuprizone a copper chelator induced histopathological changes similar to scrapie in mice (Pattison and Jebbet, 1971). Furthermore, metal induced free radicals expedite neurotoxicity in other neurodegenerative diseases including Alzheimer's, Huntington's and Parkinson's diseases (Lehmann, 2002; Singh *et al.*, 2010).

Various researchers have established a relationship between prion disease and metal ions. For example, Thackray *et al.* (2002) showed that manganese levels increased and copper levels decreased in the brain prior to clinical onset of prion disease. Additionally, manganese replaces copper competitively when bound to PrP^C (Brown *et al.* 2000) and alters recombinant PrP^C to PrP^{Sc} in a time dependant manner (Brown *et al.* 2000; Hesketh *et al.*, 2012).

Prion strain specific phenotype can be determined by the glycosylation pattern and conformation of a PrP^{Sc} specie (Collinge, 2001; Jackson, 2001). Since metal ion occupancy influences the conformation of PrP^{Sc} strains, therefore, PrP^{Sc} interaction with metal ions possibly explains the diversity of prion strains in human and animals (Wadsworth *et al.*, 1999). For example, two different strains of classical human CJD can be interconverted *in vitro* by altering their metal ion occupancy (Wadsworth *et al.*, 1999). Also, Brim *et al.* (2016) showed using high speed centrifugation that PrP^C–Zn²⁺ interaction reduces the solubility of full length glycosylated PrP^C while aminoterminally truncated full length PrP^C and unglycosylated PrP^C remained in solution. This study examines the possible phenotypic effects of expressing recombinant mPrP in transgenic tobacco plants.

5.2 Results

5.2.1 Kanamycin induced phenotypic changes in transgenic tobacco plants transformed with the pGreen-35S-mPrP-Cyto construct

To select tobacco transformants, regenerated shoots were excised from tobacco calli and transferred to MS media supplemented with kanamycin (100 µg/ml). Phenotypic alternations were observed in transgenic plants transformed with the pGreen-35S-mPrP-Cyto construct (Figure 5.1). All pGreen-35S-mPrP-Cyto transformants exhibited no root development while plants transformed with either the pGreen35SmPrP-ER construct or the control pGreen vector (Figure 5.2) developed roots when transplanted to MS media supplemented with kanamycin. However, transgenic plants transformed with the pGreen-35S-mPrP-Cyto construct developed roots when transplanted to MS media only (Figure 5.2).

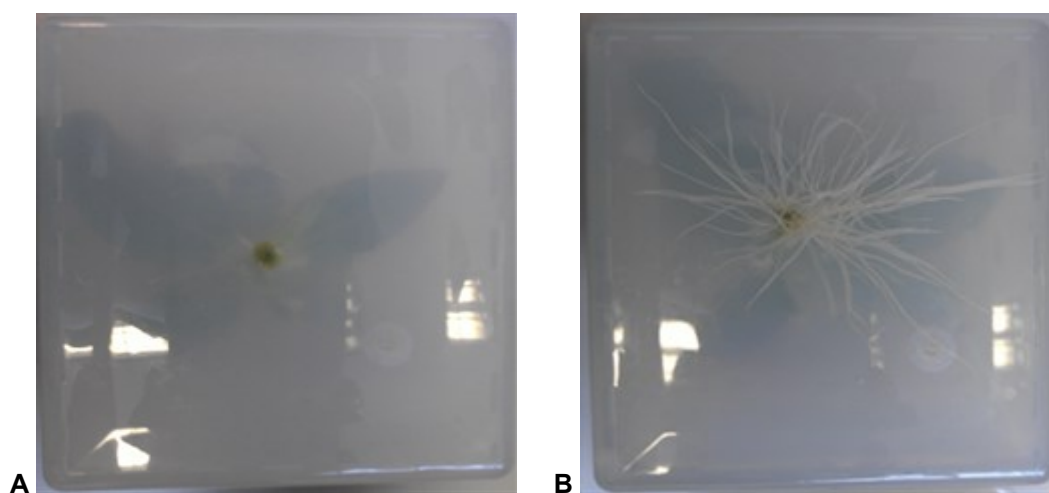


Figure 5.1: 15-day-old transgenic plant transformed with the pGreen-35S-mPrP-Cyto construct grown either in MS media supplemented with kanamycin (A) or MS media only (B).

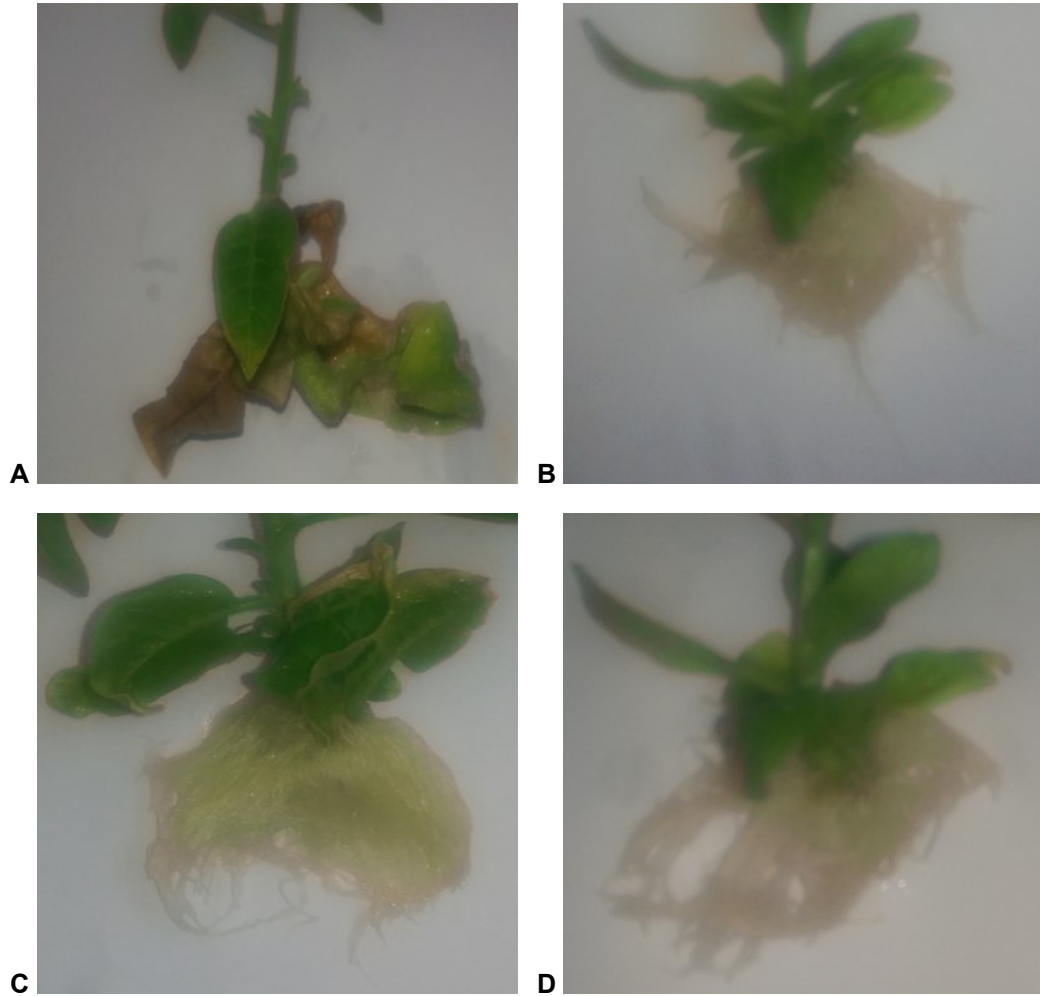


Figure 5.2: 30-day-old transgenic plants grown either in MS media supplemented with kanamycin: pGreen-35S-mPrP-Cyto construct (A) and pGreen construct (C) or MS media only: pGreen-35S-mPrP-Cyto construct (B) and pGreen construct (D)

5.2.2 Chemical analysis of transgenic tobacco plant leaves

To screen for possible phenotypic effects of expressing recombinant mPrP in transgenic tobacco plants, leaves from 30-day-old transgenic tobacco lines transformed with either the pGreen-35S-mPrP-Cyto construct (Lines C4, C9 and C12), pGreen-35S-mPrP-ER construct (Lines E1, E4 and E7) and control plants transformed with the pGreen vector (Lines P1, P2 and P3) were chemically analysed to determine the concentration of several macroelements and

microelements. The transgenic plants expressing recombinant mPrP were chosen based on similar RNA expression levels. Furthermore, the plants were either micropropagated in MS media only or MS media supplemented with kanamycin (100 µg/ml) to evaluate possible effects of the non-rooting phenotype exhibited by pGreen-35S-mPrP-Cyto constructs when exposed to kanamycin.

5.2.2.1 Analysis of macroelements

The macroelements nitrogen (N; Figure 5.3), phosphorus (P; Figure 5.4), potassium (K; Figure 5.5), calcium (C; Figure 5.6), and magnesium (Mg; Figure 5.7) were analysed.

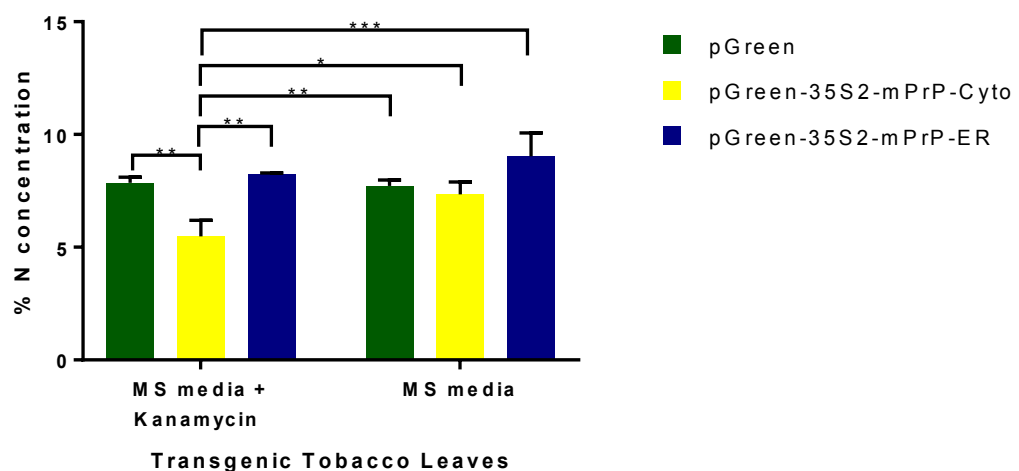


Figure 5.3: Comparison of nitrogen content of transgenic tobacco leaves from the pGreen, pGreen-35S2-mPrP-Cyto and pGreen-35S2-mPrP-ER constructs grown either in MS media or MS media supplemented with kanamycin (100 µg/ml). Data represents mean and standard error of mean of three independent plants from each construct. Two-way ANOVA with Bonferroni *post hoc* analysis indicates that subcellular localization of the recombinant mPrP factor and kanamycin factor each has a statistically significant effect on nitrogen concentration. Also, the interaction between both factors has a statistically significant effect on nitrogen concentration. Significant differences are depicted as * $P < 0.05$, ** $P < 0.001$, and *** $P < 0.0001$.

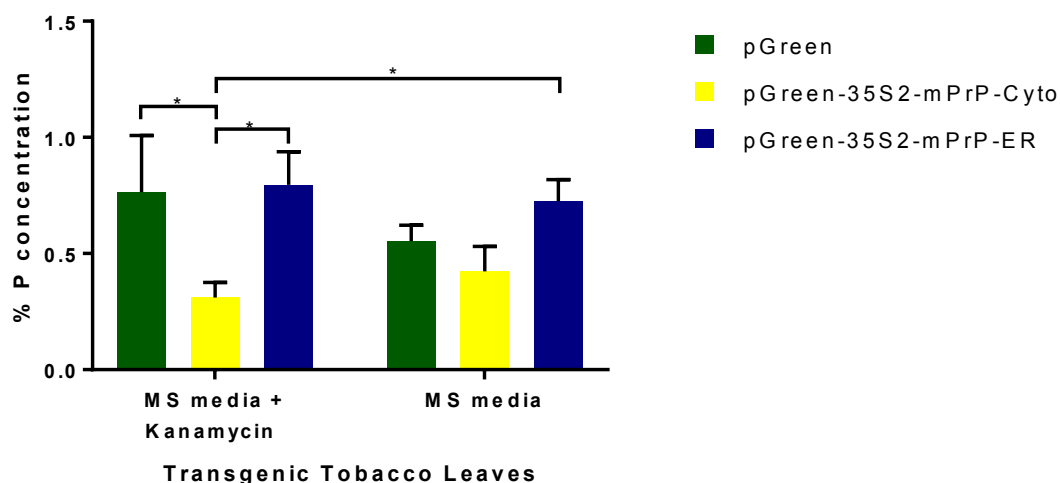


Figure 5.4: Comparison of phosphorus content of transgenic tobacco leaves from the pGreen, pGreen-35S2-mPrP-Cyto and pGreen-35S2-mPrP-ER constructs grown either in MS media or MS media supplemented with kanamycin (100 µg/ml). Data represents mean and standard error of mean of three independent plants from each construct. Two-way ANOVA analysis with Bonferroni *post hoc* analysis indicates that only the subcellular localization of the recombinant mPrP has a statistically significant effect on phosphorus concentration. Significant differences are depicted as $*P < 0.05$.

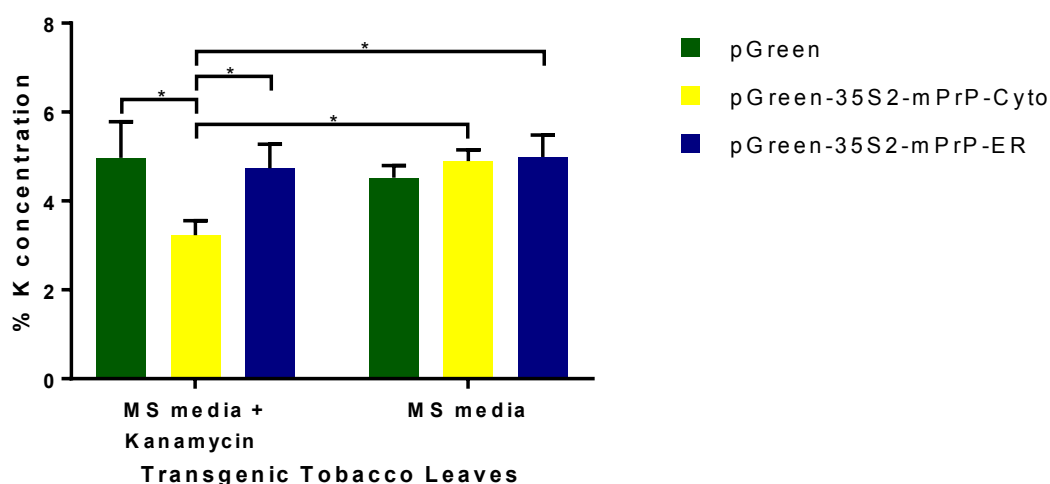


Figure 5.5: Comparison of potassium content of transgenic tobacco leaves from the pGreen, pGreen-35S2-mPrP-Cyto and pGreen-35S2-mPrP-ER constructs grown either in MS media or MS media supplemented with kanamycin (100 µg/ml). Data represents mean and standard error of mean of three independent plants from each construct. Two-way ANOVA analysis with Bonferroni *post hoc* analysis indicates the interaction between subcellular localization of the mPrP factor and kanamycin factor has a statistically significant effect on potassium concentration. Also, subcellular localization of the mPrP factor has a significant effect on potassium concentration. Significant differences are depicted as $*P < 0.05$.

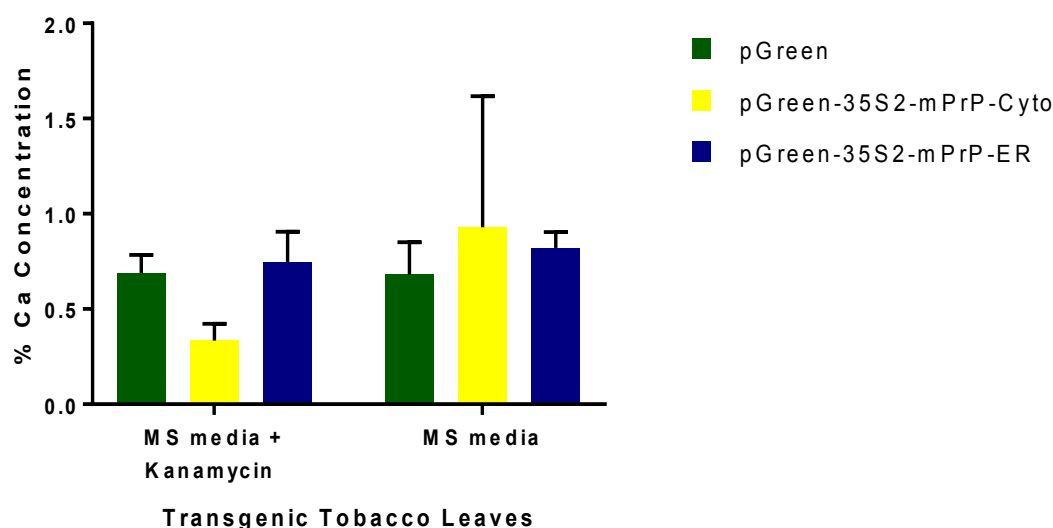


Figure 5.6: Comparison of calcium content of transgenic tobacco leaves from the pGreen, pGreen-35S2-mPrP-Cyto and pGreen-35S2-mPrP-ER constructs grown either in MS media or MS media supplemented with kanamycin (100 µg/ml). Data represents mean and standard error of mean of three independent plants from each construct. Two-way ANOVA analysis indicates no statistically significant effect on calcium concentration.

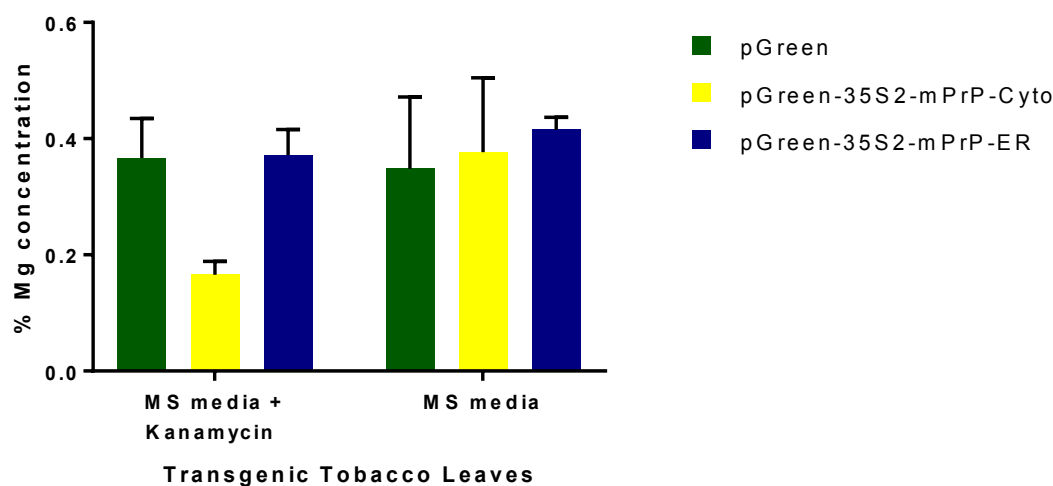


Figure 5.7: Comparison of magnesium content of transgenic tobacco leaves from the pGreen, pGreen-35S2-mPrP-Cyto and pGreen-35S2-mPrP-ER constructs grown either in MS media or MS media supplemented with kanamycin (100 µg/ml). Data represents mean and standard error of mean of three independent plants from each construct. Two-way ANOVA analysis indicates no statistically significant effect on magnesium concentration.

The results indicates that nitrogen concentration was affected by the subcellular localisation of the recombinant mPrP ($P < 0.0001$), kanamycin treatment ($P = 0.0093$) and the interaction of subcellular localisation and kanamycin treatment ($P = 0.00358$). Bonferroni *post hoc* analysis revealed that kanamycin-treated transgenic tobacco plants transformed with the pGreen-35S-mPrP-Cyto construct had reduced nitrogen concentration compared to untreated plants transformed with either the pGreen-35S-mPrP-Cyto construct ($P = 0.0296$), pGreen-35S-mPrP-ER construct ($P = 0.0001$) or pGreen vector (0.0073) and kanamycin-treated transgenic plants transformed with either the pGreen vector ($p = 0.0045$) or pGreen-35S-mPrP-ER construct ($P = 0.0013$).

Phosphorus concentration was significantly affected solely by the subcellular localisation of the recombinant protein ($P = 0.0008$). Transgenic leaves from kanamycin-treated plants transformed with the pGreen-35S-mPrP-Cyto construct had significantly reduced phosphorus concentration compared to kanamycin-treated plants transformed with either the pGreen vector ($P = 0.0207$) or pGreen-35S-mPrP-ER construct ($P = 0.0127$) and untreated plants transformed with the pGreen-35S-mPrP-ER construct ($P = 0.0398$) as observed by Bonferroni *post hoc* analysis.

Potassium concentration was significantly influenced by subcellular localisation of the recombinant mPrP (0.0316) and the interaction between kanamycin treatment and subcellular localisation ($P = 0.0087$). Bonferroni *post hoc* analysis showed that kanamycin-treated plants transformed with the pGreen-35S-mPrP-Cyto construct had significantly reduced potassium content compared to kanamycin-treated plants transformed with the pGreen vector ($P = 0.0142$) or pGreen-35S-mPrP-ER construct ($P = 0.0405$) and untreated plants transformed

with either the pGreen-35S-mPrP-Cyto construct ($P=0.0200$) or the pGreen-35S-mPrP-ER construct ($P=0.0132$). Kanamycin treatment, subcellular localisation and the interaction between subcellular localisation and kanamycin treatment had no significant effect on magnesium and calcium concentrations.

5.2.2.2 Analysis of microelements

The microelements iron (Fe; Figure 5.8), manganese (Mn; Figure 5.9), copper (Cu; Figure 5.10), boron (B; Figure 5.11), nickel (Ni; Figure 5.12) and zinc (Zn; Figure 5.13) were analysed.

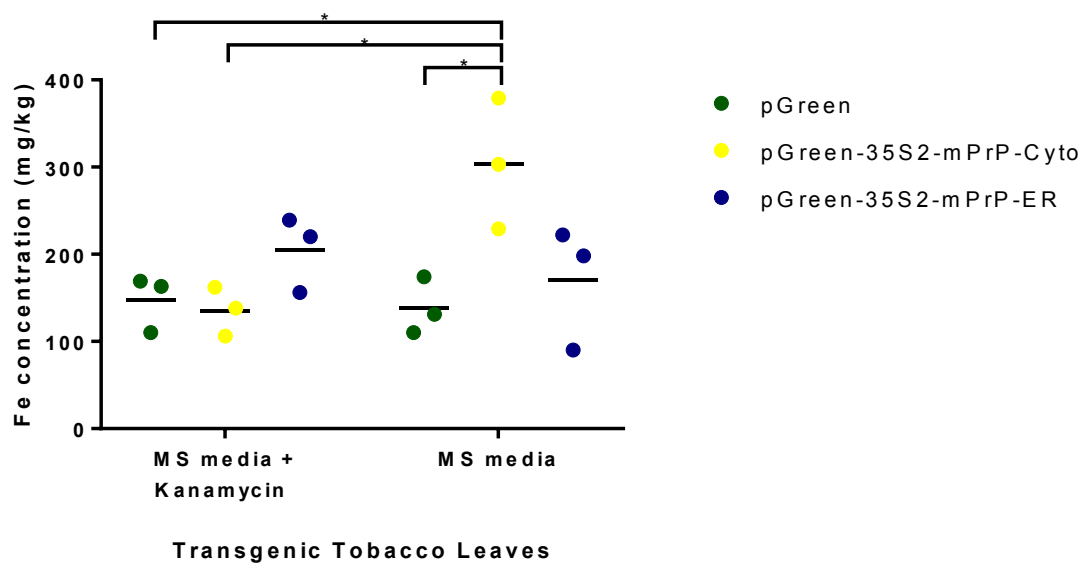


Figure 5.8: Comparison of iron content of transgenic tobacco leaves from the pGreen, pGreen-35S2-mPrP-Cyto and pGreen-35S2-mPrP-ER constructs grown either in MS media or MS media supplemented with kanamycin (100 µg/ml). Data and mean of three independent plants from each construct are depicted. Two-way ANOVA with Bonferroni *post hoc* analysis indicates the interaction between subcellular localization of the recombinant mPrP and kanamycin has a statistically significant effect on iron concentration. Significant differences are depicted as $*P<0.05$.

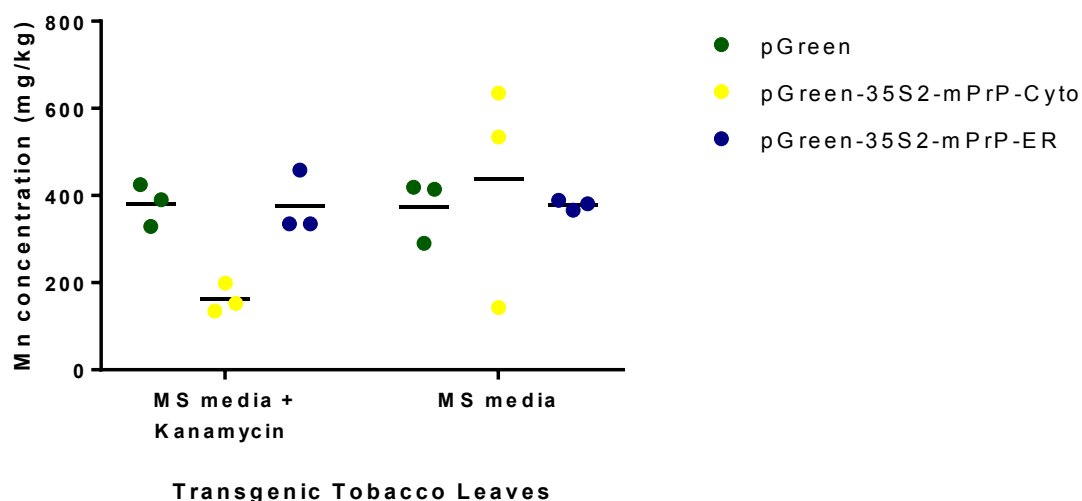


Figure 5.9: Comparison of manganese content of transgenic tobacco leaves from the pGreen, pGreen-35S2-mPrP-Cyto and pGreen-35S2-mPrP-ER constructs grown either in MS media or MS media supplemented with kanamycin (100 µg/ml). Data and mean of three independent plants from each construct are depicted. Two-way ANOVA analysis indicates no statistically significant effect on manganese concentration.

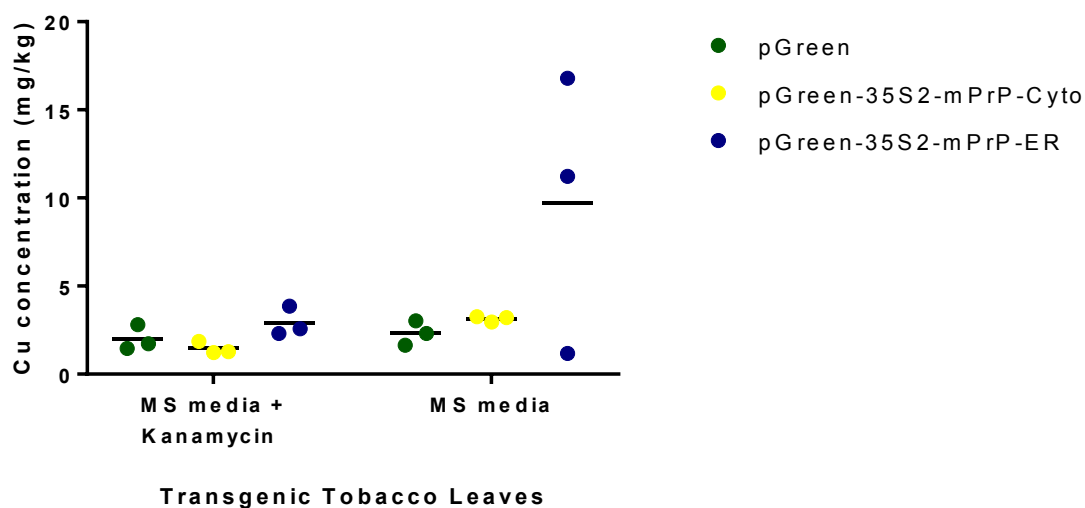


Figure 5.10: Comparison of copper content of transgenic tobacco leaves from the pGreen, pGreen-35S2-mPrP-Cyto and pGreen-35S2-mPrP-ER constructs grown either in MS media or MS media supplemented with kanamycin (100 µg/ml). Data and mean of three independent plants from each construct are depicted. Two-way ANOVA analysis indicates no statistically significant effect on copper concentration.

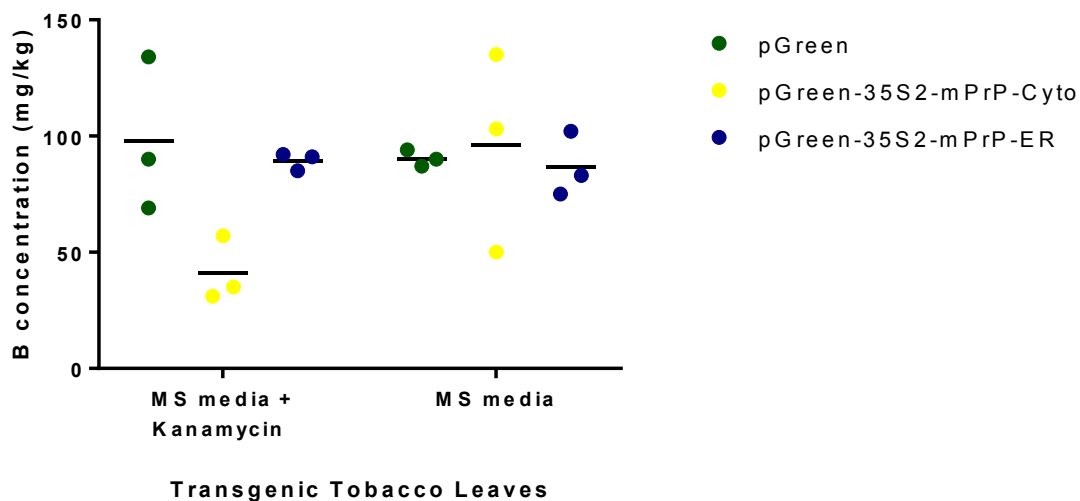


Figure 5.11: Comparison of boron content of transgenic tobacco leaves from the pGreen, pGreen-35S2-mPrP-Cyto and pGreen-35S2-mPrP-ER constructs grown either in MS media or MS media supplemented with kanamycin (100 µg/ml). Data and mean of three independent plants from each construct are depicted. Two-way ANOVA analysis indicates no statistically significant effect on boron concentration.

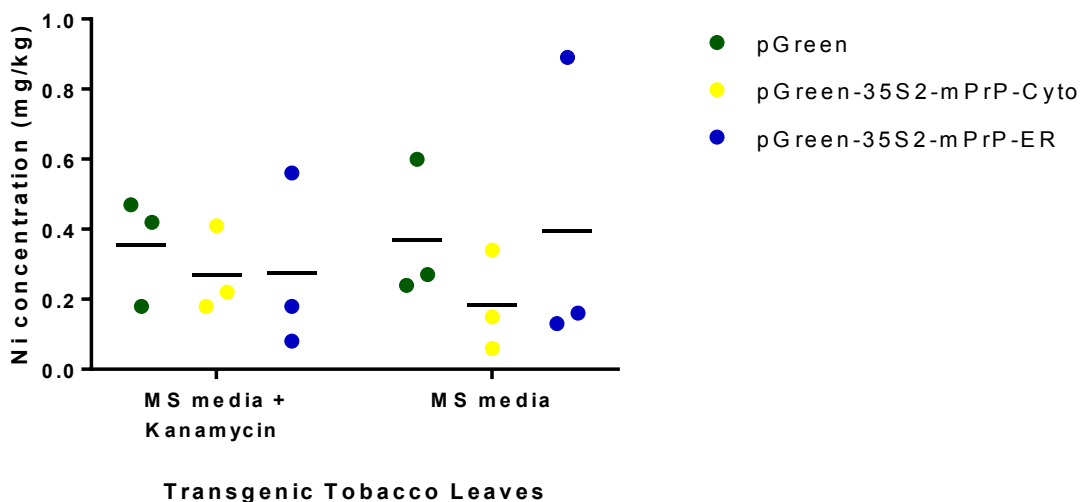


Figure 5.12: Comparison of nickel content of transgenic tobacco leaves from the pGreen, pGreen-35S2-mPrP-Cyto and pGreen-35S2-mPrP-ER constructs grown either in MS media or MS media supplemented with kanamycin (100 µg/ml). Data and mean of three independent plants from each construct are depicted. Two-way ANOVA analysis indicates no statistical significant effect on nickel concentration.

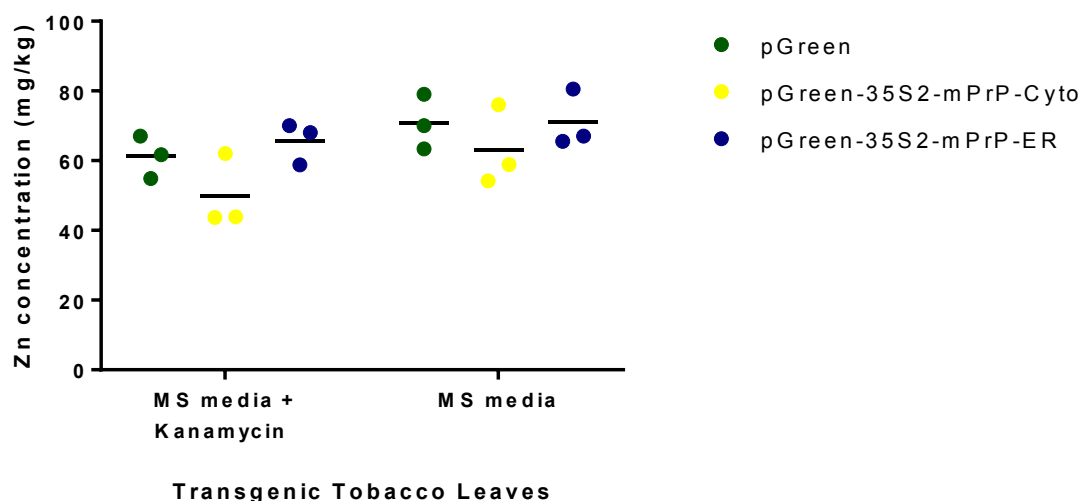


Figure 5.13: Comparison of zinc content of transgenic tobacco leaves from the pGreen, pGreen-35S2-mPrP-Cyto and pGreen-35S2-mPrP-ER constructs grown either in MS media or MS media supplemented with kanamycin (100 µg/ml). Data and mean of three independent plants from each construct are depicted. Two-way ANOVA analysis indicates that only kanamycin has a statistically significant effect on zinc concentration.

From the results, iron concentration was significantly influenced solely by the interaction of subcellular localisation of the recombinant mPrP and kanamycin treatment ($P=0.0089$). Bonferroni *post hoc* analysis showed that untreated leaves from plants transformed with the pGreen-35S-mPrP-Cyto construct had significantly higher concentration of iron than kanamycin-treated plants transformed with either the pGreen vector ($P=0.0391$) or the pGreen-35S-mPrP-Cyto construct ($P=0.0232$) and untreated plants transformed with the pGreen construct ($P=0.0264$).

Zinc concentration was significantly affected solely by kanamycin treatment ($P=0.0391$). However, Bonferroni *post hoc* analysis revealed no significant pairwise comparisons. Subcellular localisation of the recombinant mPrP, kanamycin treatment and their interaction had no significant effect on manganese, copper, boron and nickel concentrations. However, average

manganese concentration was increased in untreated transgenic lines transformed with cytosolic-mPrP compared to kanamycin-treated plants. Although, this result is not statistically significant because of the spread in the untreated data set. Similarly, the mean copper concentration was increased ~3-fold in transgenic lines transformed with the ER-mPrP construct compared to other tested transgenic lines and kanamycin-treated plants transformed with the pGreen-35S-mPrP-ER construct. However, this result is not significant due to the spread of the data.

5.2.3 Effect of recombinant prion expression and kanamycin treatment on peroxidase activity in transgenic tobacco leaves

Transgenic tobacco leaves were analysed to determine if recombinant mPrP expression had any effect on peroxidase activity of transgenic tobacco leaves. The transgenic lines analysed were identical to those used for chemical analysis. However, two way ANOVA analysis indicates that neither the subcellular localisation, kanamycin treatment nor their interaction had a statistically significant influence on peroxidase activity in the transgenic lines analysed.

Seemingly, recombinant mPrP may have a modulatory effect on peroxidase activity in transgenic tobacco plants. As shown in Figure 5.14, compared to the control plants, there was less interplant variability of peroxidase activity in plants transformed with both the pGreen-35S-mPrP-Cyto construct and the pGreen-35S-mPrP-ER construct grown on MS media only.

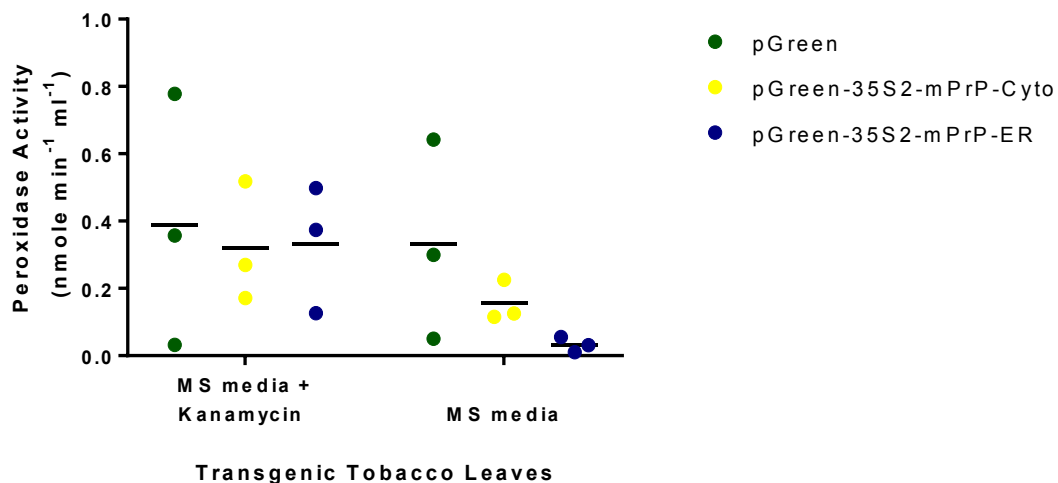


Figure 5.14: Peroxidase assay of transgenic tobacco leaves from the pGreen, pGreen-35S2-mPrP-Cyto and pGreen-35S2-mPrP-ER constructs grown either in MS media or MS media supplemented with kanamycin (100 µg/ml). Data and mean of three independent plants from each construct are depicted. Two-way ANOVA analysis indicates no statistically significant effect on peroxidase activity.

5.3 Discussion

Putative transgenic tobacco shoots were screened based on their resistance to kanamycin, an aminoglycoside antibiotic which has a negative effect on non-transformed shoots. Several studies have shown that in plants, aminoglycoside antibiotics binds to mitochondria and chloroplast ribosomes to subdue translation termination, cause misreading of the mRNA, interact with the plasma membrane and its receptors and at high concentrations inhibit protein synthesis (Padilla and Burgos, 2010). The transgene constructs used in this study included the selectable marker gene *NptI* which codes for neomycin phosphotransferase, a bacterial enzyme that inhibits the activity of aminoglycoside antibiotics (Yenofsky *et al.*, 1990). Transgenic plants transformed with the pGreen vector and the pGreen-35S-mPrP-ER construct developed roots when treated with kanamycin (100ug/ml). Unexpectedly, root morphogenesis was inhibited when transgenic tobacco plants transformed with the pGreen-35S-mPrP-Cyto construct were exposed to kanamycin treatment. Although, this effect was reversible when the transgenic plants were micropropagated on untreated MS media. Detailed analysis is required to determine the effect of kanamycin treatment on root morphogenesis in transgenic plants transformed with the cytosolic-mPrP construct.

The non-rooting phenotype occurred, possibly because transgenic tobacco plants expressing recombinant mPrP in the cytosol were all periclinal chimeras. Chimeric shoots may have reduced *nptI* activity, thereby not providing essential resistance levels to prevent kanamycin treatment from inhibiting root morphogenesis (Faize *et al.*, 2010; Schmulling and Schell, 1993). However, since identical pGreen vectors and procedures were used to transform all the

constructs this scenario seems highly implausible given the 100% prevalence of this effect amongst independent transgenic plants transformed with the pGreen-mPrP-35S-Cyto construct. Alternatively, recombinant mPrP may enhance the effect of kanamycin on plant cells. According to Padilla and Burgos (2010) growth media constituents affects kanamycin activity. For instance, chelators such as EDTA enhance the effect of kanamycin while Ca^{2+} alleviates the toxic effect of kanamycin. Nevertheless, the non-rooting phenomenon did not occur in plants transformed with the ER construct rendering this hypothesis improbable except the interaction of kanamycin is dependent on the subcellular localisation of the recombinant mPrP.

The most plausible explanation is that changes in essential nutrients profile of transgenic plants transformed with the cytosolic construct affected root initiation in the presence of kanamycin. For instance, primary root elongation is inhibited in *Arabidopsis thaliana* when grown on phosphate deficient soils in the presence of optimal iron levels, however, reduced iron concentration without increased phosphate concentration altered this phenotype (Ward *et al.*, 2008). Additionally, Niu *et al.* (2015) showed that root elongation directly correlates with the level of phosphorus in the growth medium and this effect was modulated by the level of magnesium in the medium. At high magnesium concentration, the effect of phosphorus on root elongation is enhanced while at low magnesium concentration the effect is reduced. In this study, nutrient analysis of various transgenic plants revealed that transgenic plants transformed with the cytosolic-mPrP construct had reduced phosphorus concentration compared to the other transgenic lines tested (Figure 5.4). Furthermore, phosphorus concentration is significantly reduced in kanamycin-treated transgenic plants expressing

cytosolic-mPrP compared to other kanamycin-treated transgenic lines. A possible explanation for upregulation of phosphorus in plants transformed with the pGreen vector and ER-mPrP construct after kanamycin treatment is that NptI inactivates kanamycin by phosphorylation. This implies that in the presence of kanamycin, phosphorus uptake is increased in transgenic plants, however, phosphorus concentration is reduced in plants transformed with the cytosolic-mPrP construct. Therefore, the non-rooting phenotype may be explained by the reduced availability of phosphorus in kanamycin-treated transgenic tobacco plants transformed with the cytosolic construct. If this theory is proven it indicates that phosphorylation assays may indicate accumulation of cytosolic PrP in cells. Although, this is dependent on analogous nutrient profiles in plant and mammalian cells overexpressing cytosolic-mPrP.

Mutation in tobacco *rac* gene causes a non-rooting phenotype in tobacco plants characterised by increased concentrations of auxin and the polyphenolic compounds chlorogenic acid and rutin (Lund *et al.*, 1997; Faivre-Rampant *et al.*, 2002). Kevers *et al.* (2001) showed that exogenous application of increasing concentrations of indole-3-butyric acid (IBA) and 1-naphthalene acetic acid (NAA) elicits a response in wild type shoot, increasing root proliferation at optimal concentration followed by inhibition at above optimal concentration whereas both homozygous and heterozygous *rac* mutants were nonresponsive. Furthermore, stem tips treated with chlorogenic acid accumulated auxin and did not develop adventitious roots compared to control plants (Faivre-Rampant *et al.*, 2002). In this study, attempts to induce rooting by supplementing growth media with NAA (5mg/L) did not reverse the kanamycin induced phenotype.

Plant neurobiologists dedicated to understanding signalling in plants have recognised analogies between the central nervous system and root cells at the apical meristem (Baluska *et al.*, 2006). For instance, the protein alastin is homologous to the RHD3 protein of *Arabidopsis*. Mutation in alastin causes hereditary spastic paraplegia a neurodegenerative disorder that affects the axons of the longest neurons and results in impaired control of leg muscles. Conversely, RHD3 protein is vital in *Arabidopsis* for the growth and development of root hairs (Baluska, 2010). Auxins are plant hormones with morphogen-like characteristics, essential for root development (Benkova *et al.*, 2009). The mechanisms of auxin transport is comparable to neurotransmitter release from neuronal cells. Also, auxins cooperate with cell wall peroxidases to induce the formation of reactive oxygen species which are important for plant signalling (Brenner *et al.*, 2006). Coincidentally, chlorogenic acid and rutin have been studied as therapeutic agents for neurodegenerative disorders. Chlorogenic acid may help alleviate neurodegenerative diseases such as ischemic stroke caused by glutamate neurotoxicity (Mikami and Yamazawa, 2015) while rutin due to its ability to chelate iron protects neurons from neurotoxicity of 6-hydroxydopamine (6-OHDA) which induces Parkinson's disease in rats (Khan *et al.*, 2012). Hypothetically, understanding the mechanism behind the inhibition of root development in kanamycin-treated transgenic plants expressing recombinant mPrP in the cytosol may offer insight into understanding the prion phenomenon.

In plants, shoots and roots are strongly interdependent on one another such that any factor that inhibits the development of one affects the other. Roots provides anchorage, synthesise hormones important for shoot development and absorbs water and inorganic nutrients from the soil or growth medium (Hodge *et al.*, 2009).

Expression of recombinant mPrP and kanamycin treatment modified nutrient uptake in plants and inhibited root morphogenesis in transgenic tobacco plants. Analysis of macronutrients showed that transgenic plants expressing recombinant mPrP in the cytosol had significantly reduced uptake of nitrogen, phosphorus and potassium. The non-rooting phenotype significantly affected nitrogen and phosphorus uptake. Furthermore, the subcellular localisation of the recombinant protein affected potassium, phosphorus and nitrogen concentration while kanamycin treatment significantly affected nitrogen concentration. Micronutrient analysis revealed that the interaction between kanamycin and cytosolic recombinant mPrP, conceivably responsible for the non-rooting phenotype significantly affected iron uptake. Compared to control plants and kanamycin-treated transgenic plants expressing cytosolic recombinant mPrP, iron concentration was significantly increased in untreated transgenic plants expressing recombinant mPrP in the cytosol while kanamycin significantly reduced the uptake of zinc in mPrP transgene constructs and the control plant. Kanamycin may act as a zinc chelator in MS media thus affecting its uptake by plants. Interestingly, the statistically significant differences observed in nutrient analysis is independent of recombinant mPrP concentrations in the transgenic plant lines analysed.

A literature search has revealed no direct association between the macronutrients, significantly affected by mPrP expression and/or kanamycin treatment of transgenic plants, and PrP^C or PrP^{Sc}. However, studies have revealed that PrP^C interacts with proteins involved in potassium ion transport. For instance, PrP^C binds potassium channel tetramerization domain containing protein (KCTD1) within its unstructured N-terminal region (Huang *et al.*, 2012)

and interacts with dipeptidyl aminopeptidase-like protein 6 (DPP6) to modulate A-type potassium currents (Mercer *et al.*, 2013). Also, phosphorus containing dendrimers interacts with PrP^C and prevents PrP^{Sc} accumulation in neuroblastoma cells. Alternatively, the observed effects on macroelements may be indirectly influenced by the effect of mPrP on microelements. Malakouti (2008) has shown that microelements especially iron influences the activity of macroelements.

PrP^C has been reported to act as a ferriredutase while pathogenesis of its aberrant isoform PrP^{Sc} is associated with iron dyshomeostasis (Singh *et al.*, 2010). According to Singh *et al.* (2009), aberrant prion protein sequesters ferritin into detergent insoluble PrP^{Sc}-ferritin complexes in PrP^{Sc} infected cells resulting in an iron deficiency phenotype. Subsequently, the phenotype induces upregulation of cellular iron content by upregulating transferrin and transferrin receptor and downregulating ferritin. However, iron is highly reactive and involved in the oxidative stress inducing Fenton and Haber-Weiss reactions. Therefore, iron dyshomeostasis probably induces neurotoxicity in prion disease (Singh *et al.*, 2014). Also, PrP^{Sc}-ferritin complex is associated with the transport of PrP^{Sc} across intestinal epithelial cells, probably enabling PrP^{Sc} infection across species barrier (Mishra *et al.*, 2004; Sunkesula *et al.*, 2010). Remarkably, ferritin is structurally conserved in plants and animals and studies in plant have associated ferritin with protection against the effects of oxidative stress (Briat *et al.*, 2010).

Compared to control plants manganese concentration increased in two transgenic lines expressing recombinant mPrP in the cytosol while copper concentration increased in two transgenic lines expressing recombinant mPrP in the endoplasmic reticulum. The variability in the result may be explained by

differences in protein concentration since samples were analysed from heterogeneous transgenic lines. This indicates that a threshold concentration may be required for PrP-metal interactions. The results also indicate that subcellular localisation affects the prion protein affinity for metal ions. Therefore, prion strains and characteristics are probably influenced by subcellular localisation of the aberrant prion protein. For instance, GSS and vCJD are associated with iron and ferritin deposits while iron deposits are absent in sCJD suggesting distinct pathogenesis pathways (Petersen *et al.*, 2005). Unexpectedly, the results show that kanamycin's interaction with the recombinant mPrP affects its ability to chelate Cu^{2+} ion, Mn^{2+} ions and regulate peroxidase activity in transgenic tobacco plants transformed with both mPrP constructs. Consequently, kanamycin should be investigated as a therapeutic agent against prion disease. However, kanamycin effectiveness as a therapeutic agent may be hindered by its inability to penetrate the blood brain barrier in adults (Nau *et al.*, 2010) and as stated earlier the possible harmful phenotype exhibited in kanamycin-treated transgenic plants expressing cytosolic recombinant mPrP.

A proposed function of the cellular prion protein is protection against oxidative stress via its influence of copper metabolism and superoxide dismutase (SOD) activity. This putative function is supported by *in vitro* recombinant prion protein superoxide dismutase-like activity, increased susceptibility to copper toxicity, oxidative stress and decreased Cu/Zn-SOD activity in *PRNP* ablated mice (Brown and Besinger, 1998; Brown *et al.*, 1999; Milhavet *et al.*, 2000). Contrarily, other *in vivo* studies suggest that PrP^{C} had no impact on SOD activity and no SOD-like activity (Hutter *et al.*, 2003). This study analysed the effect of expressing recombinant mPrP expression in the endoplasmic reticulum and cytosol on

peroxidase activity in transgenic tobacco leaves. Interestingly, the results showed that transgenic leaves treated with kanamycin and untreated control displayed variation in peroxidase activity while untreated plants expressing recombinant mPrP had less variable peroxidase activity. This suggests that the recombinant mPrP may have a modulatory effect on peroxidase activity in transgenic tobacco leaves. Brown and Besinger (1998) discovered that Tg35 cerebellar cells overexpressing PrP^C had increased glutathione peroxidase (GPX) expression and sensitivity to hydrogen peroxide compared to wildtype and *PRNP* ablated cells. Therefore, they hypothesised that increased superoxide dismutase activity increased the levels of hydrogen peroxide which induces oxidative stress. Alternatively, peroxidase contains haem and is probably affected by iron sequestration. Additionally, Rout *et al.* (2013) showed that copper toxicity reduced the activities of the antioxidant enzymes superoxide dismutase, glutathione peroxidase and catalase in *Withania somnifera* L. seedlings. Therefore, it is probable that overexpression of recombinant mPrP in transgenic tobacco leaves and its effect on metal homeostasis impaired peroxidase activity.

The aberrant isoform of the prion protein is neurotoxic and associated with increased susceptibility to oxidative stress. Reduced superoxide dismutase and glutathione peroxidase activity has been associated with impaired resistance to reactive oxygen species in prion infected and *PRNP* ablated cells and onset of clinical symptoms of prion disease in mice (White *et al.*, 1999; Wong *et al.*, 2001; Gudmundsdóttir *et al.*, 2008). For instance, hypothalamic neuronal GT1 cells infected with prions had drastically reduced glutathione and superoxide dismutase antioxidant activity compared to uninfected control cells (Milhavet *et al.*, 2000). Furthermore, analysis of glutathione peroxidase activity in ewes from

farms in scrapie infected and scrapie free area revealed that ewes from scrapie infected farms had significantly lower glutathione peroxidase activity (Gudmundsdóttir *et al.*, 2008). Therefore, it is conceivable that the transgenic tobacco leaves produces structurally aberrant recombinant mPrP in both the cytosol and endoplasmic reticulum.

6 Purification strategy for recombinant mPrP expressed in tobacco plants

6.1 Introduction

Prion research over several decades has generated significant information to support the infectious misfolded protein theory. Firstly, the genetic sequence of normal cellular prion protein has been isolated and cloned successfully (Lee *et al.*, 1998). Secondly, *PRNP* knockout mice are resistant to prion infectivity (Bueler *et al.*, 1992). Thirdly, the prion phenomenon occurs in yeast and other fungi, useful systems for studying the role of chaperones in prion infectivity (Wickner, 2007). Fourthly, novel infectious prion aggregates have been generated *in vitro* using recombinant prion protein produced in bacteria (Castilla *et al.*, 2005). Finally, development of protein misfolding cyclic amplification (PMCA) has the potential to improve prion disease diagnosis significantly (Saborio *et al.*, 2001). However, despite the advances in prion research, the biophysical and biochemical aspects of prion disease are still an enigma (Cobb and Surewicz, 2009). Therefore, research to elucidate the mechanism of prion propagation will require purified recombinant prion protein in substantial quantities for detailed studies of prion pathogenicity and the role of glycosylation in its conversion.

This study evaluates the possibility of purifying recombinant mouse prion protein from tobacco plants using IMAC technology. Recombinant mouse prion protein has been expressed in transgenic tobacco plants. To facilitate its purification, a C-terminal hexahistidine-tag was fused to the synthetic mouse prion gene. Histidine-tagged proteins are purified using immobilised metal affinity chromatography (IMAC) (Hochuli *et al.*, 1988). IMAC purification of affinity tagged proteins (Porath *et al.*, 1975) is cheap and usually only requires a single step process. Affinity purification of recombinant protein since its inception has been widely used to purify recombinant proteins from various heterologous expression

systems. Furthermore, greater than 60% of structurally studied proteins were purified via a polyhistidine-tag (Arnau *et al.*, 2006). Histidine affinity tails have been successfully used to purify recombinant proteins from tobacco plants (Leelavathi and Reddy, 2003; Lige *et al.*, 1998; Valdez-Ortiz, 2005). Bacterially expressed recombinant mouse prion protein has been purified using histidine affinity tails (Makarava and Baskakov, 2012).

6.2 Results

6.2.1 Purification Strategy

The purification strategy for recombinant mPrP is summarised in Figure 6.1. Transgenic tobacco leaves expressing recombinant mPrP were homogenised and dispersed in a variety of buffers (Table 2.2). the physicochemical properties of the two detergents used, Triton X-100 and CHAPS are reported in Table 2.3. The resulting lysate was centrifuged and the supernatant was either pretreated with ammonium sulphate fractionation prior to the IMAC step or passed directly through an IMAC column. Subsequently, various IMAC fractions were analysed for protein purity by SDS-PAGE or western blot.

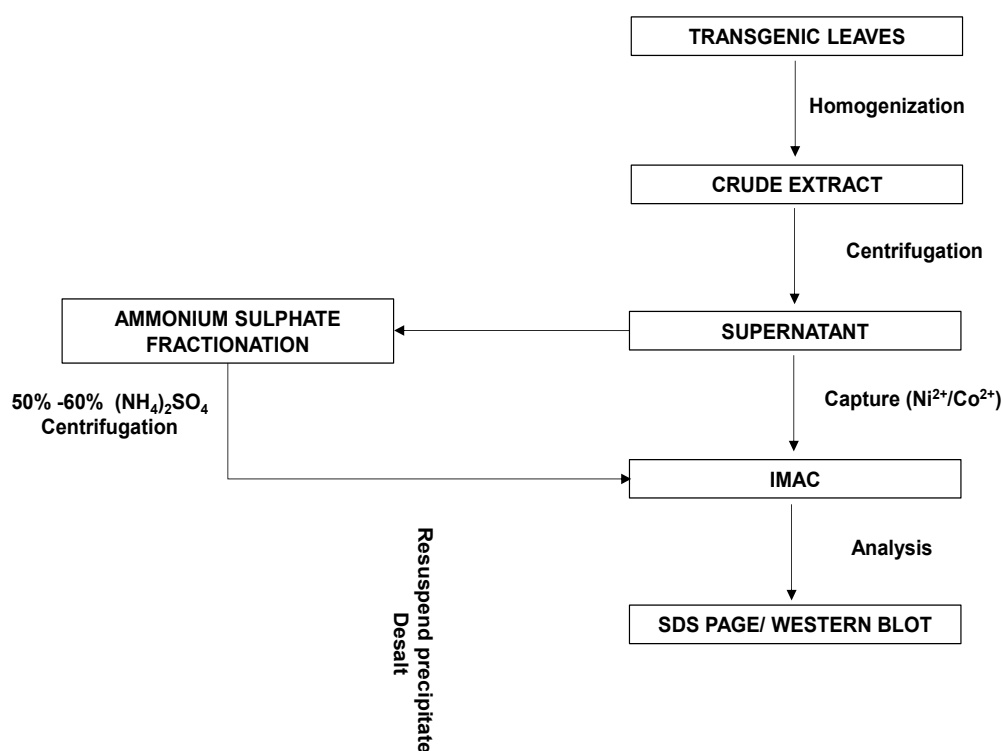


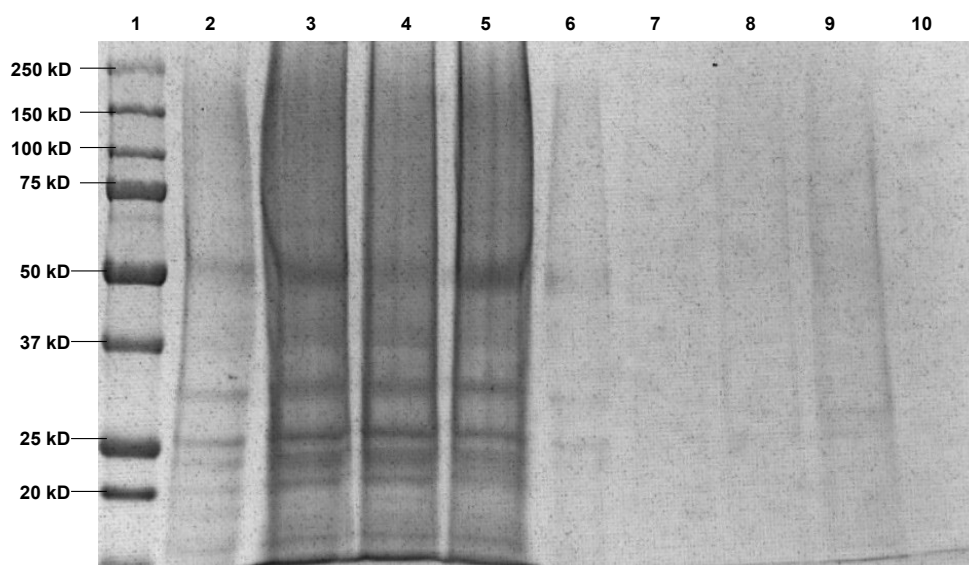
Figure 6.1: Flowchart of steps involved in recombinant mPrP extraction from transgenic tobacco plants

6.2.2 Extraction of recombinant mPrP

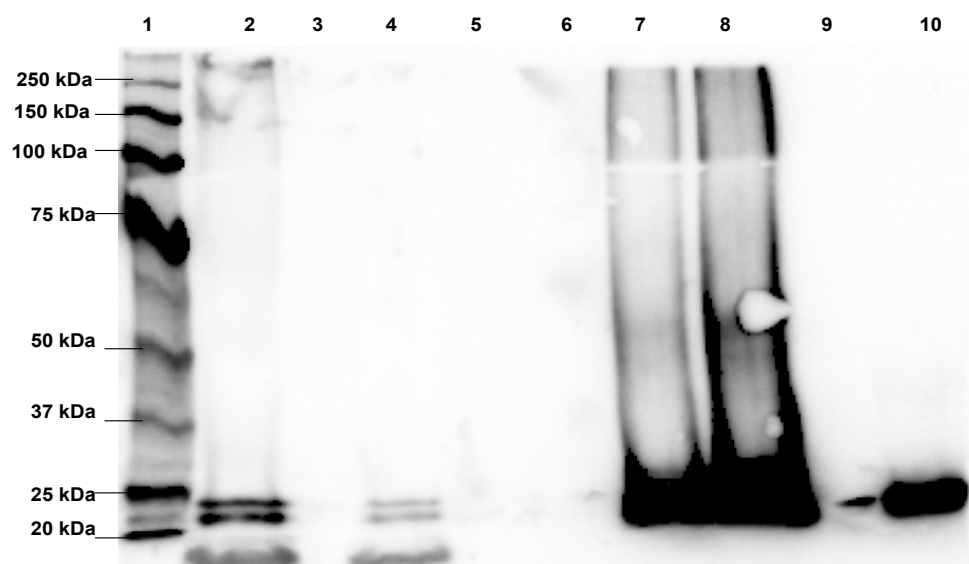
Membrane-associated recombinant mPrP was present in transgenic tobacco plants expressing both the cytosolic and the endoplasmic reticulum (ER) gene constructs. In an attempt to purify the recombinant protein using IMAC chromatography the leaves were lysed under various buffer conditions given in Table 2.2 and described below.

6.2.2.1 Transgenic leaves lysed with buffer A

Aglycosylated mPrP was expressed in the cytosol of transgenic tobacco leaves transformed with cytosolic-mPrP constructs. Homogenised transgenic leaves was mixed with buffer A at a 1:5 ratio (tissue: buffer). The mixture frozen in liquid nitrogen and thawed in a bath sonicator (Clifton MU-8) for 5 minutes. This process was repeated 10 times to lyse the cells prior to centrifugation. The clarified lysate subjected to IMAC purification using a HiTrap Chelating HP column (GE Healthcare) charged with nickel (Ni^{2+}) ions. From the result (Figure 6.2), a 24 kDa protein indicating the recombinant aglycosylated prion protein was successfully purified from the cytosolic fraction of transgenic leaves in a one-step IMAC process.



A



B

Figure 6.2: Purification of His-tagged cytosolic recombinant mPrP from transgenic tobacco leaves extract. Tobacco leaves were lysed with Buffer A and IMAC fractionated. Fractions were collected during the purification process and analysed by A) SDS-PAGE followed by coomassie blue staining and B) Western Blot, probed using HRP conjugated 6X-His-tag antibody (1:2,500 dilution). Lane 1: Protein standard. Lane 2: Lysate. Lane 3: Flow through. Lanes 4 – 6: Washes. Lanes 7 – 8: Eluates. Lane 10: Control – recombinant mPrP from *E. coli*.

6.2.2.2 Transgenic leaves lysed with buffer B

In order to extract the recombinant mPrP in its native form, transgenic plant leaves expressing both gene constructs and wild type tobacco plants were lysed with buffer B at a 1:10 ratio (tissue: buffer) and passed through a HiTrap Chelating HP column (GE Healthcare) charged with nickel (Ni^{2+}) ions. The eluate fractions were pooled, buffer exchanged to deionised water and concentrated using Pierce protein concentrators, 10K MWCO (Thermo Fisher Scientific). Fractions from plants expressing the transgenic constructs and the control plant were analysed by SDS-PAGE electrophoresis and western blot (Figure 6.3). From SDS-PAGE analysis, the recombinant protein was not purified to homogeneity (Figure 6.3 a). Western blot analysis (Figure 6.3 b) was negative for the wild type plant extract, eluate from transgenic plants expressing the ER constructs displayed a faint positive band of 24 kDa, similar to the control protein while the cytosolic construct eluate while eluate from the cytosolic construct indicated a strong positive band of approximately 60 kDa.

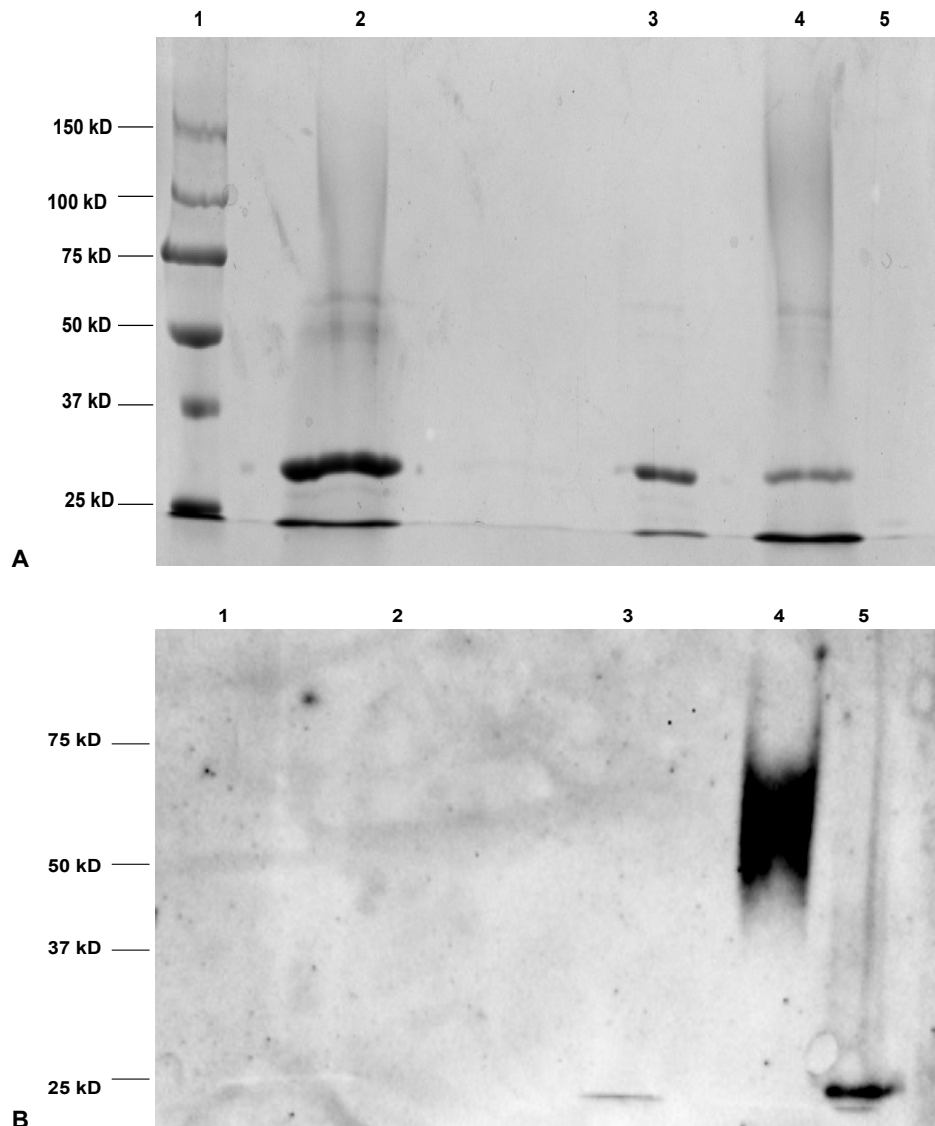


Figure 6.3: Purification of His-tagged recombinant mPrP from transgenic tobacco leaves extract. Tobacco leaves expressing both the cytosolic and ER constructs were lysed with Buffer B and IMAC fractionated. Fractions were collected during the purification process and analysed by A) SDS-PAGE followed by coomassie blue staining and B) Western Blot, probed using HRP conjugated 6X-His-tag antibody (1:2,500 dilution). Lane 1: Protein standard. Lane 2: Wild type eluate. Lane 3: Eluate from transgenic lines expressing mPrP in the ER. Lane 4: Eluate from transgenic lines expressing mPrP in the cytosol. Lane 5: Control – recombinant mPrP from *E. coli*.

6.2.2.3 Transgenic leaves lysed with buffer C

To investigate the lack of recombinant mPrP in the eluate lysed with buffer B, transgenic tobacco plants expressing cytosolic-mPrP were lysed with a denaturing buffer (Buffer C) at a 1:2 ratio (tissue: buffer). The clarified lysate was fractionated using HiTrap Chelating HP column (GE Healthcare) charged with nickel (Ni^{2+}) ions. The resultant fractions were analysed by western blot (Figure 6.4). The result suggests the recombinant mPrP misfolded as soluble aggregates present in the clarified lysate. Also, the recombinant protein was found in the flow through fraction, indicating that the prion aggregates had no affinity for nickel ions.

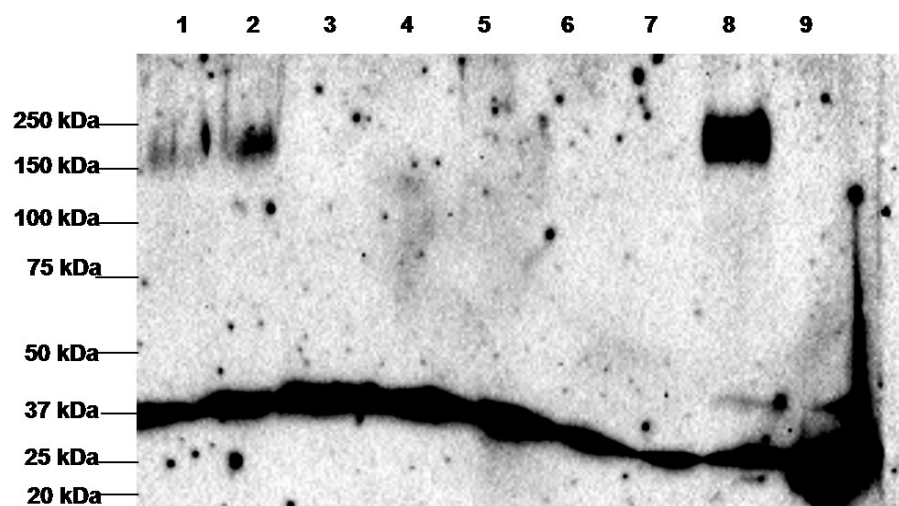


Figure 6.4: Purification of His-tagged cytosolic recombinant mPrP from transgenic tobacco leaves extract. Tobacco leaves were lysed with Buffer C and IMAC fractionated. Fractions were collected during the purification process and analysed by Western Blot, probed using HRP conjugated 6X-His-tag antibody (1:2,500 dilution). Lane 1: Lysate. Lane 2: Flow through. Lanes 3 – 5: Washes. Lanes 6 – 7: Eluates. Lane 8: Control 1 – crude extract from transgenic tobacco leaves expressing recombinant mPrP in the ER. Lane 9: Control 2 – recombinant mPrP from *E. coli*.

6.2.2.4 Ammonium Sulphate fractionation of extracts

To examine if soluble plant contaminants such as alkaloids affected recombinant mPrP solubility, transgenic tobacco leaves expressing the ER-mPrP construct were lysed with non-denaturing buffer C at a 1:5 ratio (tissue: buffer). The clarified lysate was fractionated using ammonium sulphate as described by Scopes (2013), the precipitate from various fractions were resuspended in buffer C and desalted prior to western blot analysis. Also, to determine if recombinant mPrP was completely solubilised, pellets obtained from crude lysate centrifugation were solubilised in Laemmli buffer at a 1:2 ratio, sonicated and incubated at 90°C for 10 minutes. Then, the clarified lysate analysed by western blot. From the result (Figure 6.5), recombinant mPrP was precipitated as a dimer in the 40% ammonium sulphate saturated fraction and as oligomers in both the 50% and 60% fractions. Therefore, the presence of plants alkaloids did not affect recombinant mPrP solubility. Additionally, no detectable level of recombinant mPrP was found in the pellets.

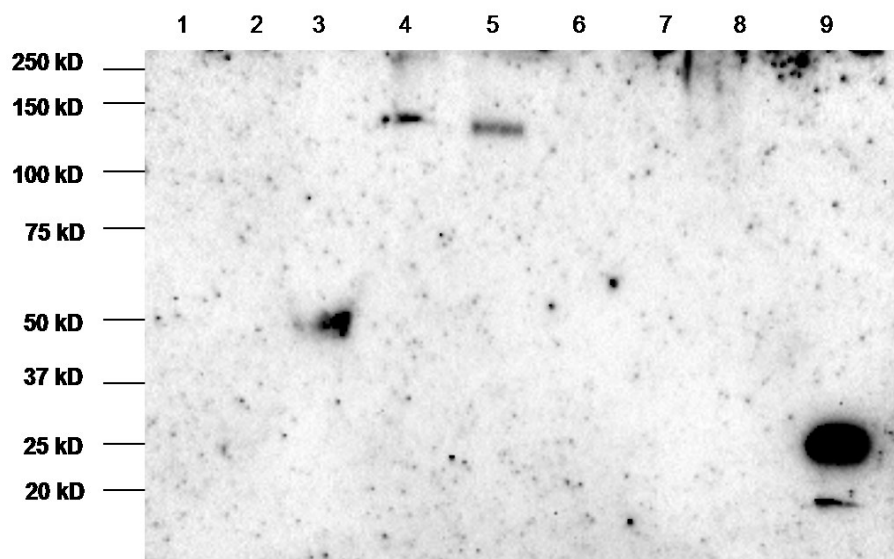


Figure 6.5: Ammonium sulphate fractionation of transgenic tobacco leaves expressing recombinant mPrP in the ER. Tobacco leaves were lysed with Buffer C without 8M urea, precipitated by ammonium sulphate in 10% fractions and the precipitate resuspended in Buffer C. Fractions were analysed by Western Blot, probed using HRP conjugated 6X-His-tag antibody (1:2,500 dilution). Lane 1: 20% precipitate. Lane 2: 30% precipitate. Lane 3: 40% precipitate. Lane 4: 50% precipitate. Lane 5: 60% precipitate. Lanes 7-8: Plant pellets solubilized in Laemmli buffer. Lane 9: Control – recombinant mPrP from *E. coli*.

6.2.2.5 Transgenic leaves lysed with buffers D and E

To determine if ionic strength had any effect on protein aggregation and protein affinity for nickel ions, transgenic plants expressing the ER constructs were lysed with medium and low ionic strength buffers (Buffers D and E) at a tissue to buffer ratio of 1:2. These buffers also included 2-mercaptoethanol, a reducing agent expected to break up aggregates linked by disulphide bonds. The clarified lysate was fractionated using His GraviTrap Talon column (GE Healthcare) charged with cobalt (Co^{2+}) ions. Various fractions were analysed by western blot as shown in Figure 6.6. The results indicate that medium ionic strength buffer (Buffer D) did not improve the binding efficiency of the recombinant protein while the low ionic strength buffer (Buffer E) improved binding affinity, but the bound recombinant

mPrP was eluted in the wash step. Neither buffer D nor buffer E improved recombinant mPrP solubility.

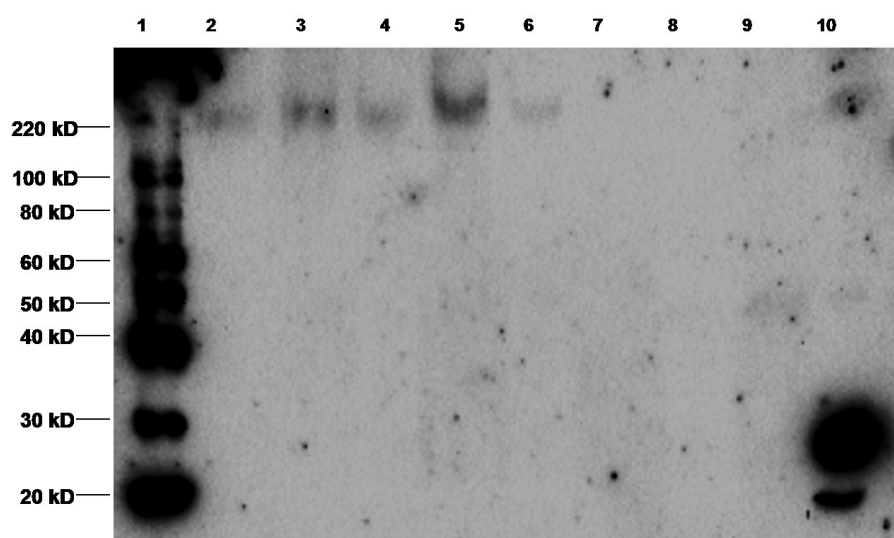


Figure 6.6: Purification of His-tagged recombinant mPrP from transgenic tobacco leaves extract. Tobacco leaves expressing recombinant mPrP in the ER were lysed with Buffer D or E and IMAC fractionated. Fractions were collected during the purification process and analysed by Western Blot, probed using HRP conjugated 6X-His-tag antibody (1:2,500 dilution). Lane 1: Protein standard. Lane 2: Buffer E Lysate. Lane 3: Buffer D lysate. Lane 4: Buffer E flow through. Lane 5: Buffer D flow through. Lane 6: Buffer E first wash. Lane 7: Buffer D first wash. Lane 8: Buffer E eluate. Lane 9: Buffer D eluate. Lane 10: Control – recombinant mPrP from *E. coli*.

6.2.2.6 Transgenic leaves lysed with buffer F

To investigate if the detergent triton X 100 had an effect on recombinant mPrP aggregation, transgenic tobacco leaves expressing the recombinant mPrP construct were lysed with buffer F at a 1:20 ratio (tissue: buffer). The clarified lysate was fractionated using His GraviTrap Talon column (GE Healthcare) charged with cobalt (Co^{2+}) ions. The resulting fractions were analysed by western blot as shown in Figure 6.7. From the result, lane 8 the eluted fraction contained heterogeneous bands. The high intensity ~19 kDa band represents unglycosylated aminoterminally truncated mPrP. A C-terminal histidine-tag was

used indicating that the truncation occurred in the N-terminal. The low intensity bands indicates ~24 kDa unglycosylated mPrP, ~31 kDa high mannose glycoform and the ~54 kDa unglycosylated dimer. Hence, changing the detergent and diluting the lysate improved the binding efficiency. However, only small quantities of the full length glycoforms were recovered. Therefore, more efficient lysis of transgenic plant is required to improve IMAC fractionation of the recombinant mPrP.

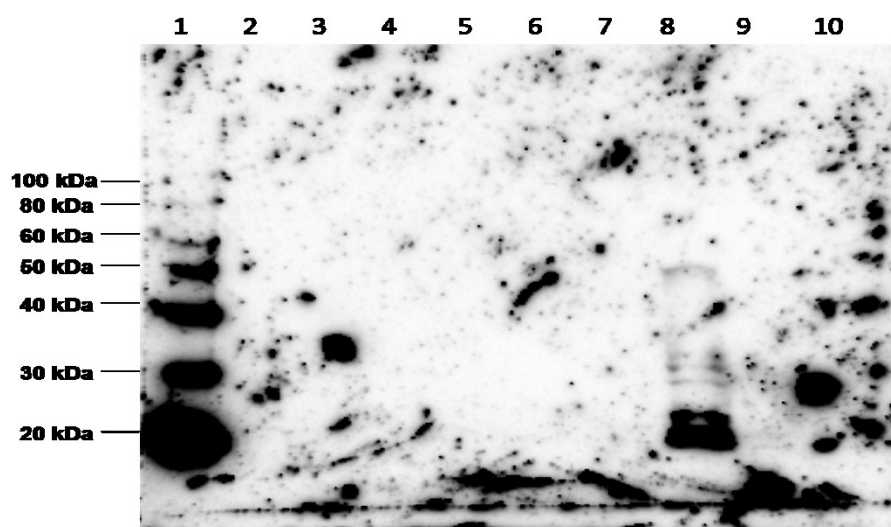


Figure 6.7: Purification of His-tagged recombinant mPrP from transgenic tobacco leaves extract. Tobacco leaves expressing recombinant mPrP in the ER were lysed with Buffer F and IMAC fractionated. Fractions were collected during the purification process and analysed by western blot, probed using HRP conjugated 6X-His-tag antibody (1:2,500 dilution). Lane 1: Protein standard. Lane 2: Lysate. Lane 3: Flow through. Lane 4 – 6: Washes. Lane 7: Eluate 1. Lane 8: Eluate 2. Lanes 9 & 10: Blank.

6.3 Discussion

Recombinant proteins produced in plant leaves are usually purified by chromatography based methods with purification strategies customised for each protein based on characteristics such as solubility, affinity to specific ligands, isoelectric point, size and charge (Chen, 2008; Wilken and Nikolov, 2012). Recombinant proteins are extracted by homogenisation in a buffer. The extraction process may be enhanced by evaluating buffer components, homogenisation technique, size distribution of particles in the extract, subcellular compartment of the recombinant protein and plant tissue to buffer ratio to limit molecular interactions between plant cell components and the recombinant protein (Wilken and Nikolov, 2012). Common buffer additives includes ascorbic acid, polyvinyl polypyrrolidone (PVPP), β -2-mercaptoethanol (B-ME) and dithiothreitol (DTT) to reduce phenolic compound interactions, detergents to solubilise membrane proteins and chlorophyll expressed proteins and proteases, antioxidants and metal chelators to prevent protein degradation (Wilken and Nikolov, 2012).

The leaf extract is clarified to separate the solid debris from the extract by dead-end filtration or centrifugation. At this stage, the clarified extracts contain various levels of phenolic compounds, alkaloids, native proteins, polysaccharides, DNA and chlorophyll pigments that foul the chromatographic resin and bind the recombinant protein, reducing the purification efficiency and quality of the recombinant protein. Therefore, the extracts are further conditioned or pre-treated, depending on the nature of the recombinant protein, by ammonium sulphate precipitation, acidification or aqueous two phase partitioning to remove contaminating plant elements and reduce native protein concentration (Wilken

and Nikolov, 2012). Acidification (Balasubramaniam *et al.*, 2003) and fractional ammonium sulphate precipitation (Desai *et al.*, 2002) removes native plant proteins including ribulose-1, 5-biphosphate carboxylase/oxygenase (rubisco) which accounts for about 50% of native plant proteins, cell debris, chlorophyll pigments and aggregates. Aqueous two-phase partitioning effectively removes plant alkaloids, phenolic compounds and reduce tobacco native proteins that foul the chromatographic resin (Chen, 2008; Platis *et al.*, 2008). Finally, proteins are purified mainly by a variety of adsorption chromatography methods as they offer higher resolution than other purification methods (Chen, 2008; Wilken and Nikolov, 2012). Recombinant antibodies expressed in tobacco plants are usually purified at above 90% purity by protein A or G affinity chromatography usually followed by an anion/cation exchange polish step (Vezina *et al.*, 2009; Bendandi *et al.*, 2010; Lai *et al.*, 2010). Recombinant fusion proteins are purified based on their affinity tags. For example, β -glucuronidase fused to calmodulin was purified from tobacco leaves based on the calcium dependent calmodulin affinity for phenothiazine affinity column (Desai *et al.*, 2002). Also, interferon gamma fused to His-tagged β -glucuronidase was purified from tobacco chloroplast in a two-step process of anion exchange chromatography followed by IMAC purification, with 75% protein yield (Leelavathi and Reddy, 2003).

The structural and chemical diversity of proteins requires elaborate downstream processes designed for isolating each protein, hence, affinity tags enables generic purification of a variety of recombinant proteins (Waugh, 2005). Hochuli *et al.* (1988) demonstrated that addition of polyhistidine-tags (H_6) to the polypeptide sequence of recombinant proteins facilitated its purification in a single step process using IMAC technology. The basis of IMAC technology is the

interaction between immobilised transition metal ions (Cu^{2+} , Ni^{2+} , Co^{2+} , Zn^{2+}) and imidazole side chains of histidine residues (Bornhorst and Falke, 2000; Arnau *et al.*, 2006). In addition to facilitating protein purification, polyhistidine-tag may affect the biochemical process of the protein positively by preventing proteolysis, protecting antigenicity, increasing solubility, improving yields and facilitating protein refolding. On the contrary, polyhistidine-tag may have a negative effect on the protein by hindering enzyme activity, changing the biological activity or structure of the protein and reducing protein yield. In cases when the polyhistidine-tag has a negative impact the tag may be cleaved by endoproteases or exopeptidases (Arnau *et al.*, 2006; Waugh, 2005).

IMAC purification of His-tagged proteins is cheap, easily scalable and optimised, protein can be purified denatured or in its native conformation. Also, IMAC resin is inexpensive, amenable to most buffers, has a high protein capacity (2-10mg/ml resin), and easily regenerated. Furthermore, purification is rapid often in a single step, up to 90% purity and 95% recovery of recombinant proteins have been achieved using IMAC technology (Bornhorst and Falke, 2000; Ueda *et al.*, 2003). However, proteins with low expression levels may not be adequately purified using IMAC technology. Such proteins may require another affinity tag or purification step (Bornhorst and Falke, 2000). Also, IMAC purification of membrane proteins have been problematic, His-tagged membrane proteins do not bind to IMAC resin when solubilised in certain detergents. This is because the detergent micelle around the protein-detergent complex may block access to the histidine-tag completely or partially. Usually detergents are screened to determine the most suitable for both protein solubilisation and purification.

Alternatively, longer histidine-tags (H₁₀) are used to improve the interaction between the recombinant protein and IMAC resin (Block *et al.*, 2009).

Purification of cellular prion protein (PrP^C) has been demonstrated in various expression systems. PrP^C was purified 13,000-fold with 17% recovery from Syrian hamster brain homogenates (Pan *et al.*, 1992). Microsomal fractions of homogenised Syrian hamster brain were solubilised with Triton X-114 digested with phosphatidylinositol-specific phospholipase C (PIPLC) to cleave the GPI anchor and phase partitioned at 37°C. The aqueous phase was precipitated with PEG and solubilised in 8% ZW 3-12, followed by IMAC fractionation and cation exchange chromatography. Finally, the enriched fractions were purified by SDS-PAGE electrophoresis. Also, recombinant mouse PrP^C expressed as insoluble inclusion bodies in *E. coli* BL21 (DE3) cells was purified by two cation exchange chromatography steps (Hornemann *et al.*, 1997). Recombinant mPrP inclusion bodies were solubilised in 8M urea, the denatured protein was purified by cation exchange chromatography and disulphide bond oxidised by atmospheric oxygen in the presence of 1µM Cu²⁺ catalyst. Subsequently, urea was removed by dialysis and refolded mPrP was purified to homogeneity by cation exchange chromatography. Furthermore, truncated recombinant mPrP (residues 23-230) expressed in Chinese hamster ovary CHOL761h cells was purified in its native form by low pressure cation exchange chromatography and IMAC steps or reverse chromatographic steps and the recombinant protein was resolved 98% pure by SDS-PAGE and silver staining analysis (Brimacombe *et al.*, 1999).

Detergents, because of their unique physical and chemical properties, interact with other molecules in a complex manner. Detergents solubilise hydrophobic and amphipathic molecules into mixed micelles or micellar aggregates at

concentrations above its critical micelle concentration (CMC) (Garavito and Ferguson-Miller, 2001). Detergents also associate with the hydrophobic surface of membrane proteins to create protein detergent complex (PDC) that are soluble in water. Researchers have observed that detergent micelles are quite fluid and can change micellar shape especially in the presence of proteins, lipids and other detergents. Therefore, solubilisation of a membrane protein depends on the choice of detergent, buffer composition, ionic conditions, detergent concentration, the presence of lipids and other proteins and experimental conditions (Fink, 1998; Garavito and Ferguson-Miller, 2001). Furthermore, membrane protein solubility depends on detergent-protein, detergent-detergent and detergent-lipid interactions. For instance, the flexibility and packing efficiency of protein-bound detergent monomers affects the stability and behaviour of the detergent layer. In turn, this detergent characteristic affects the solubility, stability and characterisation of membrane proteins and may result in inefficient protein solubility or protein aggregation (Garavito and Ferguson-Miller, 2001).

In prior attempts at prion purification, several detergents were tested for their ability to solubilise precipitated microsomal fractions of Syrian hamster brain homogenates. Pan *et al.* (1992) solubilised PEG precipitated pellets in either SDS, sarkosyl, triton x-100, triton x-114, β -octyl glucopyranoside or zwittergent 3-12. The pellets were almost completely solubilised by SDS and sarkosyl, β -octyl glucopyranoside and zwittergent 3-12 solubilised approximately 90% of the pellets while triton X-100 and triton x-114 solubilised 50% - 60% of the pellets. However, SDS and sarkosyl were unsuitable for IMAC fractionation but PrP^C binds to the Cu²⁺-IMAC resin in the presence of other detergents. In another study Turk *et al.* (1988), examined the effect of detergents and chaotropes on the

adsorption of PrP^C to immobilised monoclonal antibody. PrP^C did not effectively bind the immobilised antibody in the presence of 1% Nonidet P-40, 0.5% CHAPS, or 0.5% sodium cholate while 0.5% zwittergent 3-14, 0.5% zwittergent 3-16, and 0.5% sodium deoxycholate increased the affinity of PrP^C for the immobilised antibody. The most effective detergent for affinity purification of PrP^C were the zwittergent series and their effectiveness was improved in the presence of 0.3M guanidum thiocyanate.

In this study, attempts to purify the His-tagged recombinant prion proteins from mature leaves of transgenic tobacco plants expressing either the cytosolic or endoplasmic reticulum constructs were based on IMAC chromatography utilising a C-terminal histidine-tag added to the expression construct. Aglycosylated recombinant prion protein were successfully purified from the cytosol in a one step process using buffer A. However, recombinant mPrP was prone to aggregation when extracted with the non-ionic detergent triton X-100. Presumably, aggregation affected the accessibility of the histidine-tag, to the metal ions used as affinity ligands resulting in loss of the protein in the flow through and wash eluates. Altering the buffer composition by varying salt concentration, buffer compounds and use of denaturing agents had no effect on disaggregating recombinant mPrP soluble aggregates or improving the adsorption of the recombinant mPrP on IMAC columns. Furthermore, ammonium sulphate precipitation to remove plant phenolic compounds from the recombinant protein had no effect on the prion aggregates or their affinity for metal ions. However, diluting the lysate 20-fold in buffer F which contained the zwitterionic detergent CHAPS resulted in eluted protein although most of the eluted protein appeared to be truncated by limited proteolysis showing a molecular weight of ~

19 kDa on SDS-PAGE (Figure 6.7). Essentially, the zwittergent detergents were compatible with immunoaffinity chromatography and IMAC chromatography in PrP^C purification from Syrian hamster brain homogenates (Pan *et al.*, 1992; Turk *et al.*, 1988), thus may solubilise recombinant PrP^C expressed in transgenic tobacco plants

Inexplicably, buffer B lysates were negative in all western blot experiments, thus buffer eluates were buffer exchanged to deionised water before the blotting procedure. Subsequent changes in the buffer composition improved the quality of the blots, perhaps due to increased concentration of the lysate. Also, addition of 8M urea did not improve the solubility of the recombinant mPrP aggregates in the presence of triton X-100, indicating that possibly the hydrophobic core of the protein detergent complex was inaccessible to urea. This phenomenon was observed by (Ruiz and Sanchez, 1994) who demonstrated using fluorescent probes that urea has no effect on the micellar core of triton X-100. Furthermore, the aggregated mPrP had no affinity for the immobilised metal ions, indicating that possibly the hexahistidine-tag was inaccessible within the aggregates and/or triton x-100 micelles prevented interaction between the hexahistidine-tag and the immobilised metal ions. In one study, triton x-100 micelles prevented association between lactate dehydrogenase enzyme and immobilised Cibarcron Blue F3GA dye in a dye-ligand affinity chromatography experiment. Although, addition of anionic detergents (SDS or deoxycholate) reversed this effect, the anionic detergents had no denaturing effect on the protein as it was sequestered by triton x-100 (Robinson *et al.*, 1980). However, IMAC purification of membrane-associated prion protein from microsomal fraction of Syrian hamster brain homogenates in the presence of triton X-100 has been demonstrated by Pan *et*

al. (1992). Therefore, the hexahistidine-tag may have a negative effect on solubility of the recombinant mPrP in non-ionic detergents. Alternatively, the insolubility of protein in the presence of Triton X-100 represents evidence that recombinant mPrP produced in the cytosol and sequestered to the endoplasmic reticulum of transgenic tobacco plants have PrP^{Sc}-like properties.

A previous attempt at glycosylated prion purification, isolated the microsomal fraction by subcellular fractionation before detergent solubilisation of membrane-associated protein (Pan *et al.*, 1992; Turk *et al.*, 1988). However, this study attempted to isolate both aglycosylated and glycosylated prion protein from clarified lysate of transgenic tobacco plants, this may have affected the solubility of the recombinant protein in triton x-100, as Kuczius and Kelsch (2013) observed that in the presence of copper and zinc ions unglycosylated prion protein was insoluble in triton x-100. However, it is unlikely that the concentration of metal ions used in this study are similar to levels in tobacco plant. Further optimisation of the purification of recombinant mPrP from transgenic tobacco plants will require high-throughput detergent screening for recombinant mPrP solubility and IMAC purification. Alternatively, expressing the recombinant protein without hexahistidine tag may improve the protein solubility and thus simplify the purification process as IMAC purification protocol for PrP^C without hexahistidine tag has already been established (Pan *et al.*, 1992).

7 Discussion

PrP^C encoded by the *PRNP* gene is a glycoprotein that is predominantly expressed in the neurons of mammals although its function is unknown. Post-translational misfolding of PrP^C due to the presence of genetic mutations, infection or spontaneous conformational change results in a deleterious isoform PrP^{Sc} (Prusiner, 1998). Prion disease is a fatal neurodegenerative disorder caused by the accumulation of PrP^{Sc} in the neurons (Prusiner, 1998). Currently, no reliable diagnostic procedure or therapy exists for the disease due to difficulties understanding the molecular mechanisms underlying the conversion from PrP^C to PrP^{Sc} (Puoti *et al.*, 2012).

This study was designed to produce recombinant mPrP in transgenic tobacco plants for studies on the prion phenomenon. There are several advantages associated with producing recombinant proteins in transgenic plants over bacterial systems, especially mammalian-like post-translational modification (Twyman *et al.*, 2005). In addition, the presence of recombinant mPrP in transgenic tobacco plants resulted in phenotypic alternations, which may help determine the function of the prion protein.

Synthetic mPrP transgene constructs were designed to target recombinant mPrP to the apoplast, cytosol and endoplasmic reticulum of transgenic tobacco plants. The cytosolic construct and ER-targeted construct were successfully integrated into several transgenic tobacco lines. The transgenic lines were characterised to determine the quality of the recombinant prion protein and its effect on plant nutrients.

Characterisation of transgenic plants targeting recombinant mPrP in the cytosol revealed that the recombinant proteins were likely to be misfolded and present in two isoforms, a ~24 kDa aglycosylated isoform and a ~19 kDa partially truncated

isoform. ELISA analysis showed that transgenic line C7 had the highest expression level at 0.0024% TSP.

Phenotypic analysis of transgenic lines showed that the average level of iron was significantly upregulated in transgenic plants expressing cytosolic-mPrP compared to control plants. Furthermore, the average level of manganese was higher in plants expressing cytosolic-mPrP compared to other transgenic lines analysed. However, this result was not significant given the spread of the data. Analysis of peroxidase activity showed that mPrP may modulate antioxidant activity in transgenic tobacco plants expressing cytosolic recombinant mPrP and kanamycin treatment of transgenic lines expressing cytosolic-mPrP inhibited root development.

Recombinant mPrP directed to the endoplasmic reticulum of transgenic tobacco plants were likely to be misfolded and present in three isoforms; an unglycosylated ~24 kDa protein; a ~19 kDa truncated isoform and a ~31 kDa presumably high mannose glycoform. The transgenic lines examined had low expression levels with the highest expression from transgenic line E4 at 0.0016% TSP. Phenotypic analysis showed that the average Cu^{2+} levels was higher in transgenic plants expressing recombinant mPrP in the cytosol compared to other analysed transgenic lines. Furthermore, peroxidase activity was inhibited in transgenic plants producing recombinant mPrP in the endoplasmic reticulum. However, kanamycin treatment had no visible phenotypic effects on transgenic plants transformed with the ER transgene construct.

Purification of recombinant mPrP from transgenic lines expressing both the cytosolic and endoplasmic reticulum constructs was abortive. The purification process was compromised by the low expression rates of the recombinant mPrP

coupled with the oligomeric and misfolded conformation of the recombinant protein. Muller *et al.* (2005), showed that unless denatured, PrP^{Sc} does not bind Cu²⁺ charged IMAC columns. Since Cu²⁺ has the highest affinity for histidine-tags, this implies that Ni²⁺ and Co²⁺ charged columns will not bind the misfolded mPrP. Therefore, the purification results indicates a PrP^{Sc}-like nature of recombinant mPrP targeted to the cytosol and ER of transgenic tobacco plants.

Future research on recombinant mPrP purification should focus on assays to isolate IMAC compatible detergents/denaturants that can solubilise recombinant mPrP. For instance, Schlager *et al.* (2012) demonstrated that SDS can be used to denature proteins prior to IMAC purification since excess detergent can be removed by cooling the lysate. Furthermore, production of recombinant mPrP in tobacco cell suspension cultures could simplify the downstream purification process. Plant cell suspension cultures have several advantages over transgenic plants. For instance, they have a shorter growth cycle, transgenes can be designed to secrete the recombinant protein into the growth media simplifying the purification process and plant suspensions cultures have low environmental and contamination risks (Plasson *et al.*, 2009). Examples of biopharmaceuticals produced in tobacco Bright Yellow-2 (BY-2) suspension cells include human growth hormone and hepatitis B surface antigen (Santos *et al.*, 2016).

This study has shown for the first time that mutant recombinant mPrP is processed in transgenic tobacco plants in a similar manner to animals establishing tobacco plants as a suitable production system for recombinant mPrP. The *PR1a* signal peptide appeared to direct recombinant mPrP to the ER due to the presence of glycosylated recombinant mPrP isoforms in transgenic lines transformed with the ER construct. In addition, the presence of the

hexahistidine-tag and/or the ER retention sequence did not affect the protein's characteristics. Further research should focus on developing plants that produce fully glycosylated recombinant mPrP. Several studies have shown that the C-terminal GPI anchor is required for synthesis of fully glycosylated recombinant mPrP. To simplify downstream processing, mutating selected amino acids in the GPI anchor signal sequence results in a correctly folded and fully glycosylated recombinant prion protein that is secreted rather than anchored to the plasma membrane (Walmsley and Hooper, 2003).

Consumption of BSE-infected beef has been associated with variant CJD in humans (Brown *et al.*, 2001). Mishra *et al.* (2004), demonstrated that treatment of sporadic CJD PrP^{Sc} molecules with digestive enzymes resulted in N-terminally truncated PrP^{Sc} fragments similar to treatment with proteinase K. Additionally, PrP^{Sc} binds ferritin and the PrP^{Sc}-ferritin complex can be transported across epithelial cells into the bloodstream. This PrP^{Sc}-ferritin association is independent of PrP concentration and indicates a possible transmission route for PrP^{Sc}. Corroboratively, *PRNP* ablated mice exhibit an iron deficiency phenotype indicating a possible role for PrP^C in iron transport (Singh *et al.*, 2009). This study has shown that expression of cytosolic-mPrP in transgenic tobacco plants increases uptake of iron in transgenic tobacco leaves irrespective of the concentration of recombinant mPrP in the leaves. Therefore, this study agrees with the suggestion that PrP has a role in iron homeostasis. Further investigations into the molecular mechanisms involved in PrP-associated uptake of iron will help elucidate the role of PrP in iron homeostasis and its contribution to PrP^{Sc}-associated neurotoxicity.

Studies of brain tissue from patients with prion disease have revealed increased concentrations of Mn^{2+} and Zn^{2+} ions with a reduced Cu^{2+} ion content. Furthermore, Brown *et al.* (2000) showed that only Mn^{2+} ions can replace Cu^{2+} ions in prion protein and that Mn^{2+} -associated PrP^C becomes protease resistant in a time dependant manner. In this study, independent transgenic lines expressing cytosolic-mPrP had elevated levels of Fe^{2+} and Mn^{2+} while independent transgenic plants with recombinant mPrP retained in the endoplasmic reticulum had elevated levels of Cu^{2+} . Consequently, this study shows for the first time that irrespective of PrP conformation its affinity for metal ions may depend on its subcellular localisation.

It has been suggested that PrP^C may be involved in maintaining zinc homeostasis in neuronal cells (Watt *et al.*, 2012). Conversely, others have demonstrated no relationship between PrP^C and zinc homeostasis (Pass *et al.* (2015). Expressing recombinant mPrP in transgenic tobacco plants had no effect on zinc levels in transgenic tobacco leaves probably because of the subcellular localisation of the recombinant protein. Future research should focus on expressing anchored mPrP in plants to determine the effect that localising recombinant mPrP to plasma membranes has on the metal ion content and antioxidant activity of transgenic tobacco leaves. Also, studies that direct mPrP to other plant organelles could be useful in the elucidation of the function of recombinant mPrP.

The prion protein has three different topologies. The fully translocated PrP that can be secreted and two transmembrane forms. The N-transmembrane form (^{Ntm}PrP) has the amino terminus in the ER and the carboxyl terminus accessible to proteases in the cytosol while the C-transmembrane form (^{Ctm}PrP) has its carboxyl terminus in the ER and the amino terminus accessible to proteases in

the cytosol (Hegde *et al.*, 1998). This study agrees with research that has suggested that high concentrations of PrP^C in the cytosol is responsible for the toxic effects associated with prion disease (Sections 5.2.2 and 5.3). The toxic effect of cytosolic PrP on neuroblastoma cells and cerebellar granular neurons (Ma and Lindquist, 2002) can probably be explained by increased Mn²⁺ concentration in the cells due to overexpression of PrP in the cytosol. To substantiate this theory, Mn²⁺-induced neurotoxicity has been documented in SK-ER3 neuroblastoma cell lines (Di Lorenzo *et al.*, 1996) and cerebellar granular neurons (Hernandez *et al.*, 2011). Also, Mn²⁺-depleted cells are not susceptible to prion infection (Pass *et al.*, 2015). Hegde *et al.* (1998) demonstrated that overexpression of the CtmPrP transmembrane topology, associated with A117V mutation of GSS, is neurotoxic to cells in the absence of PrP^{Sc} aggregates. Therefore, it is important to design studies that will determine if overexpression of CtmPrP and cytosolic PrP is associated with increased manganese uptake and NtmPrP increased copper uptake in neuronal cells.

This study has also shown for the first time that the interaction of mPrP with kanamycin sulphate inhibits the protein's ability to bind Cu²⁺ ions and Mn²⁺ ions and to modulate peroxidase activity. However, root morphogenesis was inhibited in kanamycin-treated transgenic plants transformed with the cytosolic transgene construct. Since the effects of this interaction could be subject to the subcellular location of the mPrP, future studies should focus on understanding the biophysical and biochemical implications of prion-kanamycin interaction and how it can be harnessed for diagnostic and therapeutic purposes.

8 References

Abskharon, R. N. N., Ramboarina, S., El Hassan, H., Gad, W., Apostol, M. I., Giachin, G., Legname, G., Steyaert, J., Messens, J. and Soror, S. H. (2012) 'A novel expression system for production of soluble prion proteins in *E. coli*', *Microbial Cell Factories*, 11(1), p. 6.

Acevedo-Morantes, C.Y. and Wille, H. (2014) 'The Structure of Human Prions: From Biology to Structural Models—Considerations and Pitfalls', *Viruses*, 6(10), pp.3875-3892.

Aguzzi, A. and Calella, A. M. (2009) 'Prions: protein aggregation and infectious diseases', *Physiological Reviews*, 89, pp.1105-1152.

Ali, G., Hadi, F., Ali, Z., Tariq, M. and Khan, M.A. (2007) 'Callus induction and *in vitro* complete plant regeneration of different cultivars of tobacco (*Nicotiana tabacum* L.) on media of different hormonal concentrations', *Biotechnology*, 6(4), pp.561-566.

Arnau, J., Lauritzen, C., Petersen, G.E. and Pedersen, J. (2006) 'Current strategies for the use of affinity tags and tag removal for the purification of recombinant proteins', *Protein Expression and Purification*, 48(1), pp.1-13.

Ashok, A. and Hegde, R.S. (2008) 'Retrotranslocation of prion proteins from the endoplasmic reticulum by preventing GPI signal transamidation', *Molecular Biology of the Cell*, 19(8), pp.3463-3476.

Ashok, A. and Hegde, R.S. (2009) 'Selective processing and metabolism of disease-causing mutant prion proteins', *PLoS Pathogens*, 5(6), p.1000479.

Balasubramaniam, D., Wilkinson, C., Van Cott, K. and Zhang, C. (2003) 'Tobacco protein separation by aqueous two-phase extraction', *Journal of Chromatography*, 989(1), pp.119-129.

Baluska, F. (2010) 'Recent surprising similarities between plant cells and neurons', *Plant signalling and behaviour*, 5(2), pp.87-89.

Baluska, F., Mancuso, S. and Volkmann, D. (2006) 'Communication in plants', *Neuronal Aspect of Plant Life*.

Barendse, G.W.M., Croes, A.F., Bosveld, M., Van Der Krieken, W.M. and Wullems, G.J. (1987) 'Uptake and metabolism of NAA and BAP in explants of tobacco in relation to *in vitro* flower bud formation', *Journal of Plant Growth Regulation*, 6(4), pp.193-200.

Barria, M. A., Mukherjee, A., Gonzalez-Romero, D., Morales, R. and Soto, C. (2009) '*De novo* generation of infectious prions *in vitro* produces a new disease phenotype', *PLoS Pathogens*, 5(5).

Baskakov, I.V. and Breydo, L. (2007) 'Converting the prion protein: what makes the protein infectious', *Biochimica et Biophysica Acta (BBA)-Molecular Basis of Disease*, 1772(6), pp.692-703.

Bendandi, M., Marillonnet, S., Kandzia, R., Thieme, F., Nickstadt, A., Herz, S., Fröde, R., Inoges, S., de Cerio, A.L.D., Soria, E. and Villanueva, H. (2010) 'Rapid, high-yield production in plants of individualized idiotypic vaccines for non-Hodgkin's lymphoma', *Annals of Oncology*, p.256.

- Benkova, E., Ivanchenko, M.G., Friml, J., Shishkova, S. and Dubrovsky, J.G., (2009) 'A morphogenetic trigger: is there an emerging concept in plant developmental biology?' *Trends in Plant Science*, 14(4), pp.189-193.
- Binns, A.N. (2002) 'T-DNA of *Agrobacterium tumefaciens*: 25 years and counting', *Trends in Plant Science*, 7(5), pp.231-232.
- Birch, R.G. (1997) 'Plant transformation: problems and strategies for practical application', *Annual Review of Plant Biology*, 48(1), pp.297-326.
- Block, H., Maertens, B., Priestersbach, A., Brinker, N., Kubicek, J., Fabis, R., Labahn, J. and Schäfer, F. (2009) 'Immobilized-metal affinity chromatography (IMAC): a review', *Methods in Enzymology*, 463, pp.439-473.
- Bornhorst, J.A. and Falke, J.J. (2000) 'Purification of proteins using polyhistidine affinity tags', *Methods in Enzymology*, 326, p.245.
- Brenner, E.D., Stahlberg, R., Mancuso, S., Vivanco, J., Baluška, F. and Van Volkenburgh, E. (2006) 'Plant neurobiology: an integrated view of plant signalling', *Trends in Plant Science*, 11(8), pp.413-419.
- Briat, J.F., Duc, C., Ravet, K. and Gaymard, F. (2010) 'Ferritins and iron storage in plants', *Biochimica et Biophysica Acta (BBA)-General Subjects*, 1800(8), pp.806-814.
- Brim, S., Groschup, M.H. and Kuczius, T. (2016) 'Copper and Zinc Interactions with Cellular Prion Proteins Change Solubility of Full-Length Glycosylated Isoforms and Induce the Occurrence of Heterogeneous Phenotypes', *PloS One*, 11(4), p.0153931.

Brimacombe, D.B., Bennett, A.D., Wusteman, F.S. and Bostock, C.J. (1999) 'Characterization and polyanion-binding properties of purified recombinant prion protein', *Biochemical Journal*, 342(3), pp.605-613.

Brown, D.R. and Besinger, A. (1998) 'Prion protein expression and superoxide dismutase activity', *Biochemical Journal*, 334(2), pp.423-429.

Brown, D.R., Hafiz, F., Glasssmith, L.L., Wong, B.S., Jones, I.M., Clive, C. and Haswell, S.J. (2000) 'Consequences of manganese replacement of copper for prion protein function and proteinase resistance', *The EMBO journal*, 19(6), pp.1180-1186.

Brown, D.R., Qin, K., Herms, J.W., Madlung, A., Manson, J., Strome, R., Fraser, P.E., Kruck, T., von Bohlen, A., Schulz-Schaeffer, W. and Giese, A. (1997) 'The cellular prion protein binds copper *in vivo*', *Nature*, 390(6661), pp.684-687.

Brown, D.R., Wong B.S., Hafiz, F., Clive, C., Haswell, S.J. and Jones, I.M. (1999) 'Normal prion protein has an activity like that of superoxide dismutase', *Biochemical Journal*, 344(1), pp.1-5.

Brown, P., Will, R.G., Bradley, R., Asher, D.M. and Detwiler, L. (2001) 'Bovine spongiform encephalopathy and variant Creutzfeldt-Jakob disease: background, evolution, and current concerns', *Emerging Infectious Diseases*, 7(1), p.6.

Brundin, P., Melki, R. and Kopito, R. (2010) 'Prion-like transmission of protein aggregates in neurodegenerative diseases', *Nature Reviews Molecular Cell Biology*, 11(4), pp.301-307.

Bueler, H., Fischer, M., Lang, Y., Bluethmann, H., Lipp, H.P., DeArmond, S.J., Prusiner, S.B., Aguet, M. and Weissmann, C. (1992) 'Normal development and

behaviour of mice lacking the neuronal cell-surface PrP protein', *Nature*, 356(6370), pp.577-582.

Cardinale, A., Filesì, I., Vetrugno, V., Pocchiari, M., Sy, M.S. and Biocca, S. (2005) 'Trapping prion protein in the endoplasmic reticulum impairs PrP^C maturation and prevents PrP^{Sc} accumulation', *Journal of Biological Chemistry*, 280(1), pp.685-694.

Castilla, J., Gonzalez-Romero, D., Saá, P., Morales, R., De Castro, J. and Soto, C. (2008) 'Crossing the species barrier by PrP^{Sc} replication *in vitro* generates unique infectious prions', *Cell*, 134(5), pp.757-768.

Castilla, J., Saá, P., Hetz, C. and Soto, C. (2005) '*In vitro* generation of infectious scrapie prions', *Cell*, 121(2), pp.195-206.

Caughey, B., Raymond, G.J. and Bessen, R.A. (1998) 'Strain-dependent differences in β -sheet conformations of abnormal prion protein', *Journal of Biological Chemistry*, 273(48), pp.32230-32235.

Chen, Q. (2008) 'Expression and purification of pharmaceutical proteins in plants', *Biological Engineering Transactions*, 1(4), pp.291-321.

Chesebro, B., Trifilo, M., Race, R., Meade-White, K., Teng, C., LaCasse, R., Raymond, L., Favara, C., Baron, G., Priola, S. and Caughey, B. (2005) 'Anchorless prion protein results in infectious amyloid disease without clinical scrapie', *Science*, 308(5727), pp.1435-1439.

Chiti, F. and Dobson, C.M. (2006) 'Protein misfolding, functional amyloid, and human disease', *Annual Review of Biochemistry*, 75, pp.333-366.

Christensen, A.H. and Quail, P.H. (1996) 'Ubiquitin promoter-based vectors for high-level expression of selectable and/or screenable marker genes in monocotyledonous plants', *Transgenic Research*, 5(3), pp.213-218.

Cobb, N.J. and Surewicz, W.K. (2009) 'Prion diseases and their biochemical mechanisms', *Biochemistry*, 48(12), pp.2574-2585.

Collinge, J. (2001) 'Prion diseases of humans and animals: their causes and molecular basis' *Annual Review of Neuroscience*, 24(1), pp.519-550.

Comai, L., Moran, P. and Maslyar, D. (1990) 'Novel and useful properties of a chimeric plant promoter combining CaMV 35S and MAS elements', *Plant Molecular Biology*, 15(3), pp.373-381.

Conrad, U. and Fiedler, U. (1998) 'Compartment-specific accumulation of recombinant immunoglobulins in plant cells: an essential tool for antibody production and immunomodulation of physiological functions and pathogen activity', *Protein Trafficking in Plant Cells*, pp.101-109.

Corrado, G. and Karali, M. (2009) 'Inducible gene expression systems and plant biotechnology', *Biotechnology Advances*, 27(6), pp.733-743.

Corsaro, A., Thellung, S., Russo, C., Villa, V., Arena, S., D'Adamo, M.C., Paludi, D., Principe, D.R., Damonte, G., Benatti, U. and Aceto, A. (2002) 'Expression in *E. coli* and purification of recombinant fragments of wild type and mutant human prion protein', *Neurochemistry International*, 41(1), pp.55-63.

Daniell, H., Streatfield, S.J. and Wycoff, K. (2001) 'Medical molecular farming: production of antibodies, biopharmaceuticals and edible vaccines in plants', *Trends in Plant Science*, 6(5), pp.219-226.

Darbani, B., Farajnia, S., Toorchi, M., Zakerbostanabad, S., Noeparvar, S. and Stewart, C.N. (2008) 'DNA-delivery methods to produce transgenic plants', *Biotechnology*, 7(3), pp.385-402.

Davies, P. and Brown, D.R. (2008) 'The chemistry of copper binding to PrP: is there sufficient evidence to elucidate a role for copper in protein function?', *Biochemical Journal*, 410(2), pp.237-244.

DeArmond, S.J. and Bouzamondo, E. (2002) 'Fundamentals of prion biology and diseases', *Toxicology*, 181, pp.9-16.

Den Dulk-Ras, A. and Hooykaas, P.J. (1995) 'Electroporation of *Agrobacterium tumefaciens*', *Plant Cell Electroporation and Electrofusion Protocols*, pp.63-72.

Desai, P. N., Shrivastava, N. and Padh, H. (2010) 'Production of heterologous proteins in plants: strategies for optimal expression', *Biotechnology Advances*, 28, pp.427-435.

Desai, U.A., Sur, G., Daunert, S., Babbitt, R. and Li, Q. (2002) 'Expression and affinity purification of recombinant proteins from plants', *Protein Expression and Purification*, 25(1), pp.195-202.

Di Lorenzo, D., Ferrari, F., Agrati, P., de Vos, H., Apostoli, P., Alessio, L., Albertini, A. and Maggi, A. (1996) 'Manganese effects on the human neuroblastoma cell line SK-ER3', *Toxicology and Applied Pharmacology*, 140(1), pp.51-57.

Dobson, C.M. (2003) 'Protein folding and misfolding', *Nature*, 426(6968), pp.884-890.

Duennwald, M.L., Echeverria, A. and Shorter, J. (2012) 'Small heat shock proteins potentiate amyloid dissolution by protein disaggregases from yeast and humans', *PLoS Biology*, 10(6), p.1001346.

Egelkrout, E., Rajan, V. and Howard, J.A. (2012) 'Overproduction of recombinant proteins in plants', *Plant Science*, 184, pp.83-101.

Faivre-Rampant, O., Charpentier, J.P., Kevers, C., Dommes, J., Van Onckelen, H., Jay-Allemand, C. and Gaspar, T. (2002) 'Cuttings of the non-rooting *rac* tobacco mutant overaccumulate phenolic compounds', *Functional Plant Biology*, 29(1), pp.63-71.

Faize, M., Faize, L. and Burgos, L. (2010) 'Using quantitative real-time PCR to detect chimeras in transgenic tobacco and apricot and to monitor their dissociation', *BMC biotechnology*, 10(1), p.53.

Fang, R.X., Nagy, F., Sivasubramaniam, S. and Chua, N.H. (1989) 'Multiple cis regulatory elements for maximal expression of the cauliflower mosaic virus 35S promoter in transgenic plants', *The Plant Cell*, 1(1), pp.141-150.

Faye, L., Boulaflous, A., Benchabane, M., Gomord, V. and Michaud, D. (2005) 'Protein modifications in the plant secretory pathway: current status and practical implications in molecular pharming', *Vaccine*, 23(15), pp.1770-1778.

Fink, A.L. (1998) 'Protein aggregation: folding aggregates, inclusion bodies and amyloid', *Folding and Design*, 3(1), pp.9-23.

Fischer, R., Emans, N.J., Twyman, R.M. and Schillberg, S. (2004) 'Molecular farming in plants: technology platforms', *Encyclopaedia of Plant and Crop Science*, pp.753-756.

Fontaine, S.N. and Brown, D.R. (2009) 'Mechanisms of prion protein aggregation', *Protein and Peptide Letters*, 16(1), pp.14-26.

Gaggelli, E., Kozlowski, H., Valensin, D. and Valensin, G. (2006) 'Copper homeostasis and neurodegenerative disorders (Alzheimer's, prion, and Parkinson's diseases and amyotrophic lateral sclerosis)', *Chemical Reviews*, 106(6), pp.1995-2044.

Gallie, D.R. (2002) 'The 5'-leader of tobacco mosaic virus promotes translation through enhanced recruitment of eIF4F', *Nucleic Acids Research*, 30(15), pp.3401-3411.

Gallie, D.R. and Walbot, V. (1990) 'RNA pseudoknot domain of tobacco mosaic virus can functionally substitute for a poly (A) tail in plant and animal cells', *Genes and Development*, 4(7), pp.1149-1157.

Garavito, R.M. and Ferguson-Miller, S. (2001) 'Detergents as tools in membrane biochemistry', *Journal of Biological Chemistry*, 276(35), pp.32403-32406.

Gasperini, L. and Legname, G. (2015) 'Prion protein and aging', *Promiscuous Functions of the Prion Protein Gene Family*, p.98.

Gelvin, S.B. (2003) 'Agrobacterium-mediated plant transformation: the biology behind the "gene-jockeying" tool', *Microbiology and Molecular Biology reviews*, 67(1), pp.16-37.

Giddings, G., Allison, G., Brooks, D. and Carter, A. (2000) 'Transgenic plants as factories for biopharmaceuticals', *Nature biotechnology*, 18(11), pp.1151-1155.

Goldstein, D.A. and Thomas, J.A. (2004) 'Biopharmaceuticals derived from genetically modified plants', *Qjm*, 97(11), pp.705-716.

Gomord, V. and Faye, L. (2004) 'Posttranslational modification of therapeutic proteins in plants', *Current Opinion in Plant Biology*, 7(2), pp.171-181.

Gomord, V., Chamberlain, P., Jefferis, R. and Faye, L. (2005) 'Biopharmaceutical production in plants: problems, solutions and opportunities', *Trends in Biotechnology*, 23(11), pp.559-565.

Gomord, V., Fitchette, A.C., Menu-Bouaouiche, L., Saint-Jore-Dupas, C., Plasson, C., Michaud, D. and Faye, L. (2010) 'Plant-specific glycosylation patterns in the context of therapeutic protein production', *Plant Biotechnology Journal*, 8(5), pp.564-587.

Goni, F., Knudsen, E., Schreiber, F., Scholtzova, H., Pankiewicz, J., Carp, R., Meeker, H.C., Rubenstein, R., Brown, D.R., Sy, M.S. and Chabalgoity, J.A. (2005) 'Mucosal vaccination delays or prevents prion infection via an oral route', *Neuroscience*, 133(2), pp.413-421.

Gudmundsdóttir, K.B., Kristinsson, J., Sigurdarson, S., Eiríksson, T. and Jóhannesson, T. (2008) 'Glutathione peroxidase (GPX) activity in blood of ewes on farms in different scrapie categories in Iceland', *Acta Veterinaria Scandinavica*, 50(1), p.1.

Gustafsson, C., Govindarajan, S. and Minshull, J. (2004) 'Codon bias and heterologous protein expression', *Trends in Biotechnology*, 22(7), pp.346-353.

Hanahan, D. (1985) 'Techniques for transformation of *E. coli*', *DNA Cloning*, 1, pp.109-135.

Hansen, G. and Wright, M.S. (1999) 'Recent advances in the transformation of plants', *Trends in Plant Science*, 4(6), pp.226-231.

Harris, D.A. (1999) 'Cellular biology of prion diseases', *Clinical Microbiology Reviews*, 12(3), pp.429-444.

Hegde, R.S., Mastrianni, J.A., Scott, M.R., DeFea, K.A., Tremblay, P., Torchia, M., DeArmond, S.J., Prusiner, S.B. and Lingappa, V.R. (1998) 'A transmembrane form of the prion protein in neurodegenerative disease', *Science*, 279(5352), pp.827-834.

Hegde, R.S., Tremblay, P., Groth, D., DeArmond, S.J., Prusiner, S.B. and Lingappa, V.R. (1999) 'Transmissible and genetic prion diseases share a common pathway of neurodegeneration', *Nature*, 402(6763), pp.822-826.

Hellens, R. P., Edwards, E. A., Leyland, N. R., Bean, S. and Mullineaux, P. M. (2000) 'pGreen: a versatile and flexible binary Ti vector for *Agrobacterium*-mediated plant transformation', *Plant Molecular Biology*, 42, pp.819-832.

Heller, U., Winklhofer, K.F., Heske, J., Reintjes, A. and Tatzelt, J. (2003) 'Post-translational Import of the Prion Protein into the Endoplasmic Reticulum Interferes with Cell Viability. A CRITICAL ROLE FOR THE PUTATIVE TRANSMEMBRANE DOMAIN', *Journal of Biological Chemistry*, 278(38), pp.36139-36147.

Hernandez, R.B., Farina, M., Espósito, B.P., Souza-Pinto, N.C., Barbosa, F. and Suñol, C. (2011) 'Mechanisms of manganese-induced neurotoxicity in primary neuronal cultures: the role of manganese speciation and cell type', *Toxicological Sciences*, 124(2), pp.414-423.

Hernandez-Garcia, C.M. and Finer, J.J. (2014) 'Identification and validation of promoters and cis-acting regulatory elements', *Plant Science*, 217, pp.109-119.

Hershberg, R. and Petrov, D.A. (2008) 'Selection on codon bias', *Annual Review of Genetics*, 42, pp.287-299.

Heske, J., Heller, U., Winklhofer, K.F. and Tatzelt, J. (2004) 'The C-terminal globular domain of the prion protein is necessary and sufficient for import into the endoplasmic reticulum', *Journal of Biological Chemistry*, 279(7), pp.5435-5443.

Hesketh, S., Thompsett, A.R. and Brown, D.R. (2012) 'Prion protein polymerisation triggered by manganese-generated prion protein seeds', *Journal of Neurochemistry*, 120(1), pp.177-189.

Hetz, C.A. and Soto, C. (2006) 'Stressing out the ER: a role of the unfolded protein response in prion-related disorders', *Current Molecular Medicine*, 6(1), pp.37-43.

Hill, A.F., Joiner, S., Beck, J.A., Campbell, T.A., Dickinson, A., Poulter, M., Wadsworth, J.D. and Collinge, J. (2006) 'Distinct glycoform ratios of protease resistant prion protein associated with *PRNP* point mutations', *Brain*, 129(3), pp.676-685.

Hochuli, E., Bannwarth, W., Dobeli, H., Gentz, R. and Stuber, D. (1988) 'Genetic approach to facilitate purification of recombinant proteins with a novel metal chelate adsorbent', *Biotechnology*, 6(11), pp.1321-1325.

Hodge, A., Berta, G., Doussan, C., Merchan, F. and Crespi, M. (2009) 'Plant root growth, architecture and function', *Plant and Soil*, 321(1-2), pp.153-187.

Holscher, C., Bach, U.C. and Dobberstein, B. '2001. Prion protein contains a second endoplasmic reticulum targeting signal sequence located at its C terminus', *Journal of Biological Chemistry*, 276(16), pp.13388-13394

Holsters, M., De Waele, D., Depicker, A., Messens, E., Van Montagu, M. and Schell, J. (1978) 'Transfection and transformation of *Agrobacterium tumefaciens*', *Molecular and General Genetics MGG*, 163(2), pp.181-187.

Hornemann, S., Korth, C., Oesch, B., Riek, R., Wider, G., Wüthrich, K. and Glockshuber, R. (1997) 'Recombinant full-length murine prion protein, mPrP (23–231): purification and spectroscopic characterization', *Febs Letters*, 413(2), pp.277-281.

Horsch, R.B., Fry, J.E., Hoffmann, N., Eichholtz, D., Rogers, S.A. and Fraley, R.T. (1985) 'A simple and general method for transferring genes into plants', *Science*, 227, pp.1229-1231.

Horsch, R.B., Fry, J., Hoffmann, N., Neidermeyer, J., Rogers, S.G. and Fraley, R.T. (1989) 'Leaf disc transformation', *Plant Molecular Biology Manual*, pp.63-71.

Hu, W., Kieseier, B., Frohman, E., Eagar, T.N., Rosenberg, R.N., Hartung, H.P. and Stüve, O. (2008) 'Prion proteins: physiological functions and role in neurological disorders', *Journal of the Neurological Sciences*, 264(1), pp.1-8.

Huang, T., Xu, J., Xiang, J., Lu, Y., Chen, R., Huang, L., Xiao, G. and Sun, G. (2012) 'PrP^C interacts with potassium channel tetramerization domain containing 1 (KCTD1) protein through the PrP 51-136 region containing octapeptide repeats', *Biochemical and Biophysical Research Communications*, 417(1), pp.182-186.

Hutter, G., Heppner, F.L. and Aguzzi, A. (2003) 'No superoxide dismutase activity of cellular prion protein *in vivo*', *Biological Chemistry*, 384(9), pp.1279-1285.

Jackson, G.S., Murray, I., Hosszu, L.L., Gibbs, N., Waltho, J.P., Clarke, A.R. and Collinge, J. (2001) 'Location and properties of metal-binding sites on the human prion protein', *Proceedings of the National Academy of Sciences*, 98(15), pp.8531-8535.

Jeffrey, M., Scholes, S.F.E., Martin, S., McGovern, G., Siso, S. and González, L. (2012) 'Increased immunohistochemical labelling for prion protein occurs in diverse neurological disorders of sheep: relevance for normal cellular PrP function', *Journal of Comparative Pathology*, 147(1), pp.46-54.

Kearse, M., Moir, R., Wilson, A., Stones-Havas, S., Cheung, M., Sturrock, S., Buxton, S., Cooper, A., Markowitz, S., Duran, C., Thierer, T., Ashton, B., Mentjies, P., and Drummond, A. (2012) 'Geneious Basic: an integrated and extendable desktop software platform for the organization and analysis of sequence data', *Bioinformatics*, 28(12), pp.1647-1649.

Kevers, C., Dommès, J., Gaspar, T., Faivre-Rampant, O. and Van Onckelen, H. (2001) 'Modified hormonal balance in rooting-recalcitrant *rac* mutant tobacco shoots', *Plant Biosystems-An International Journal Dealing with all Aspects of Plant Biology*, 135(1), pp.85-93.

Khan, M.M., Raza, S.S., Javed, H., Ahmad, A., Khan, A., Islam, F., Safhi, M.M. and Islam, F. (2012) 'Rutin protects dopaminergic neurons from oxidative stress in an animal model of Parkinson's disease', *Neurotoxicity Research*, 22(1), pp.1-15.

Kiachopoulos, S., Bracher, A., Winklhofer, K.F. and Tatzelt, J. (2005) 'Pathogenic mutations located in the hydrophobic core of the prion protein interfere with folding and attachment of the glycosylphosphatidylinositol anchor', *Journal of Biological Chemistry*, 280(10), pp.9320-9329.

Kozziel, M.G., Carozzi, N.B. and Desai, N. (1996) 'Optimizing expression of transgenes with an emphasis on post-transcriptional events', *Post-Transcriptional Control of Gene Expression in Plants*, pp.393-405.

Kralovicova, S., Fontaine, S.N., Alderton, A., Alderman, J., Ragnarsdottir, K.V., Collins, S.J. and Brown, D.R. (2009) 'The effects of prion protein expression on metal metabolism', *Molecular and Cellular Neuroscience*, 41 (2), pp.135-147.

Kristiansen, M., Messenger, M.J., Klöhn, P.C., Brandner, S., Wadsworth, J.D., Collinge, J. and Tabrizi, S.J. (2005) 'Disease-related prion protein forms aggregates in neuronal cells leading to caspase activation and apoptosis', *Journal of Biological Chemistry*, 280(46), pp.38851-38861.

Kuczius, T. and Kelsch, R. (2013) 'Effects of metal binding on solubility and resistance of physiological prions depend on tissues and glycotypes', *Journal of Cellular Biochemistry*, 114(12), pp.2690-2698.

Kusnadi, A.R., Nikolov, Z.L. and Howard, J.A. (1997) 'Production of recombinant proteins in transgenic plants: practical considerations', *Biotechnology and Bioengineering*, 56(5), pp.473-484.

Lai, H., Engle, M., Fuchs, A., Keller, T., Johnson, S., Gorlatov, S., Diamond, M.S. and Chen, Q. (2010) 'Monoclonal antibody produced in plants efficiently treats

West Nile virus infection in mice' *Proceedings of the National Academy of Sciences*, 107(6), pp.2419-2424.

Lazo, G.R., Stein, P.A. and Ludwig, R.A. (1991) 'A DNA transformation-competent *Arabidopsis* genomic library in *Agrobacterium*', *Nature Biotechnology*, 9(10), pp.963-967.

Lee, I.Y., Westaway, D., Smit, A.F., Wang, K., Seto, J., Chen, L., Acharya, C., Ankener, M., Baskin, D., Cooper, C. and Yao, H. (1998) 'Complete genomic sequence and analysis of the prion protein gene region from three mammalian species', *Genome Research*, 8(10), pp.1022-1037.

Leelavathi, S. and Reddy, V.S. (2003) 'Chloroplast expression of His-tagged GUS-fusions: a general strategy to overproduce and purify foreign proteins using transplastomic plants as bioreactors', *Molecular Breeding*, 11(1), pp.49-58.

Lehmann, S. (2002) 'Metal ions and prion diseases', *Current Opinion in Chemical Biology*, 6(2), pp.187-192.

Lerouge, P., Bardor, M., Pagny, S., Gomord, V. and Faye, L. (2000) 'N-glycosylation of recombinant pharmaceutical glycoproteins produced in transgenic plants towards a humanisation of plant N-glycans', *Current Pharmaceutical Biotechnology*, 1(4), pp.347-354.

Lessard, P.A., Kulaveerasingam, H., York, G.M., Strong, A. and Sinskey, A.J. (2002) 'Manipulating gene expression for the metabolic engineering of plants', *Metabolic Engineering*, 4(1), pp.67-79.

- Lige, B., Ma, S., Zhao, D. and van Huystee, R.B. (1998) 'Cationic peanut peroxidase: expression and characterization in transgenic tobacco and purification of the histidine-tagged protein', *Plant Science*, 136(2), pp.159-168.
- Lin, J.J. (1995) 'Electrotransformation of *Agrobacterium*', *Electroporation Protocols for Microorganisms*, pp.171-178.
- Linden, R., Martins, V.R., Prado, M.A., Cammarota, M., Izquierdo, I. and Brentani, R.R. (2008) 'Physiology of the prion protein', *Physiological Reviews*, 88(2), pp.673-728.
- Lund, S.T., Smith, A.G. and Hackett, W.P. (1997) 'Differential gene expression in response to auxin treatment in the wild type and *rac*, an adventitious rooting-incompetent mutant of tobacco', *Plant Physiology*, 114(4), pp.1197-1206.
- Ma, J. and Lindquist, S. (2001) 'Wild-type PrP and a mutant associated with prion disease are subject to retrograde transport and proteasome degradation', *Proceedings of the National Academy of Sciences*, 98(26), pp.14955-14960.
- Ma, J., Wollmann, R. and Lindquist, S. (2002) 'Neurotoxicity and neurodegeneration when PrP accumulates in the cytosol', *Science*, 298(5599), pp.1781-1785.
- Ma, J.K., Drake, P.M. and Christou, P. (2003) 'The production of recombinant pharmaceutical proteins in plants', *Nature Reviews Genetics*, 4(10), pp.794-805.
- Makarava, N. and Baskakov, I.V. (2012) 'Purification and fibrillation of full-length recombinant PrP', *Amyloid Proteins: Methods and Protocols*, pp.33-52.

- Malakouti, M.J. (2008) 'The effect of micronutrients in ensuring efficient use of macronutrients', *Turkish Journal of Agriculture and Forestry*, 32(3), pp.215-220.
- Marusic, C., Nuttall, J., Buriani, G., Lico, C., Lombardi, R., Baschieri, S., Benvenuto, E. and Frigerio, L. (2007) 'Expression, intracellular targeting and purification of HIV Nef variants in tobacco cells', *BMC biotechnology*, 7(1), p.12.
- Mastrianni, J.A. (2004) 'Prion diseases', *Clinical Neuroscience Research*, 3(6), pp.469-480.
- Matzke, A.J. and Matzke, M.A. (1998) 'Position effects and epigenetic silencing of plant transgenes', *Current Opinion in Plant Biology*, 1(2), pp.142-148.
- McKintosh, E., Tabrizi, S.J. and Collinge, J. (2003) 'Prion diseases', *Journal of Neurovirology*, 9(2), pp.183-193.
- McNally, K.L., Ward, A.E. and Priola, S.A. (2009) 'Cells expressing anchorless prion protein are resistant to scrapie infection', *Journal of Virology*, 83(9), pp.4469-4475.
- Mejare, M., Lilius, G. and Bülow, L. (1998) 'Evaluation of genetically attached histidine affinity tails for purification of lactate dehydrogenase from transgenic tobacco', *Plant Science*, 134(1), pp.103-114.
- Menkhaus, T.J., Bai, Y., Zhang, C., Nikolov, Z.L. and Glatz, C.E. (2004) 'Considerations for the recovery of recombinant proteins from plants', *Biotechnology Progress*, 20(4), pp.1001-1014.
- Mercer, R.C., Ma, L., Watts, J.C., Strome, R., Wohlgemuth, S., Yang, J., Cashman, N.R., Coulthart, M.B., Schmitt-Ulms, G., Jhamandas, J.H. and

Westaway, D. (2013) 'The prion protein modulates A-type K⁺ currents mediated by Kv4. 2 complexes through dipeptidyl aminopeptidase-like protein 6', *Journal of Biological Chemistry*, 288(52), pp.37241-37255.

Miesbauer, M., Rambold, A.S., Winklhofer, K.F. and Tatzelt, J. (2010) 'Targeting of the prion protein to the cytosol: mechanisms and consequences', *Current issues in Molecular Biology*, 12(2), p.109.

Mikami, Y. and Yamazawa, T. (2015) 'Chlorogenic acid, a polyphenol in coffee, protects neurons against glutamate neurotoxicity', *Life Sciences*, 139, pp.69-74.

Milhavet, O., McMahon, H.E., Rachidi, W., Nishida, N., Katamine, S., Mangé, A., Arlotto, M., Casanova, D., Riondel, J., Favier, A. and Lehmann, S. (2000) 'Prion infection impairs the cellular response to oxidative stress', *Proceedings of the National Academy of Sciences*, 97(25), pp.13937-13942.

Mironov, A., Latawiec, D., Wille, H., Bouzamondo-Bernstein, E., Legname, G., Williamson, R.A., Burton, D., DeArmond, S.J., Prusiner, S.B. and Peters, P.J., (2003) 'Cytosolic prion protein in neurons', *The Journal of Neuroscience*, 23(18), pp.7183-7193.

Mishra, R.S., Basu, S., Gu, Y., Luo, X., Zou, W.Q., Mishra, R., Li, R., Chen, S.G., Gambetti, P., Fujioka, H. and Singh, N. (2004) 'Protease-resistant human prion protein and ferritin are cotransported across Caco-2 epithelial cells: implications for species barrier in prion uptake from the intestine', *The Journal of Neuroscience*, 24(50), pp.11280-11290.

Moore, R. A., Taubner, L. M., and Priola, S. A. (2009) 'Prion protein misfolding and disease', *Current Opinion in Structural Biology*, 19(1), pp.14-22.

Morales, R., Abid, K. and Soto, C. (2007) 'The prion strain phenomenon: molecular basis and unprecedented features', *Biochimica et Biophysica Acta (BBA)-Molecular Basis of Disease*, 1772(6), pp.681-691.

Moustafa, K., Makhzoum, A. and Trémouillaux-Guiller, J. (2016) 'Molecular farming on rescue of pharma industry for next generations', *Critical reviews in biotechnology*, 36(5), pp.840-850.

Muller, H., Strom, A., Hunsmann, G. and Stuke, A.W. (2005) 'Separation of native prion protein (PrP) glycoforms by copper-binding using immobilized metal affinity chromatography (IMAC)', *Biochemical Journal*, 388(Pt 1), p.371.

Munch, C. and Bertolotti, A. (2012) 'Propagation of the prion phenomenon: beyond the seeding principle', *Journal of Molecular Biology*, 421(4), pp.491-498.

Munro, S. and Pelham, H.R. (1987) 'A C-terminal signal prevents secretion of luminal ER proteins', *Cell*, 48(5), pp.899-907.

Murashige, T. and Skoog, F. (1962) 'A revised medium for rapid growth and bio assays with tobacco tissue cultures' *Physiologia Plantarum*, 15(3), pp.473-497

Nau, R., Sörgel, F. and Eiffert, H. (2010) 'Penetration of drugs through the blood-cerebrospinal fluid/blood-brain barrier for treatment of central nervous system infections', *Clinical Microbiology Reviews*, 23(4), pp.858-883.

Neuendorf, E., Weber, A., Saalmueller, A., Schatzl, H., Reifenberg, K., Pfaff, E. and Groschup, M.H. (2004) 'Glycosylation deficiency at either one of the two glycan attachment sites of cellular prion protein preserves susceptibility to bovine spongiform encephalopathy and scrapie infections', *Journal of Biological Chemistry*, 279(51), pp.53306-53316.

Nikolov, Z.L. and Woodard, S.L. (2004) 'Downstream processing of recombinant proteins from transgenic feedstock', *Current Opinion in Biotechnology*, 15(5), pp.479-486.

Niu, Y., Jin, G., Li, X., Tang, C., Zhang, Y., Liang, Y. and Yu, J. (2015) 'Phosphorus and magnesium interactively modulate the elongation and directional growth of primary roots in *Arabidopsis thaliana* (L.) Heynh', *Journal of experimental botany*, 66(13), pp.3841-3854.

Norstrom, E.M., Ciaccio, M.F., Rassbach, B., Wollmann, R. and Mastrianni, J.A. (2007) 'Cytosolic prion protein toxicity is independent of cellular prion protein expression and prion propagation', *Journal of Virology*, 81(6), pp.2831-2837.

Nunziante, M., Gilch, S. and Schätzl, H.M. (2003) 'Essential role of the prion protein N terminus in subcellular trafficking and half-life of cellular prion protein', *Journal of Biological Chemistry*, 278(6), pp.3726-3734.

Obembe, O.O., Popoola, J.O., Leelavathi, S. and Reddy, S.V. (2011) 'Advances in plant molecular farming', *Biotechnology Advances*, 29(2), pp.210-222.

Oberpichler, I., Rosen, R., Rasouly, A., Vugman, M., Ron, E.Z. and Lamparter, T. (2008) 'Light affects motility and infectivity of *Agrobacterium tumefaciens*', *Environmental Microbiology*, 10(8), pp.2020-2029.

Odell, J.T., Nagy, F. and Chua, N.H. (1985) 'Identification of DNA sequences required for activity of the cauliflower mosaic virus 35S promoter', *Nature*, 313(6005), pp.810-812.

Olinger, G.G., Pettitt, J., Kim, D., Working, C., Bohorov, O., Bratcher, B., Hiatt, E., Hume, S.D., Johnson, A.K., Morton, J. and Pauly, M. (2012) 'Delayed

treatment of Ebola virus infection with plant-derived monoclonal antibodies provides protection in rhesus macaques', *Proceedings of the National Academy of Sciences*, 109(44), pp.18030-18035.

Padilla, I.M.G. and Burgos, L. (2010) 'Aminoglycoside antibiotics: structure, functions and effects on *in vitro* plant culture and genetic transformation protocols', *Plant Cell Reports*, 29(11), pp.1203-1213.

Page, A.F. and Minocha, S.C. (2004) 'Analysis of gene expression in transgenic plants', *Transgenic Plants: Methods and Protocols*, pp.291-311.

Pan, K.M., Stahl, N. and Prusiner, S.B. (1992) 'Purification and properties of the cellular prion protein from Syrian hamster brain' *Protein Science*, 1(10), pp.1343-1352.

Pan, T., Li, R., Wong, B.S. and Liu, T. (2002) 'Heterogeneity of normal prion protein in two-dimensional immunoblot: presence of various glycosylated and truncated forms', *Journal of Neurochemistry*, 81(5), pp.1092-1101.

Pass, R., Frudd, K., Barnett, J.P., Blindauer, C.A. and Brown, D.R. (2015) 'Prion infection in cells is abolished by a mutated manganese transporter but shows no relation to zinc', *Molecular and Cellular Neuroscience*, 68, pp.186-193.

Pattison, I.H. and Jebbett, J.N. (1971) 'Histopathological similarities between scrapie and cuprizone toxicity in mice', *Nature*, 230(5289), pp.115-117.

Pavlíček, A., Bednarova, L. and Holada, K. (2007) 'Production, purification and oxidative folding of the mouse recombinant prion protein', *Folia Microbiologica*, 52(4), pp.391-397.

Pen, J., van Ooyen, A.J., van den Elzen, P.J., Quax, W.J. and Hoekema, A. (1992) 'Efficient production of active industrial enzymes in plants', *Industrial Crops and Products*, 1(2), pp.241-250.

Perera, W.S.S. and Hooper, N.M. (2001) 'Ablation of the metal ion-induced endocytosis of the prion protein by disease-associated mutation of the octarepeat region', *Current Biology*, 11(7), pp.519-523.

Petersen, R.B., Siedlak, S.L., Lee, H.G., Kim, Y.S., Nunomura, A., Tagliavini, F., Ghetti, B., Cras, P., Moreira, P.I., Castellani, R.J. and Guentchev, M. (2005) 'Redox metals and oxidative abnormalities in human prion diseases', *Acta neuropathologica*, 110(3), pp.232-238.

Pfaffl, M.W. (2001) 'A new mathematical model for relative quantification in real-time RT-PCR', *Nucleic acids research*, 29(9), p.45.

Piccardo, P., Cervenak, J., Yakovleva, O., Gregori, L., Pomeroy, K., Cook, A., Muhammad, F.S., Seuberlich, T., Cervenakova, L. and Asher, D.M. (2012) 'Squirrel monkeys (*Saimiri sciureus*) infected with the agent of bovine spongiform encephalopathy develop tau pathology', *Journal of Comparative Pathology*, 147(1), pp.84-93.

Plasson, C., Michel, R., Lienard, D., Saint-Jore-Dupas, C., Sourrouille, C., March, G.G.D. and Gomord, V. (2009) 'Production of Recombinant Proteins in Suspension-Cultured Plant Cells', *Recombinant Proteins from Plants: Methods and Protocols*, pp.145-161.

Platis, D., Drossard, J., Fischer, R., Ma, J.C. and Labrou, N.E. (2008) 'New downstream processing strategy for the purification of monoclonal antibodies from transgenic tobacco plants', *Journal of Chromatography*, 1211(1), pp.80-89.

Porath, J., Carlsson, J.A.N., Olsson, I. and Belfrage, G. (1975) 'Metal chelate affinity chromatography, a new approach to protein fractionation', *Nature*, 258, pp.598-599.

Prusiner, S.B. (1998) 'Prions', *Proceedings of the National Academy of Sciences*, 95(23), pp.13363-13383.

Prusiner, S.B. (2001) 'Neurodegenerative diseases and prions', *New England Journal of Medicine*, 344(20), pp.1516-1526.

Prusiner, S.B. (2012) 'A unifying role for prions in neurodegenerative diseases', *Science*, 336(6088), pp.1511-1513.

Puig, B., Altmeyden, H.C., Ulbrich, S., Linsenmeier, L., Krasemann, S., Chakraborty, K., Acevedo-Morantes, C.Y., Wille, H., Tatzelt, J. and Glatzel, M. (2016) 'Secretory pathway retention of mutant prion protein induces p38-MAPK activation and lethal disease in mice', *Scientific Reports*, 6.

Puoti, G., Bizzi, A., Forloni, G., Safar, J.G., Tagliavini, F. and Gambetti, P. (2012) 'Sporadic human prion diseases: molecular insights and diagnosis', *The Lancet Neurology*, 11(7), pp.618-628.

Rambold, A.S., Miesbauer, M., Rapoport, D., Bartke, T., Baier, M., Winklhofer, K.F. and Tatzelt, J. (2006) 'Association of Bcl-2 with misfolded prion protein is linked to the toxic potential of cytosolic PrP', *Molecular Biology of the Cell*, 17(8), pp.3356-3368.

Rana, A., Gnaneswari, D., Bansal, S. and Kundu, B. (2009) 'Prion metal interaction: Is prion pathogenesis a cause or a consequence of metal imbalance?' *Chemico-biological Interactions*, 181(3), pp.282-291.

Rane, N.S., Chakrabarti, O., Feigenbaum, L. and Hegde, R.S. (2010) 'Signal sequence insufficiency contributes to neurodegeneration caused by transmembrane prion protein', *The Journal of Cell Biology*, 188(4), pp.515-526.

Robinson, J.B., Strottmann, J.M., Wick, D.G. and Stellwagen, E. (1980) 'Affinity chromatography in nonionic detergent solutions', *Proceedings of the National Academy of Sciences*, 77(10), pp.5847-5851.

Rogers, M., Yehiely, F., Scott, M. and Prusiner, S.B. (1993) 'Conversion of truncated and elongated prion proteins into the scrapie isoform in cultured cells', *Proceedings of the National Academy of Sciences*, 90(8), pp.3182-3186.

Ross, C.A. and Poirier, M.A. (2004) 'Protein aggregation and neurodegenerative disease', *Nature Medicine*, 10(7), pp.10–17.

Rout, J.R., Ram, S.S., Das, R., Chakraborty, A., Sudarshan, M. and Sahoo, S.L. (2013) 'Copper-stress induced alterations in protein profile and antioxidant enzymes activities in the *in vitro* grown *Withania somnifera* L', *Physiology and Molecular Biology of Plants*, 19(3), pp.353-361.

Rouwendal, G.J., Mendes, O., Wolbert, E.J. and De Boer, A.D. (1997) 'Enhanced expression in tobacco of the gene encoding green fluorescent protein by modification of its codon usage', *Plant Molecular Biology*, 33(6), pp.989-999.

Rudd, P.M., Merry, A.H., Wormald, M.R. and Dwek, R.A. (2002) 'Glycosylation and prion protein', *Current opinion in structural biology*, 12(5), pp.578-586.

Ruiz, C.C. and Sánchez, F.G. (1994) 'Effect of urea on aggregation behavior of triton X-100 micellar solutions: a photophysical study', *Journal of Colloid and Interface Science*, 165(1), pp.110-115.

Russelakis-Carneiro, M., Saborio, G.P., Anderes, L. and Soto, C. (2002) 'Changes in the Glycosylation Pattern of Prion Protein in Murine Scrapie IMPLICATIONS FOR THE MECHANISM OF NEURODEGENERATION IN PRION DISEASES', *Journal of Biological Chemistry*, 277(39), pp.36872-36877.

Saborio, G.P., Permanne, B. and Soto, C. (2001) 'Sensitive detection of pathological prion protein by cyclic amplification of protein misfolding', *Nature*, 411(6839), pp.810-813.

Sambrook, J., Fritsch, E.F. and Maniatis, T. (1989) 'Molecular cloning: a laboratory manual', *CSHL press*, pp.14-9.

Santos, R.B., Abranches, R., Fischer, R., Sack, M. and Holland, T. (2016) 'Putting the Spotlight Back on Plant Suspension Cultures', *Frontiers in Plant Science*, 7.

Sayre, L.M., Perry, G., Atwood, C.S. and Smith, M.A. (2000) 'The role of metals in neurodegenerative diseases', *Cellular and molecular biology*, 46(4), pp.731-741.

Schillberg, S., Fischer, R. and Emans, N. (2003) 'Molecular farming of recombinant antibodies in plants', *Cellular and Molecular Life Sciences CMLS*, 60(3), pp.433-445.

Schillberg, S., Twyman, R.M. and Fischer, R. (2005) 'Opportunities for recombinant antigen and antibody expression in transgenic plants—technology assessment', *Vaccine*, 23(15), pp.1764-1769.

Schlager, B., Straessle, A. and Hafen, E. (2012) 'Use of anionic denaturing detergents to purify insoluble proteins after overexpression', *BMC Biotechnology*, 12, p.95.

Schmidt, G.W. and Delaney, S.K. (2010) 'Stable internal reference genes for normalization of real-time RT-PCR in tobacco (*Nicotiana tabacum*) during development and abiotic stress', *Molecular Genetics and Genomics*, 283(3), pp.233-241.

Schmulling, T. and Schell, J. (1993) 'Transgenic tobacco plants regenerated from leaf disks can be periclinal chimeras' *Plant Molecular Biology*, 21(4), pp.705-708.

Scopes, R.K. (2013). *Protein Purification: Principles and Practice*. Springer Science and Business Media.

Sethuraman, N. and Stadheim, T.A. (2006) 'Challenges in therapeutic glycoprotein production', *Current Opinion in Biotechnology*, 17(4), pp.341-346.

Sharma, A.K. and Sharma, M.K. (2009) 'Plants as bioreactors: Recent developments and emerging opportunities', *Biotechnology Advances*, 27(6), pp.811-832.

Sharp, P.M. and Li, W.H. (1987) 'The codon adaptation index-a measure of directional synonymous codon usage bias, and its potential applications', *Nucleic Acids Research*, 15(3), pp.1281-1295.

Singh, A., Kong, Q., Luo, X., Petersen, R.B., Meyerson, H. and Singh, N. (2009) 'Prion protein (PrP) knock-out mice show altered iron metabolism: a functional role for PrP in iron uptake and transport', *PLoS One*, 4(7), p.6115.

Singh, N., Das, D., Singh, A. and Mohan, M.L. (2010) 'Prion protein and metal interaction: physiological and pathological implications', *Current Issues in Molecular Biology*, 12(2), P.99.

Singh, N. (2014) 'The role of iron in prion disease and other neurodegenerative diseases', *PLoS Pathog*, 10(9), p.e1004335.

Soto, C. (2003) 'Unfolding the role of protein misfolding in neurodegenerative diseases', *Nature Reviews Neuroscience*, 4(1), pp.49-60.

Soto, C. (2004) 'Diagnosing prion diseases: needs, challenges and hopes', *Nature Reviews Microbiology*, 2(10), pp.809-819.

Stam, M., Mol, J.N. and Kooter, J.M. (1997) 'Review article: the silence of genes in transgenic plants', *Annals of Botany*, 79(1), pp.3-12.

Stoger, E., Ma, J.K., Fischer, R. and Christou, P. (2005) 'Sowing the seeds of success: pharmaceutical proteins from plants', *Current Opinion in Biotechnology*, 16(2), pp.167-173.

Strasser, R., Castilho, A., Stadlmann, J., Kunert, R., Quendler, H., Gattinger, P., Jez, J., Rademacher, T., Altmann, F., Mach, L. and Steinkellner, H. (2009) 'Improved virus neutralization by plant-produced anti-HIV antibodies with a homogeneous β 1, 4-galactosylated N-glycan profile', *Journal of Biological Chemistry*, 284(31), pp.20479-20485.

Sunkesula, S.R.B., Luo, X., Das, D., Singh, A. and Singh, N. (2010) 'Iron content of ferritin modulates its uptake by intestinal epithelium: implications for co-transport of prions', *Molecular Brain*, 3(1), p.1.

Taraboulos, A., Scott, M., Semenov, A., Avrahami, D., Laszlo, L., Prusiner, S.B. and Avraham, D. (1995) 'Cholesterol depletion and modification of COOH-terminal targeting sequence of the prion protein inhibit formation of the scrapie isoform', *The Journal of cell biology*, 129(1), pp.121-132.

Thackray, A.M., Knight, R., Haswell, S.J., Bujdoso, R. and Brown, D.R. (2002) 'Metal imbalance and compromised antioxidant function are early changes in prion disease', *Biochemical Journal*, 362(2), pp.253-258.

Trick, H.N. and Finer, J.J. (1997) 'SAAT: sonication-assisted *Agrobacterium*-mediated transformation', *Transgenic Research*, 6(5), pp.329-336.

Turk, E., Teplow, D., Hood, L.E. And Prusiner, S.B. (1988) 'Purification and properties of the cellular and scrapie hamster prion proteins', *European Journal of Biochemistry*, 176(1), pp.21-30.

Tuzi, N.L., Cancellotti, E., Baybutt, H., Blackford, L., Bradford, B., Plinston, C., Coghill, A., Hart, P., Piccardo, P., Barron, R.M. and Manson, J.C. (2008) 'Host PrP glycosylation: a major factor determining the outcome of prion infection', *PLoS Biology*, 6(4).

Twyman, R.M. (2006) 'Host plants, systems and expression strategies for molecular farming', *Molecular Farming: Plant-Made Pharmaceuticals and Technical Proteins*, p.338.

Twyman, R.M., Schillberg, S. and Fischer, R. (2005) 'Transgenic plants in the biopharmaceutical market', *Expert Opinion on Emerging Drugs*, 10(1), pp.185-218.

Twyman, R.M., Stoger, E., Schillberg, S., Christou, P. and Fischer, R. (2003) 'Molecular farming in plants: host systems and expression technology', *Trends in Biotechnology*, 21(12), pp.570-578.

Ueda, E.K.M., Gout, P.W. and Morganti, L. (2003) 'Current and prospective applications of metal ion–protein binding', *Journal of Chromatography*, 988(1), pp.1-23.

Ullrich, K.K., Hiss, M. and Rensing, S.A. (2015) 'Means to optimize protein expression in transgenic plants', *Current Opinion in Biotechnology*, 32, pp.61-67.

Valdez-Ortiz, A., Rascón-Cruz, Q., Medina-Godoy, S., Sinagawa-García, S.R., Valverde-González, M.E. and Paredes-López, O. (2005) 'One-step purification and structural characterization of a recombinant His-tag 11S globulin expressed in transgenic tobacco', *Journal of Biotechnology*, 115(4), pp.413-423.

Vezina, L.P., Faye, L., Lerouge, P., D'Aoust, M.A., Marquet-Blouin, E., Burel, C., Lavoie, P.O., Bardor, M. and Gomord, V. (2009) 'Transient co-expression for fast and high-yield production of antibodies with human-like N-glycans in plants', *Plant biotechnology journal*, 7(5), pp.442-455.

Vogel, C. and Marcotte, E.M. (2012). Insights into the regulation of protein abundance from proteomic and transcriptomic analyses. *Nature Reviews Genetics*, 13(4), pp.227-232.

Vrentas, C.E., Onstot, S. and Nicholson, E.M. (2012) 'A comparative analysis of rapid methods for purification and refolding of recombinant bovine prion protein', *Protein Expression and Purification*, 82(2), pp.380-388.

Wadsworth, J.D., Hill, A.F., Joiner, S., Jackson, G.S., Clarke, A.R. and Collinge, J. (1999) 'Strain-specific prion-protein conformation determined by metal ions', *Nature Cell Biology*, 1(1), pp.55-59.

Walmsley, A.R. and Hooper, N.M. (2003) 'Distance of sequons to the C-terminus influences the cellular N-glycosylation of the prion protein', *Biochemical Journal*, 370(1), pp.351-355.

Walmsley, A.R., Zeng, F. and Hooper, N.M. (2001) 'Membrane topology influences N-glycosylation of the prion protein', *The EMBO journal*, 20(4), pp.703-712.

Wang, X., Wang, F., Arterburn, L., Wollmann, R. and Ma, J. (2006) 'The interaction between cytoplasmic prion protein and the hydrophobic lipid core of membrane correlates with neurotoxicity', *Journal of Biological Chemistry*, 281(19), pp.13559-13565.

Ward, J.T., Lahner, B., Yakubova, E., Salt, D.E. and Raghothama, K.G. (2008) 'The effect of iron on the primary root elongation of Arabidopsis during phosphate deficiency', *Plant Physiology*, 147(3), pp.1181-1191.

Watt, N.T., Taylor, D.R., Kerrigan, T.L., Griffiths, H.H., Rushworth, J.V., Whitehouse, I.J. and Hooper, N.M. (2012) 'Prion protein facilitates uptake of zinc into neuronal cells', *Nature Communications*, 3, p.1134.

Waugh, D.S. (2005) 'Making the most of affinity tags', *Trends in Biotechnology*, 23(6), pp.316-320.

Weber, P., Giese, A., Piening, N., Mitteregger, G., Thomzig, A., Beekes, M. and Kretzschmar, H.A. (2007) 'Generation of genuine prion infectivity by serial PMCA', *Veterinary microbiology*, 123(4), pp.346-357.

Westergard, L., Christensen, H.M. and Harris, D.A. (2007) 'The cellular prion protein (PrP^C): its physiological function and role in disease', *Biochimica et Biophysica Acta (BBA)-Molecular Basis of Disease*, 1772(6), pp.629-644.

White, A.R., Collins, S.J., Maher, F., Jobling, M.F., Stewart, L.R., Thyer, J.M., Beyreuther, K., Masters, C.L. and Cappai, R. (1999) 'Prion protein-deficient neurons reveal lower glutathione reductase activity and increased susceptibility to hydrogen peroxide toxicity', *The American Journal of Pathology*, 155(5), pp.1723-1730.

Wickner, R.B., Edskes, H.K., Shewmaker, F. and Nakayashiki, T. (2007) 'Prions of fungi: inherited structures and biological roles', *Nature Reviews Microbiology*, 5(8), pp.611-618.

Wilken, L.R. and Nikolov, Z.L. (2012) 'Recovery and purification of plant-made recombinant proteins', *Biotechnology Advances*, 30(2), pp.419-433.

Winklhofer, K.F., Heller, U., Reintjes, A. and Tatzelt, J. (2003) 'Inhibition of complex glycosylation increases the formation of PrP^{Sc}', *Traffic*, 4(5), pp.313-322.

Wong, B.S., Chen, S.G., Colucci, M., Xie, Z., Pan, T., Liu, T., Li, R., Gambetti, P., Sy, M.S. and Brown, D.R. (2001) 'Aberrant metal binding by prion protein in human prion disease', *Journal of Neurochemistry*, 78(6), pp.1400-1408.

Xu, J., Tan, L., Goodrum, K.J. and Kieliszewski, M.J. (2007) 'High-yields and extended serum half-life of human interferon α 2b expressed in tobacco cells as arabinogalactan-protein fusions', *Biotechnology and Bioengineering*, 97(5), pp.997-1008.

Yang, D., Guo, F., Liu, B., Huang, N. and Watkins, S.C. (2003) 'Expression and localization of human lysozyme in the endosperm of transgenic rice', *Planta*, 216(4), pp.597-603.

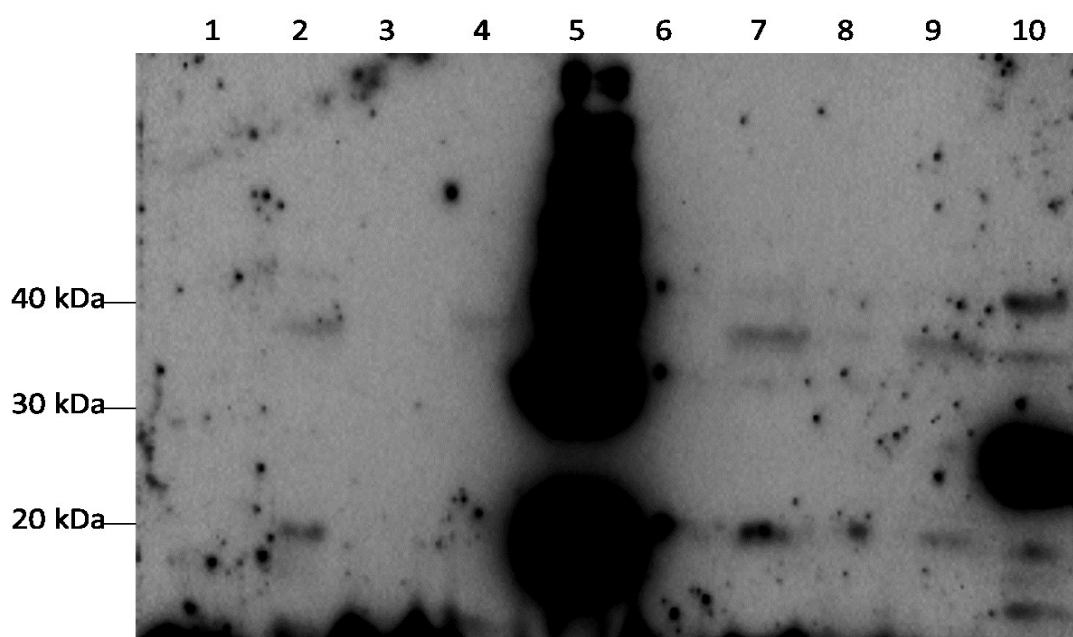
Yedidia, Y., Horonchik, L., Tzaban, S., Yanai, A. and Taraboulos, A. (2001) 'Proteasomes and ubiquitin are involved in the turnover of the wild-type prion protein', *The EMBO Journal*, 20(19), pp.5383-5391.

Yenofsky, R.L., Fine, M. and Pellow, J.W. (1990) 'A mutant neomycin phosphotransferase II gene reduces the resistance of transformants to antibiotic selection pressure', *Proceedings of the National Academy of Sciences*, 87(9), pp.3435-3439.

Yin, S.M., Zheng, Y. and Tien, P. (2003) 'On-column purification and refolding of recombinant bovine prion protein: using its octarepeat sequences as a natural affinity tag', *Protein Expression and Purification*, 32(1), pp.104-109.

9 Appendices

9.1 Appendix A: Protease Digestion of recombinant mPrP

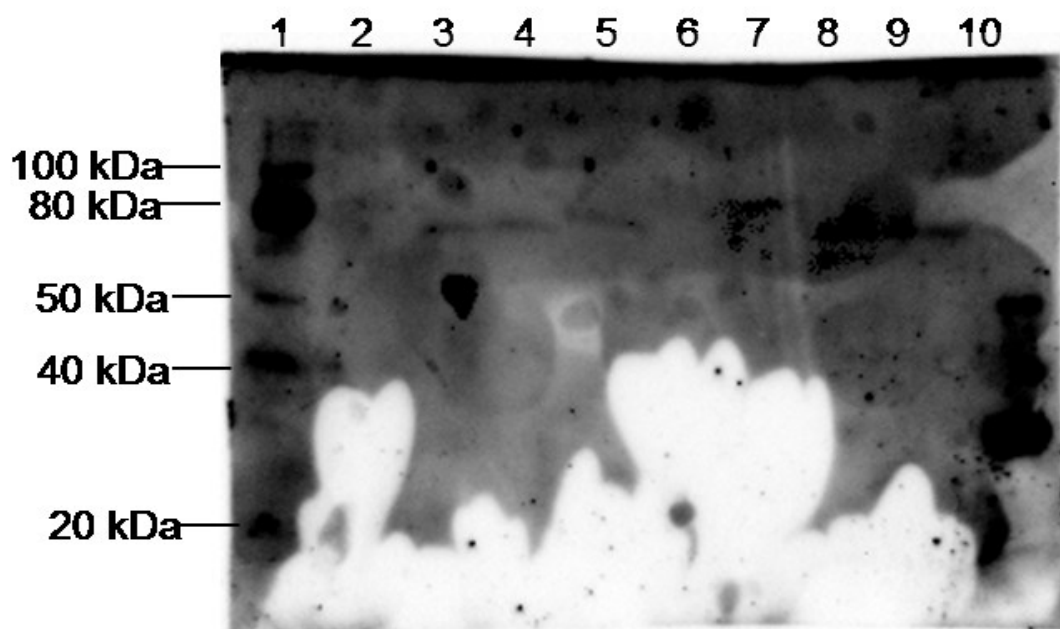


Appendix 9.1: Proteinase K digestion of transgenic plants expressing mPrP.

Lanes 1 & 3: Proteinase K treated lysate from transgenic lines C9 & C12. Lanes 2 & 4: Untreated lysate from transgenic lines C9 & C12. Lane 5: Molecular weight marker. Lanes 6 & 8: Proteinase K treated lysate from transgenic lines E4 & E10. Lanes 7 & 9 – Untreated lysate from transgenic lines E4 & E10. Lane 10: Control – recombinant mPrP from *E. coli*.

500 mg of transgenic plant leaves was solubilised in 1 ml of Lysis Buffer (50 mM Tris-HCl (pH 8), 5mM β -mercaptoethanol, 1% CHAPS). The lysate was precipitated with methanol/chloroform and resuspended in 500 μ l of reaction buffer (50 mM Tris-HCl (pH 7.5), 5mM CaCl_2). 12.5 μ g of proteinase K (Promega) was added to 250 μ l aliquot of the solution and incubated at 37°C overnight. The control aliquots were stored at -20°C overnight. Subsequently, the reaction was analysed by western blot using the anti 6X his-tag antibody (Abcam). The results indicate that the ~19kDa aminoterminally truncated mPrP molecules from plants expressing either the cytosolic or ER constructs are not authentic PrP^{Sc} molecules.

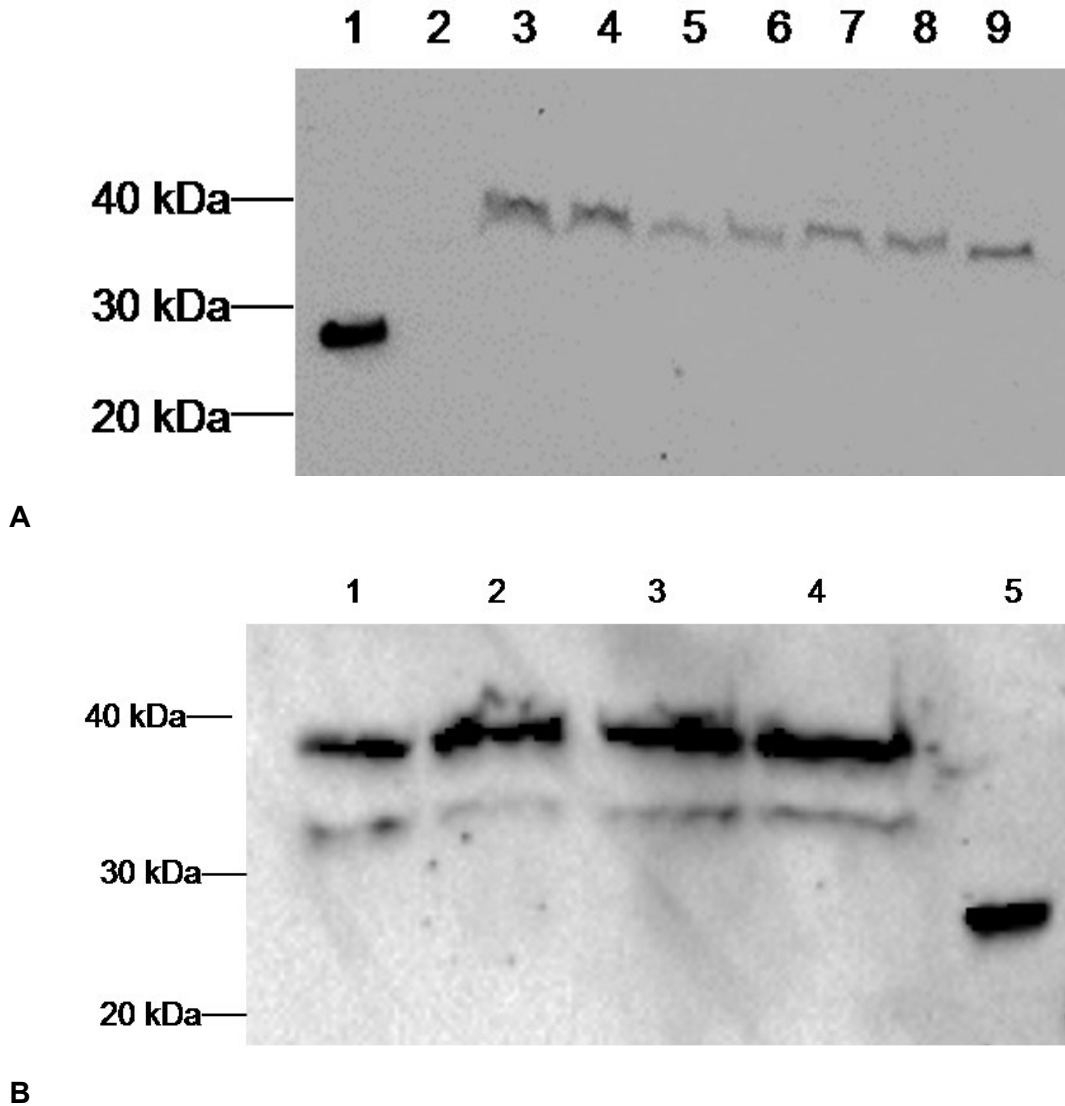
9.2 Appendix B: Deglycosylation of recombinant mPrP



Appendix 9.2: Deglycosylation of transgenic plants transformed with the ER construct. Lane 1: Molecular weight marker. Lanes 2 & 4: Untreated lysate from transgenic lines E4 & E10. Lanes 3 & 5: N-glycosidase A treated lysate from transgenic lines E4 & E10. Lane 10: Control – recombinant mPrP from *E. coli*.

250 mg of plant leaves was solubilised in 500 μ l of Lysis Buffer (10 mM sodium acetate, 100 mM β -mercaptoethanol; 0.5% SDS). 250 μ l aliquot of the clarified lysate was treated with 20 μ l (1 mU) of N-glycosidase A (Roche) and incubated at 37°C for 3 hours. The control aliquot was incubated on ice for three hours. Subsequently, the reaction was analysed by western blot using the anti 6X his-tag antibody (Abcam). From the results, deglycosylation of recombinant mPrP sequestered in the endoplasmic reticulum was unsuccessful because of its aggregated state (Appendix 9.2; lanes 3, 4 and 5 above 50 kDa) of the recombinant protein.

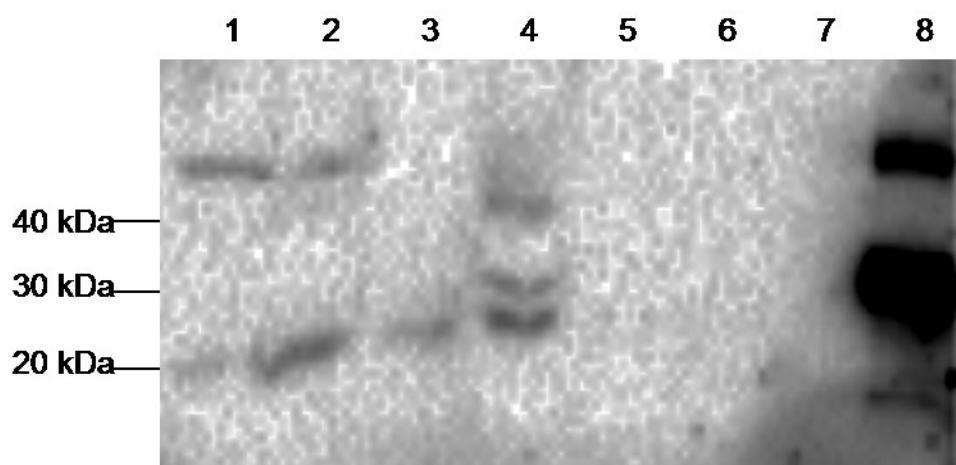
9.3 Appendix C: Western Blot analysis of recombinant mPrP



Appendix 9.3: Western blot analysis of recombinant mPrP using PrP antibody C-20 (1:1000 dilution). **A:** Transgenic lines transformed with the cytosolic transgene construct. Lane 1: Control - recombinant mPrP from *E. coli*. Lanes 3 – 9: Clarified Lysate from independent transgenic lines, C1, C4, C7, C9, C12, C15 and C23 respectively. **B:** Transgenic lines transformed with ER transgene construct. Lanes 1 – 4: Clarified Lysate from independent transgenic lines E1, E2, E4 and E7 respectively. Lane 5: Control – recombinant mPrP from *E. coli*.

100 mg of homogenised transgenic tobacco leaves were lysed in 200 µl of 2X laemmli sample buffer. The lysate was incubated for 10 minutes at 90°C and clarified by centrifugation at 13, 000 rpm for 5 minutes. The clarified lysate was analysed by western blot using the PrP antibody C-20 (Santa Cruz biotechnology) as described in section 2.3.3.1. As shown in Appendix 9.3, analysis of recombinant mPrP from transgenic lines transformed with the cytosolic construct indicated a single band of ~38 kDa, indicating a dimer of the aminoterminally truncated mPrP while recombinant mPrP sequestered in the endoplasmic reticulum indicated two bands of ~38kDa and ~32kDa

9.4 Appendix D: Non-detergent lysis of transgenic tobacco leaves expressing cytosolic-mPrP



Appendix 9.4: Western blot analysis of cytosolic-mPrP in transgenic tobacco lines. Lanes 1-4: recombinant mPrP from independent transgenic lines C4, C7, C9 and C12 transformed with the cytosolic transgene construct. Lane 8: Control - recombinant mPrP from *E. coli*.

100 mg of transgenic tobacco leaves were lysed in extraction buffer (200 mM Tris HCl (pH 7.5), 10 mM EDTA, 1 mM PMSF, 100 mM NaCl). The extract was clarified by centrifugation at 13,000 rpm for 15 minutes and precipitated with methanol/chloroform. The precipitate was resuspended in 50 μ l of 2X Laemmli buffer and incubated at 90°C for 10 minutes. The resulting solution was analysed by western blot.

The analytes in Appendix 9.3 constitutes 0.5 mg of homogenised leaves per μ l of extraction buffer compared to Appendix 9.4 which constitutes 2 mg of homogenised leaves per μ l of extraction buffer. The results indicate in spite of a 4-fold difference in analytes concentration, the non-detergent lysis buffer had

lower protein concentration. This implies that cytosolic recombinant mPrP may be membrane-associated or binds to other membrane associated proteins.

9.5 Appendix E: Recombinant mPrP concentration

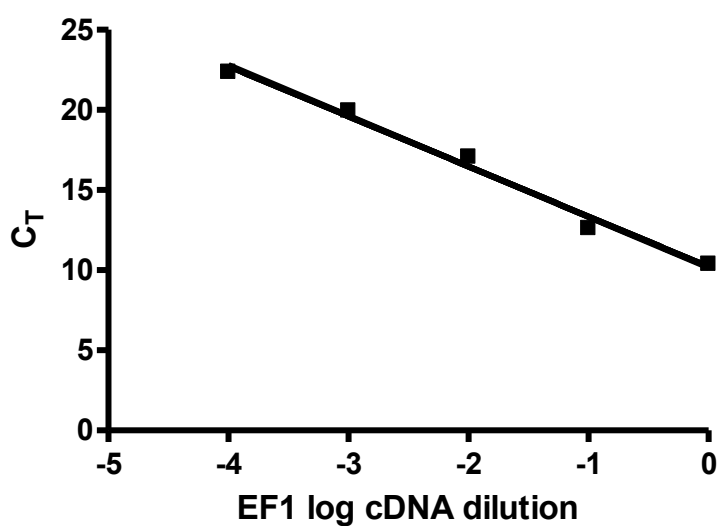
The concentration of recombinant mPrP in transgenic plant lines as determined by ELISA analysis is shown in Appendix 9.5.

Appendix 9.5: Recombinant mPrP concentration

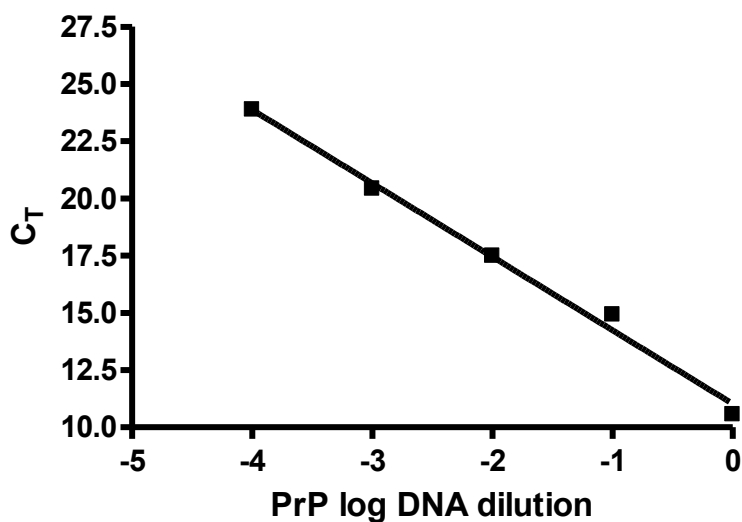
Transgenic lines	Average mPrP Concentration (ng/ 100 µl of lysate)	Average Total soluble protein (ng/ 100 µl of lysate)	mPrP as %(TSP)
E1	1.495814	148384.5	0.001008066
E2	0.606289	119138.5	0.000508894
E4	2.360312	146125.9	0.00161526
E7	0.776333	257027.5	0.000302043
E10	1.951788	129715.4	0.00150467
C4	0.912424	212776.3	0.000428819
C7	2.44075	100588.9	0.002426462
C9	1.218471	86874.95	0.001402557
C12	1.726432	128731.7	0.001341109
C15	2.031893	151215.8	0.001343704

9.6 Appendix F: qRT-PCR Analysis

Data in Appendix 9.6 shows an example of relative mRNA estimation for transgenic plants expressing cytosolic-mPrP using the Pfaffl (2001) method.



A



B

Appendix 9.6a: qRT-PCR Efficiency

A) EF1 Standard; Slope = -3.128; Efficiency (E_{EF1}) = 2.09

B) PrP Standard; Slope = -3.212; Efficiency (E_{PrP}) = 2.05

Appendix 9.6b: Relative RNA quantification

Plant lines	C _T PrP	C _T EF1	ΔC _T PrP	ΔC _T EF1	(E _{PrP}) ΔC _T PrP	(E _{EF1})ΔC _T EF1	Normalised Relative Quantity
C4	24.10	26.56	0.00	0.00	1.00	1.00	1.00
C12	23.22	25.94	0.88	0.62	1.87	1.58	1.19
C7	23.92	21.24	0.17	5.32	1.13	50.49	0.02
C15	23.38	27.11	0.72	-0.55	1.67	0.67	2.51
C9	23.89	25.60	0.20	0.97	1.16	2.04	0.57

$$\text{Normalised relative quantity} = \frac{(E_{\text{PrP}})^{\Delta C_T (\text{PrP calibrator-sample})}}{(E_{\text{EF1}})^{\Delta C_T (\text{EF1 calibrator-sample})}}$$